Università degli Studi di Urbino Carlo Bo

Dipartimento di Scienze Pure e Applicate (DiSPeA)

Ph.D. Program in: Research Methods in Science and Technology

CYCLE: XXXV

BENTHIC FORAMINIFERA AS BIOINDICATORS OF THE ENVIRONMENTAL QUALITY STATUS OF MARINE HABITATS: DIFFERENT TECHNIQUES AND APPLICATIONS

ACADEMIC DISCIPLINE: GEO/01 (Paleontology and Paleoecology)
BIO/07 (Ecology)

Coordinator: Prof. Alessandro Bogliolo

Supervisor: Prof. Fabrizio Frontalini

Ph.D. student: Marco Cavaliere

ACADEMIC YEAR
2021/22

A mia madre

Ma che affare!
Vendo Bagnoli chi la vuol comprare?

E. BENNATO

List of contents

List of contents 3
List of figures 5
List of tables 7
1. Background and summary 8
2. Assessing the Ecological Quality Status of the Highly Polluted Bagnoli Area (Tyrrhenian Sea, Italy) using Foraminiferal eDNA Metabarcoding 12
2.1. Introduction 12
2.2 The study area 14
2.3 Materials and Methods 15
2.4. Results 25
2.5. Discussion 35
2.6. Conclusions 43
3. Encapsulated in sediments: eDNA deciphers the ecosystem history of one of the most polluted European marine sites 44
3.1. Introduction 44
3.2. Methods 46
3.3. Results 52
3.4. Discussion 60
3.5. Conclusion and future perspectives 66
4. Paleoenvironmental Impact: the Morphometric Variation of Benthic Foraminiferal Species in Bagnoli-Coroglio SIN (Site of National Interest) 68
4.1. Introduction 68
4.2. Study area and historical changes 70
4. Materials and methods 73
4.4. Results 75
4.5. Discussion 78
4.6. Conclusions 81
5. Paleoenvironmental changes in the Gulf of Gaeta (central Tyrrhenian Sea, Italy): a perspective from benthic foraminifera after dam construction 82

5.1. Introduction 82
5.2. Study area 84
5.3. Materials and Methods 86
5.4. Results 88
5.5. Discussion 92
5.6. Conclusion 97
6. Conclusions and future challenges 98
6.1. State of the art and research impact 98
6.2. Future challenges 99
References 101
Acknowledgments 122
Supplementary materials 124

List of figures

Figure 2.1. Study area: a) location of Campania Region in Southern Italy; b) location of Bagnoli area in the Campania region; c) sampling locations and relative water depth within the Pozzuoli Gulf. Geographical coordinates refer to the World Geodetic System 1984 (WGS-84). 17

Figure 2.2. Spatial plots of a) mud content (%); b) sand content (%); c) total organic carbon (TOC) (%); and d) C/N ratio. 26

Figure 2.3. Spatial plots of a) enrichment factor of As; b) enrichment factor of Hg c) enrichment factor of Pb; d) enrichment factor of Zn; e) modified contamination degree (mCd); and f) pollution load index (PLI). 27

Figure 2.4. Chord diagram based on a) morphospecies and the eDNA dataset: b) molecular classes; b) Globothalamea; and d) Monothalamea-Tubothalamea; the top part shows the stations, whereas the lower part refers to morphospecies and MOTUs. A complete list of abbreviations is reported in Table S2.9. 28

Figure 2.5. PCA diagram based on environmental parameters and a) morphospecies, b) unassigned OTUs > 5%, c) assigned Monothalamea, and d) assigned Globothalamea. Secondary variables are marked with an *. 31

Figure 2.6. Spearman's rho matrix of correlation between environmental parameters (i.e., PLI and TOC) and biotic indices (i.e., Foram-AMBI, FSI, TSI-Med, exp(H'bc), g-exp(H'bc), g-Foram-AMBI, and g-Foram-AMBI MOTUs). The distribution (histogram) of each variable is shown on the diagonal. On the bottom of the diagonal, the bivariate scatter plots with a fitted line are displayed. On the top of the diagonal, the Rho values and the relative p-values are provided. Significance levels are reported as stars: 0.001, 0.01, 0.05, 0.1, 1 <=> "***", "**", "*", ".", " ". 35

Figure 2.7. Spatial plots of a) environmental stress (ES) based on PCA first axis scores, b) Foram Stress Index (FSI), c) Tolerance Stress Index (TSI-Med), d) Foram-AMBI, e) g-exp(H'bc), f) g-Foram-AMBI, and d) g-Foram-AMBI MOTUs. The ecological quality status categorizations are also reported following Table 2.1. Two categorizations I and II are provided for Foram-AMBI based on Borja et al. (2003) and Parent (2019), respectively. 37

Figure 3.1 Geochemical, historical and biological archives. Plot of selected geochemical proxies (PLI: Pollution Load Index; PAHs: Polycyclic Aromatic Hydrocarbons, TOC: Total Organic Carbon; C/N: carbon-nitrogen ratio). Classification of PLI after Zhang et al. (2011) with modification, sediment quality guidelines for PAHs (TEL: threshold effect level; ERL: effects range low; ERM: effect range median; CB-MEC: Consensus Based - midrange effect concentration) after Burton (2002) and TOC after Bouchet et al. (2018a). Historical archives with significant human-induced changes and activities. Hierarchical Cluster Analyses (HCAs) based on prokaryotes, protists, dinoflagellates, diatoms, benthic foraminifera (molecular and morphological) and metazoa. The colour-shaded areas over HCAs denote the stepwise temporal phases along the AB01 core in the Bagnoli-Coroglio SIN (Gulf of Pozzuoli, Tyrrhenian Sea), namely I: Pre-industrial (1827-1851; blue), II: Initial industrial phase & land-use change (1851-1911; green), III: Industrial phase (1911-1950; yellow), IV: Industrial peak and productivity expansion (1950-1992; red) and V: Post-industrial/partial decommission (1992-2016; orange). 57

Figure 3.2. Paleo-community composition shift. Eukaryote, protists, metazoa, and benthic foraminifera (molecular and morphological) composition changes along the AB01 core in the Bagnoli-Coroglio SIN (Gulf of Pozzuoli, Tyrrhenian Sea) inferred from multimarker sedaDNA data from 1827 to 2013. The different colours over the ages refer to the main phases (I: blue; II: green; III: yellow; IV: red and V: orange) as identified in Figure 1. 58

Figure 3.3. Changes in diversity and ecological indices. Diversity (H') plots of prokaryotes, protists, dinoflagellates, diatoms, benthic foraminifera (molecular and morphological) and metazoa coupled with relative abundance of Posidonia oceanica, land plants, epifaunal and epiphytic foraminifera and encrusting metazoa percentages. Ecological indices for prokaryotes (microgAMBI, m-ERM-q-HM, and m-ERM-q-PAHs), foraminifera (Foram AMBI) and metazoa (AMBI) are also plotted. The different colour over the ages refer to the main phases (I: blue; II: green; III: yellow; IV: red and V: orange) as identified in Figure 3.1. .. 60

Figure 4.1 Study area. Location of the Bagnoli-Coroglio SIN within the Campi Flegrei Caldera. Geographical coordinates referred to the World Geodetic System 1984 (WGS-84).....71

Figure 4.2. Abiotic (PAHs, PLI, C/N, TOC) and biotic (V. bradyana and R. bradyi relative abundance, tests size and P. oceanica relative abundance) factors temporal variations. 77

Figure 5.1. Location map of the Gulf of Gaeta in Southern Italy and SW104_C5 core site. 85

Figure 5.2. Temporal relative abundance variations of selected benthic foraminiferal species. 91

Figure 5.3. Paleoclimate periods (blue and red from Margaritelli et al., 2016) and anthropogenic interventions. a) HCA (Hierarchical cluster analysis) based on benthic foraminiferal relative abundances; b) Enhanced Benthic Foraminifera Oxygen Index (EBFOI) temporal variations; c) Paleoenvironmental reconstruction and land-use change in 1857 (Annali delle Bonificazioni – Anno I – 1858. Pianta Generale del Bacino Inferiore del Volturno con la indicazione delle opere di strade e di canali eseguite dal Real Governo), 1915 (Istituto Geografico Militare, 1914, Cartografia 1:25000) and 1990 (Satellite Imagery, Google Earth, 1990)..... 96

List of tables

Table 2.1. Indices categorization to assess the ecological quality status: Tolerance Stress Index-Med (TSI-Med; Barras et al., 2014; Parent et al., 2021), exp(H'bc) (Bouchet et al., 2012), Foram Stress Index (FSI; Dimiza et al., 2016), Foram-AMBI (Borja et al., 2003) *Foram-AMBI, *g-Foram-AMBI (Parent, 2019), and *g-exp(H'bc) (present paper).

Table 2.2. Ecological quality status calculated on the selected indices (see Table 2.1 for categorization). Spearman's rho correlation coefficients between indices and environmental stress (ES that is the scores of PCA1) are also reported. Bold values *p*. <0.05. The sum of the score agreement (acceptable: high or good EcoQS scored as 1 and not acceptable: moderate-to-bad EcoQS scored as 0) is reported with the interpretation of the agreement (i.e., full 0/7 or 7/7, partial 1/7, 2/7, 5/7 or 6/7, and disagreement 4/7).

Chapter I

1. Background and summary

The increase of human activities prompted by population growth and economic development is severely affecting global ecosystems and ecological diversity, rapidly altering sustainability, environmental balances and biogeochemical cycles (Plant et al. 2001; Logermann et al., 2022). These shifts have led scientists to re-name the current human-dominated epoch we are living in as the Anthropocene (Curtzen and Stoermer, 2000; Lewis and Maslin, 2015). Global pollution, climate changes and ecosystems degradation are causing a deterioration of the environmental (i.e., water quality, ecological diversity) quality and posing a threat to the human health (McMichael, 1993).

In this scenario, environmental researches are crucial for providing tools by which assessing the human impact, monitoring the ecological and geochemical status, distinguishing the anthropogenic influence (i.e., pollution) from the natural background and applying restorations programmes.

Human impact is severely damaging aquatic ecosystems. In fact, marine environments are the final sink of pollutants pathways and waterways, transported from the continent to the oceans (Salomons et al., 1987), and coastal areas are singularly sensitive to anthropic impact (Lu et al., 2018). Indeed, the human activities (i.e., industrial development, urbanization, illegal dumping, contamination runoff) are mostly set along the coast and have progressively risen. The importance of evaluating the quality of water bodies and marine sediment (Burton et al., 2002) has been underlined in many EU directive (WFD,2000/60/EC; MSFD, 2008/56/EC). Also for the 2030 Agenda for Sustainable Environment (United Nations, 2015), one of the 17 Goals is to conserve and sustain marine environments (goal number 14: Life below water).

In addition to geochemical analysis, organisms can be successfully used to assess the present and past environmental quality of marine areas. The analyses of biotas or their biological processes, called bioindicators or biomarkers, can accurately reveal the conditions of an environment and quantify the anthropogenic pressure (Holt and Miller 2010). Among them, foraminifera, a single-cell group of organisms (i.e., protozoa), have been widely studied for evaluating global changes and the environmental health of marine ecosystems (Martins et al., 2019; Frontalini et al., 2020). Benthic foraminifera inhabit all marine environments and have the ability to construct a hard test (i.e., shell) made up by calcium carbonate (hyaline and porcelaneous types) or sediment (agglutinated ones). Their occurrence as living or along fossil records assemblages can reveal important information regarding the physical and chemical (e.g., organic matter input, salinity, trace elements concentrations) marine dynamics and history. Since they have a relatively short-life cycle, are abundant, and highly diversified, they can be used as early warning indicators of environmental changes (Frontalini and Coccioni, 2008). Indeed, because of their high test fossilization potential they can be used for paleoenvironmental reconstructions (Murray, 2006). Living assemblages' analysis (i.e., faunal density, diversity) can provide detailed spatial information about the current marine conditions (Alve et al., 2016), recorded as diversity reduction (Bergamin et al., 2005) and test-size variation (Ferraro et al., 2020). Foraminiferal assemblages (preserved in the sedimentary records) can also reveal temporal variations and paleo-ecological shifts over time (Francescangeli et al., 2016) and represent an accurate proxy for paleoenvironmental reconstructions. Moreover, the development of foraminiferal eDNA metabarcoding offers a reliable and suitable alternative to morphology-based foraminiferal biomonitoring (Pawlowski et al., 2014b). The combination and agreement between these two techniques has been recently proved (Frontalini et al., 2020).

In this PhD thesis, benthic foraminifera have been used to evaluate and to infer the present and paleo-ecological quality status (EcoQS and paleo-EcoQS) in two coastal areas of Campania Region (Tyrrhenian Sea, Italy).

In Chapter II, the response of benthic foraminifera in the Bagnoli-Coroglio area (Tyrrhenian Sea, Italy), one of the most polluted marine coastal sites in Europe, has been evaluated based on a traditional morphology-based approach and eDNA metabarcoding. The Bagnoli-Coroglio area hosted industrial plants till the 1992 and the geochemical data show that the marine area in front of the former industrial plant contain high concentrations of potentially toxic elements. Significant differences (i.e., diversity and assemblage composition; ecological indices) in both morphological and molecular datasets resulted in a clear separation following the environmental stress gradient. The congruent and complementary trends between morphological and metabarcoding data observed in the case of the Bagnoli site further support the application of foraminiferal metabarcoding in routine biomonitoring to assess the environmental impacts of heavily polluted marine areas.

In **Chapter III**, a marine sediment core has been analyzed, at high resolution, for reconstructing the ecological history of the Bagnoli-Coroglio area. The sedimentary ancient DNA (*sedaDNA*) has been evaluated through all trophic levels of biodiversity (i.e., planktonic and benthic protists, metazoan and seagrasses) as well as the geochemical data along the core. The *sedaDNA* analysis reveals a five-phase evolution of the area, where changes appear as the result of a multi-level cascade effect of impacts associated with industrial activities, urbanization, water circulation and land-use changes. The *sedaDNA* allows to infer reference conditions that must be considered when restoration actions are implemented.

In **Chapter IV**, the historical changes of the Bagnoli-Coroglio marine site has been assessed using the morphological measurement of tests (i.e., shells) in two benthic foraminiferal species. *Rosalina bradyi* and *Valvulineria bradyana* were chosen as target species for their abundance and their ecological behaviour. The tests sizes were measured along the historical record to reveal potential environmental stress resulted as morphometric variations of tests. The temporal results have also been compared with *Posidonia oceanica* abundance, pollutants' temporal variations and historical information about the area. Results confirmed how the human impact altered the ecological equilibrium of the coastal area, changing the hydrodynamic circulation as well as the amount and the

nature of organic matter inputs. These temporal variations are partially recorded in *R. bradyi* as density and test-size reduction and in *V. bradyana* as a "delayed" response to pollution.

In Chapter V, a paleo-environmental reconstruction of the continental shelf environment in proximity of the Volturno River's mouth (Northern Campania Region) has been based on the benthic foraminiferal historical record analysis in a marine sediment log-core. The log-core was dated back to 1686 and the benthic foraminiferal assemblages' variations have been statistically analysed and compared to historical changes occurred in the Volturno River catchment basin. In this research, interesting relations between human interventions (i.e., land use changes happened on the continent like dams' constructions) and foraminiferal assemblages' changes have been observed and described as results of sediment and organic matter input variations.

Chapter II

2. Assessing the Ecological Quality Status of the Highly Polluted Bagnoli Area (Tyrrhenian Sea, Italy) using Foraminiferal eDNA Metabarcoding

Published in Science of the Total Environment (Cavaliere et al., 2021).

M. Cavaliere, I. Barrenechea Angeles, M. Montresor, C. Bucci, L. Brocani, E. Balassi, F. Margiotta, F. Francescangeli, V.M.P. Bouchet, J. Pawlowski, F. Frontalini, Science of The Total Environment, Volume 790, 2021, 147871, ISSN 0048-9697, https://doi.org/10.1016/j.scitotenv.2021.147871.

2.1. Introduction

In recent years, the implementation of several marine legislations has emphasized the need to characterize the worldwide increasing degree of marine pollution of coastal environments (Lu et al., 2018). Coastal marine sediments act as the final sink of contamination (Salomons et al., 1987), posing a high anthropogenic stress on marine habitats and the species living therein. In this context, several areas marked by strong anthropogenic impact have been recognized in Italy and defined as sites of national interest (SINs), some of which are marine locations, such as Bagnoli (NW sector of Naples, Italy) (Ausili et al., 2020).

Bagnoli was Italy's former second-largest steel factory (Trifuoggi et al., 2017), an area where intensive industrial activities widely operated until 1992. The former industrial plant hosted steel, asbestos, and concrete industries on a wide territory facing the sea. In 2000, the area was declared a

SIN, and the first remediation programmes were planned. Today, Bagnoli is a large brownfield area, the marine sediments of which are still intensively impacted, as shown by several ecological and geochemical surveys (Romano et al., 2004, 2018; Sprovieri et al., 2020). Although the area has been largely investigated, the assessment of its ecological quality is crucial to highlight potential changes in the anthropogenic stress on the aquatic biota of the area. The evaluation of the impact is commonly carried out through geochemical analyses aimed at recognizing pollutants that, at high concentrations, could trigger serious imbalances within the aquatic ecosystem. However, chemical analyses are not directly related to an ecosystem's ecological status. The ecological quality is instead more linked to the biota living therein. Indeed, the detection of unforeseen impacts can be achieved through biological monitoring (i.e., bioindicators). In this context, the European Union has implemented the Water Framework Directive (WFD, 2000/60/EC) to protect, maintain, and restore the environmental quality of water bodies and the sustainable use of water and the Marine Strategy Framework Directive (MSFD, 2008/56/EC) to identify strategies to achieve a Good Environmental Status also through the consideration of biological elements. Among the numerous biological groups used to assess the health of marine ecosystems, benthic foraminifera—single-cell organisms with a test (i.e., shell)—are increasingly applied as environmental proxies (Alve, 1995; Francescangeli et al., 2020) and, more recently, in environmental biomonitoring to evaluate ecological quality status (EcoQS) (e.g., Alve et al., 2009, 2019; Bouchet et al., 2012, 2018a, 2021; Francescangeli et al., 2016; El Kateb et al., 2020).

Morphology-based taxonomy is still the preferred approach for evaluating changes in benthic foraminiferal species and assemblages' composition in response to stress conditions. Recently, environmental DNA (eDNA) metabarcoding has been successfully applied to characterize a benthic foraminiferal community (Pawlowski et al., 2014b). This innovative and effective methodology has been used for investigating the response of benthic foraminifera to different human-related activities and stress in, for example, fish farms (Pawlowski et al., 2014a; He et al., 2019) and oil and gas platforms (Laroche et al., 2016, 2018; Cordier et al., 2019; Frontalini et al., 2020). Compared to the classic morphology-based approach, eDNA metabarcoding allows a larger number of samples and

data to be processed rapidly and accurately (Pawlowski et al., 2014b). However, only a limited number of studies has simultaneously evaluated and compared the performance and congruence of the traditional morphology-based biomonitoring with eDNA metabarcoding (e.g., Frontalini et al., 2020). Furthermore, foraminiferal biotic indices are still to be implemented on eDNA-based datasets.

The aims of the present research are, therefore, to 1) provide an environmental characterization of the Bagnoli area, highlighting the spatial variations of the anthropogenic impact on the marine ecosystem, 2) test foraminiferal biotic indices on eDNA datasets, and 3) assess and compare the EcoQS based on both molecular- and morphology-based benthic foraminiferal communities.

2.2 The study area

The Bagnoli area is located in the NW metropolitan territory of Naples (Campania Region, Southern Italy), along the coastline of the Pozzuoli Gulf (Tyrrhenian Sea) (Fig. 2.1a,b). The area of Bagnoli is part of the Campi Flegrei caldera, a large territory influenced by active volcanism and hydrothermal activity that modify the chemical composition of local groundwater (Celico et al., 2000).

The first industrial activities started at the beginning of the 20th century, and in the first decades of 1900, large plants of steel (ILVA-Italsider), asbestos (Eternit), and concrete (Cementir) were operating, reaching their development peak in the late 1960s. For stimulating productivity, the natural landscape of the territory has also been deeply modified. In 1920, two piers were built to provide factory access to large ships carrying fossil coal, iron ores, and limestone, and in 1935, the Island of Nisida was connected to the mainland by the construction of a long strip of land, changing the water circulation system in the gulf. High concentrations of heavy metals (i.e., Cu, Fe, Hg, Mn, Pb, and Zn) and hydrocarbons, particularly polycyclic aromatic hydrocarbons (PAHs), occur in marine sediments in front of the former plant area (Damiani et al., 1987; Romano et al., 2009; Arienzo et al., 2017). Contamination is particularly high between the two long piers, where, in 1960–62, a large amount of

polluted materials was disposed to expand the plant operating area. The industrial production ceased in the 1990s, and the industrial facilities were completely dismantled in the early 2000s (Romano et al., 2004; Ausili et al., 2020). In 2000, the Bagnoli-Coroglio site was listed among the Italian SINs. These SINs are areas where a threat to human health occurs, and a recovery programme must be implemented. In recent years, the brownfield site has been the object of a governmental remediation project aimed at environmental restoration. In particular, marine sediments from Bagnoli should be treated as special waste and physically removed from the site, although this technique is invasive and may seriously impact the environment.

Several studies have accurately addressed the response of benthic foraminifera to pollution in the Bagnoli area (Bergamin et al., 2003, 2005; Romano et al., 2008, 2009). Overall, these studies have evidenced from an absence to a very low abundance of living foraminifera near the plant, particularly between the two piers, given that the total assemblages were always considered (Bergamin et al., 2003; Romano et al., 2008). Additionally, several species have been either identified as tolerant (i.e., *H. germanica, Miliolinella subrotunda,* and *Quinqueloculina parvula*) or sensitive (*L. lobatula, A. mamilla and R. bradyi, Elphidium macellum* and *Miliolinella dilatata*) to pollution (Bergamin et al., 2003, 2005; Romano et al., 2008, 2009).

2.3 Materials and Methods

2.3.1 Sampling and samples treatment

The superficial marine sediment samples were collected at 12 sites with a box-corer along 4 transects (B1, B2, B3, and B4) at different water depths (10, 20, and 40 m) in the Bagnoli area (Fig. 2.1c). The transects B3 and B4 were placed in the axis of the two piers within the internal area so that they would reflect the most impacted areas, whereas B1 and B2 were approximately 2.5 km away from the ex-industrial plant and would, therefore, represent a lower level of contamination.

Sediments were collected in three replicates for both morphological and molecular benthic foraminiferal analyses by independent deployments of the box-corer. The sediments from only the first deployment were sub-sampled for geochemical and grain-size analyses. Only the uppermost part of the sediment (1 cm) was sampled and used for morphological, molecular, grain-size, and geochemical analyses. Once collected, samples (50 cm^3) for foraminiferal morphological analyses were immediately stained with a rose Bengal solution (2 g/L) for the identification of living, stained foraminifera. Samples (~10 g) for eDNA metabarcoding were immersed in 10 mL of Life Guard™ Soil Preservation Solution (Qiagen), stored on ice during transportation to the laboratory, and then frozen (−20 °C) until processing. All manipulations were carried out using sterile gloves and spoons. Samples were then delivered to the University of Geneva (Switzerland). Sediments for geochemical analyses (i.e., organic matter and trace element) were stored on ice, and another aliquot for grain size was preserved at room temperature.

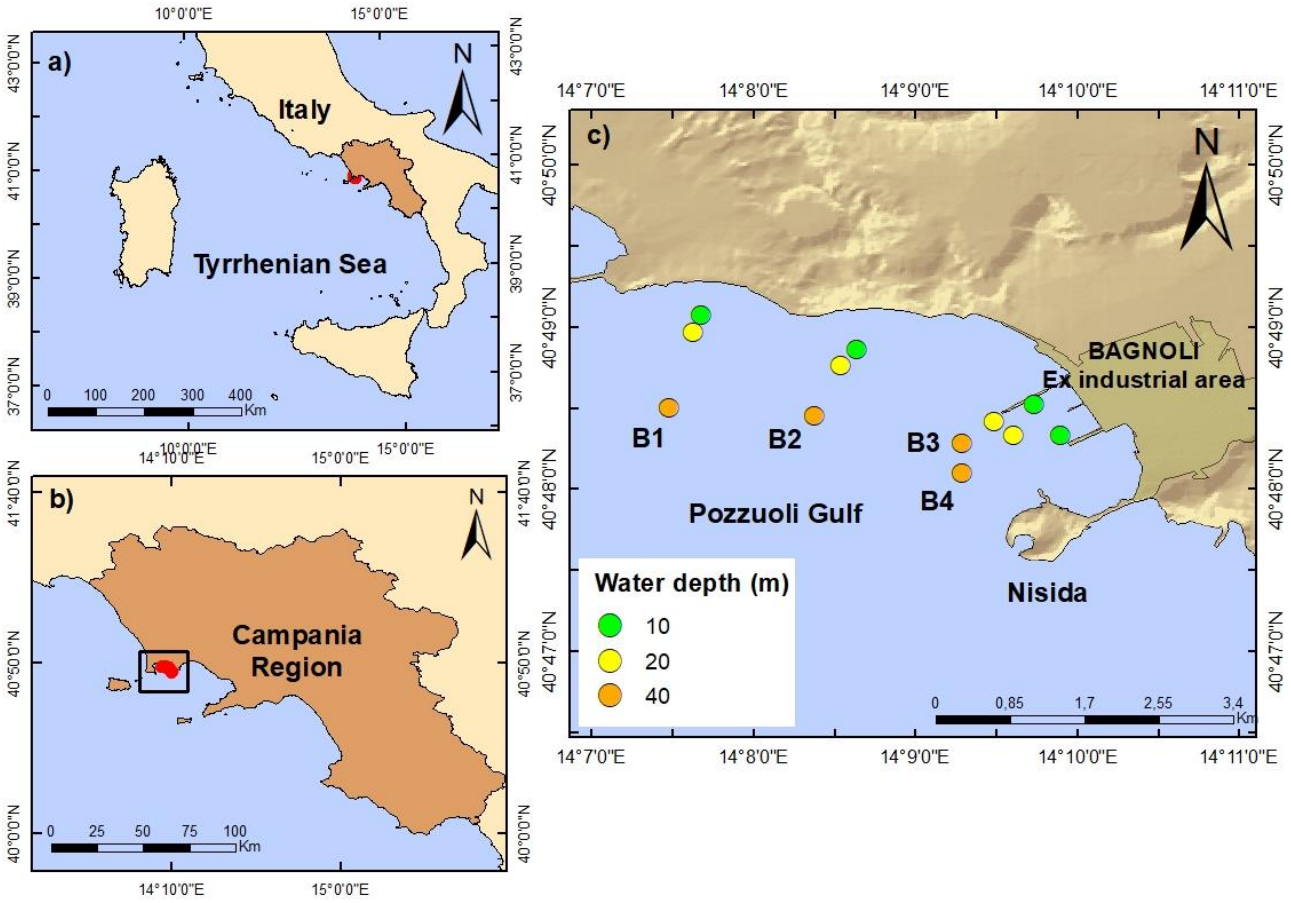

Figure 2.1. Study area: a) location of Campania Region in Southern Italy; b) location of Bagnoli area in the Campania region; c) sampling locations and relative water depth within the Pozzuoli Gulf. Geographical coordinates refer to the World Geodetic System 1984 (WGS-84).

2.3.2. Sediment analysis

2.3.2.1 Grain size

For grain-size analysis, sediment samples (~50 g) were dried and weighted. They were then wet-sieved on a 63-μm mesh sieve (sand-silt limit) and a 2-mm mesh sieve (gravel-sand limit), re-dried, and weighted. The weights of gravel, sand, and mud + silt components were then weighted, and the relative proportions were calculated for characterizing the sedimentological features of the sediment samples according to Blott and Pye, 2012.

2.3.2.2 Organic matter characterization

Sediment samples were thawed at room temperature and dried in an oven at 60 °C. They were subsequently ground and homogenized. Sub-samples were then weighed (~10–20 mg) in silver capsules and treated with 1 M HCl (three/four times) to completely remove carbonates. Total organic carbon (TOC) and total nitrogen (TN) were analyzed using a Thermo Electron Flash Elemental Analyzer (EA 1112) calibrated with acetanilide (C_8H_9ON, elemental composition: 71.09% carbon and 10.36% nitrogen) standards. The C/N ratios were calculated to investigate the origin of sedimentary organic matter (Meyers, 1994).

2.3.2.3 Inorganic geochemistry

One aliquot of sediment was used for geochemical analysis by the certified laboratory Bureau Veritas (Canada). Sediments were digested in aqua regia (1:1:1 HNO_3:HCl:H_2O) to better understand the bioavailability. Chemical analyses were performed on the fine (<63 µm) fraction because potential toxic elements (PTEs) (i.e., trace elements) are commonly adsorbed in the organic matter, which predominantly occurs in the finest sediment fractions (Baran et al., 2019). The PTE concentrations were analyzed by inductively coupled plasma-mass spectrometry (ICP-MS). Quality control involving the use of replicate and reference materials was also performed. To identify potential anthropic contributions, selected pollution indicators were computed: enrichment factor (*EF*), contamination factor (C*f*), modified degree of contamination index (mC_d), and pollution load index (*PLI*).

The *EF* defines the contamination level by minimizing the grain-size effect through the normalization of one metal concentration with respect to the concentration of a reference element. The *EF* was calculated for each of the nine selected PTEs (i.e., As, Cd, Co, Cr, Cu, Hg, Ni, Pb, and Zn) using Al as reference element. Aluminum is adopted by many authors in marine assessments (Francescangeli et al., 2020) because it is not normally influenced by anthropogenic processes. *EF* was calculated as follows (2.1):

$$EF = \frac{[X_i]/[Al_i]}{[X_0]/[Al_0]} \quad (2.1)$$

where X_i and Al_i are the concentrations of the element X and Al, respectively, in the sample i; X_0 and Al_0 are the local geochemical background concentrations of the element X and Al, respectively. The background values are based on different studies carried out near the Bagnoli area (Damiani et al., 1987; Cicchella et al., 2005; De Vivo and Lima, 2008) (Table S2.1). The *EF* levels were assigned using the classes proposed by Müller (1979) (Table S2.2).

C*f* represents the degree of sediment contamination by a single element and was calculated for the nine selected PTEs using the following equation:

$$Cf = \frac{[element]i}{[element]background} \quad (2.2)$$

mC_d represents the sum of all *Cf*s of the considered elements. It was obtained as follows (1.3):

$$mC_d = \frac{\sum_{i=1}^{i=n} C_f}{n} \quad (2.3)$$

where n is the number of analyzed elements and *i*=ith element. The categories of mC_d, from Hakanson (1980) are reported in Table S2.2.

PLI represents a synthetic parameter to evaluate the degree of contamination (Tomlinson et al., 1980). It was calculated with equation (2.4):

$$PLI = \sqrt[n]{Cf_1\ Cf_2 \dots Cfn} \quad (2.4)$$

where n is the number of potentially contaminant elements, and C*f*i is the Cf of the element.

To define the environmental quality of marine sediment, chemical concentrations of PTEs were compared with different sediment quality guidelines (Burton, 2002 for a review) (Table S2.1). The effect range median (ERM), which expresses values above which effects are frequently observed (Long and Morgan, 1990; Long et al., 1995), and the effect range low (ERL), indicating low concentrations of pollutants (O'Connor, 2004) (that is, approximately related to toxicity), were considered.

2.3.3. Benthic foraminifera

2.3.3.1 Morphological analysis

Benthic foraminiferal analyses were performed following the FOBIMO protocol (Schönfeld et al., 2012). Samples were gently washed through a 63-µm sieve to eliminate mud particles and excess staining. Residues were then oven-dried at 40 °C overnight. Because the number of living specimens was low in the >125-µm fraction, the picking was also extended to the 63–125-µm fraction. Replicates were independently processed, and the resulting picked specimens were pooled before statistical analyses. The taxonomical classification was carried out through microscopic observation following comparisons with Cimerman and Langer (1991), Sgarella and Moncharmont Zei (1993), and Milker and Schmiedl (2012). The World Register of Marine Species (Hayward et al., 2022) was followed for the systematic classification of the benthic foraminiferal species.

2.3.3.2 eDNA metabarcoding

Extraction of sedimentary eDNA was performed with a DNeasy® PowerMax® Soil Kit (QIAGEN). The eDNA extracts were concentrated with 10.4 ml of ethanol and 200 µl of NaCl as in the manufacturer's guidelines and resuspended in 400 µl of elution buffer. The eDNA extracts were then stored at -20 °C. The 37f–41f region of the 18S rRNA gene was amplified using the primer 14F1: 5'– AAGGGCACCACAAGAACGC –3' and S17: 5' – CGGTCACGTTCGTTGC – 3'. To enable the multiplexing of polymerase chain reactions (PCR) products in sequencing libraries, we used tagged primers bearing 8 nucleotides attached at each primer's 5′-extremity (Esling et al., 2015). The PCR program is detailed in S1. Per each extracted sample, three PCR replicates and one PCR-negative control were amplified. Then, the PCR products were verified through agarose gel electrophoresis. The total volume of three PCR replicates was combined to be quantified using high-resolution capillary electrophoresis (QIAxcel System, QIAGEN). The combined PCR products were pooled in equimolar concentrations and then purified using a Purification High Pure PCR Product Purification kit (Roche).

The library was prepared using a TruSeq® DNA PCR-Free Library Preparation Kit (Illumina). It was then quantified using a Kapa Library Quantification Kit for Illumina Platforms (Kapa Biosystems). Finally, the library was sequenced on a MiSeq instrument using paired-end sequencing for 2*250 cycles with kit v2.

The raw data were analyzed using the SLIM v0.4 web application (Dufresne et al., 2019). The sequences were demultiplexed with no mismatch allowed in the tagged primers (module demultiplexer). The paired-end reads were merged using a VSEARCH toolkit (Rognes et al., 2016), with a minimum overlap of 16 base pairs and 5 mismatches allowed (module mergepair-vsearch). Potential chimeras were removed using the UCHIME *de novo* algorithm (Edgar et al., 2011). All sequences with ambiguous bases were removed (module chimera-vsearch). Then, the sequences were clustered into molecular operational taxonomic units (MOTU) using a VSEARCH algorithm (Rognes et al., 2016) with a 97% similarity threshold (module out-vsearch). A MOTUs table was generated, and the representative sequences were compared to our local database using the VSEARCH toolkit and annotated if the minimum similarity between the reference and a sequence was 95%.

The raw data were submitted to the SRA public database under accession number PRJNA723313.

2.3.4. Diversity and biotic indices

For both morphological and eDNA datasets, the richness (S), dominance (D), Shannon-Weaver (H'), and equitability (J) were calculated using Past 4.0 (Hammer et al., 2001).

Four biotic indices were calculated to evaluate the EcoQS based on the morphological and eDNA data: 1) the quality index based on diversity $\exp(H'_{bc})$ (i.e., effective number of species) (Bouchet et al., 2012 for details); 2) the Foram Stress Index (FSI) based on the relative percentages of two ecological groups according to their tolerance/sensitivity to organic matter enrichment (Dimiza et al., 2016); 3) the Tolerant Species Index (TSI-Med) based on the relative proportion of stress-tolerant taxa normalized for grain size (<63 μm) (Barras et al., 2014) using the reference equation provided

by Parent et al. (2021); and 4) the Foram-AMBI, an adaptation of the macrofauna AMBI (Borja et al., 2000) to benthic foraminifera, where foraminiferal species are classified into five ecological groups (EGs) in relation to their response to organic matter enrichment (Alve et al., 2016; Jorissen et al., 2018; Bouchet et al., 2021). For TSI-Med and Foram-AMBI, we used the species list provided by Jorissen et al. (2018) for the Mediterranean coastal environments. The categorizations to assess the EcoQS are reported in Table 2.1.

For the eDNA data, exp(H'$_{bc}$) and Foram-AMBI are referred to as g-exp(H'$_{bc}$), and g-Foram-AMBI, respectively, and were calculated. The EcoQS class boundaries have not been defined yet for the g-exp(H'$_{bc}$). Because the molecular diversity is much higher than the morphological one, class boundaries developed for morphological datasets (Bouchet et al., 2012) cannot be applied. Therefore, an attempt was made using the ecological quality ratio (EQR), as suggested in the WFD (WFD, 2000/60/EC). The EQR is the ratio between the value of a biological metric, such as g-exp(H'bc), and the expected value under reference conditions (van de Bund and Solimini, 2007). The EQR varies, therefore, between 0 (i.e., bad EcoQS) and 1 (i.e., high EcoQS). Local-specific reference conditions are the anchor point to calculate the EQR; here, we use the sites (B1–20 and B2–20) with lowest deviance from reference conditions to define the boundaries for the five classes of EcoQS (Table 2.1).

Because not all of the MOTUs could be identified at species level, and/or only 70 MOTUs are assigned to an ecological group, in the present study, we computed the g-Foram-AMBI by assigning MOTUs to EGs following the method proposed by Bouchet et al. (2021). Although some of the MOTUs could have been assigned to EGs based on previous studies (e.g. Jorissen, 2018; Keeley et al. 2018), the number of these assigned species was too low to evaluate reliably the EcoQS using AMBI. As matter of fact, this work constitutes the first attempt of using g-Foram-AMBI for the assessment of EcoQS. Previous works have been principally referred to other taxonomical groups (e.g. Aylagas et al., 2014; macrofauna). Specifically, the weighted averaging (WA) optimum and tolerance to TOC content were calculated for each MOTU using the R Software Analogue package

(Simpson and Oksanen, 2020). The estimated optimum provides an effective evaluation of the MOTUs' environmental requirements. According to Birks et al. (1990), the WA optimum method is a rapid, easy, and reliable tool to define the species-specific (i.e., MOTUs) indicative values. Afterwards, MOTUs' assignment to EGs was performed as follows: if a MOTU had an optimum in the TOC range 0–2%, it was assigned to EGI; in the range 2–2.5%, 2.5–3.4%, 3.4–4.1%, and above 4.1%, it was assigned to EGII, EGIII, EGIV, and EGV, respectively (see more details in Bouchet et al., 2021).

Index	**Ecological Quality Status**				
	High	**Good**	**Moderate**	**Poor**	**Bad**
exp(H'bc)	<20	15-20	10-15	5-10	<5
FSI	9-10	5.5-9	2-5.5	2-1	<1
TSI-Med	<4	4-16	16-36	36-64	>64
Foram-AMBI	<1.2	1.2-3.3	3.3-4.3	4.3-5.5	>5.5
Foram-AMBI*and g-Foram-AMBI*	<0.9	0.9-1.8	1.8-3.2	3.2-5	>5
g-exp(H'bc)*	>105	105-88	88-65	65-35	<35

Table 2.1. Indices categorization to assess the ecological quality status: Tolerance Stress Index-Med (TSI-Med; Barras et al., 2014; Parent et al., 2021), exp(H'bc) (Bouchet et al., 2012), Foram Stress Index (FSI; Dimiza et al., 2016), Foram-AMBI (Borja et al., 2003) *Foram-AMBI, *g-Foram-AMBI (Parent, 2019), and *g-exp(H'bc) (present paper).

To compare the agreement/disagreement among biotic indices in assessing EcoQS, two EcoQS (i.e., 'Acceptable' or 'Not acceptable') were considered, following Blanchet et al. (2008). The 'Acceptable' results from High or Good EcoQS and scores as 1, whereas 'Not acceptable' from Moderate, Poor, or Bad EcoQS and scores as 0 (Blanchet et al., 2008; Bouchet and Sauriau, 2008). Then, the scores were summed for any station that reflected the level of agreement/disagreement of the biotic indices and categorized (i.e., full agreement 0/7 or 7/7, partial agreement 1/7, 2/7, 5/7 or 6/7, and disagreement 4/7).

2.3.5. Statistical analyses and spatial distributional maps

Before performing statistical analyses, the three replicates of each station were pooled for both morphological and molecular datasets. For the morphological dataset, only species with a relative abundance of > 5% in at least one sample were considered for multivariate statistical purposes. The molecular dataset was filtered considering only MOTUs represented by > 100 reads in at least one sample.

A chord diagram was plotted to show the variations in the foraminiferal taxonomic composition among the stations for both morphological and molecular datasets. This diagram was computed using R software and the Circlize package (Gu et al., 2014). A Mantel's test (999 permutations) was performed to test the significance of Spearman's correlation between the relative abundances of morphological foraminiferal species and eDNA MOTUs dissimilarity matrices (Bray-Curtis) using the R Package Vegan (Oksanen et al., 2019). To observe the capability of foraminiferal-based biotic indices to reflect the ecological quality, a Spearman's rho matrix of correlation was computed considering *PLI*, TOC, and biotic indices (for both morphological and molecular datasets) using the R package PerformanceAnalytics (Peterson et al., 2020). Prior to statistical analyses, all biotic and abiotic data were log-normalized. A Q-mode cluster analysis (CA), based on environmental variables and geochemical indices (i.e., *EF*s, TOC, C/N, mud, *PLI*, and mC_d) using Ward's linkage method and the Euclidean distance was carried out. Principal component analyses (PCAs) were also performed considering environmental variables and geochemical indices as primary variables and the foraminiferal relative abundance from both morphological datasets and molecular ones (unassigned and assigned MOTUs) as secondary variables. The PCA does not include the EFs to simplify the plot as the degree of contamination is underlined by the PLI. The PCA and CA were performed using the software STATISTICA 13.5.

The distributional maps were generated using the software ArcMap 10.5 (Esri). For plotting the abiotic factors and geochemical indices, the inverse distance weighted (IDW) method was used to interpolate the data. This method is fast and easy to compute and interpret (Lu and Wong, 2008). The

IDW interpolation method was also adopted for creating maps showing the spatial distribution of the biotic indices.

2.4. Results

2.4.1. Environmental characterization

The grain-size analysis revealed that in the study area, most of the sea bottom is composed of sand. The sandy fraction varies from 71.7 to 95.5%, whereas the mud content (<63 μm) ranges from 0.10 to 27.2% (Fig. 2.2a,b, Tables S2.3–4). A clear increase of the mud fraction was found seaward, with all stations at 40 m exhibiting the highest values, particularly in transects B3 and B4 (Fig. 2.2a). This trend was more evident along transects B3 and B4 in front of the former industrial plant. Indeed, these transects showed higher values of mud than transects B1 and B2. The TOC content ranged between 0.1 and 20.3%. The highest percentages of TOC were found in transect B3, particularly at 20 and 40 meters depth (Fig. 2.2c, Table S2.3). In the external area, the TOC values strongly decreased compared to B3 stations and ranged from 0.1 to 0.7%. The C/N ratios varied from 5 to 52.5, with the highest values associated with the area in front of the ex-industrial plant (Fig. 2d).

The concentrations of PTEs varied substantially in the study area (Fig. 2.3a–d, Table S2.3). In particular, Pb and Zn ranged between 31 and 322 mg/kg and 102 and 795 mg/kg, respectively. The highest values of As (19–84 mg/kg) and Hg (41–728 ng/kg) were found at stations along transects B3 and B4. The *EF*s of Pb (0.55–7.27) and Zn (0.69–5.79) were constantly higher than 4 at stations in front of the former industrial area (Fig. 2.3c, d). A similar trend was observed for the *EF*s of As (0.58–3.17) and Hg (0.18–3.07) (Fig. 2.3a,b).

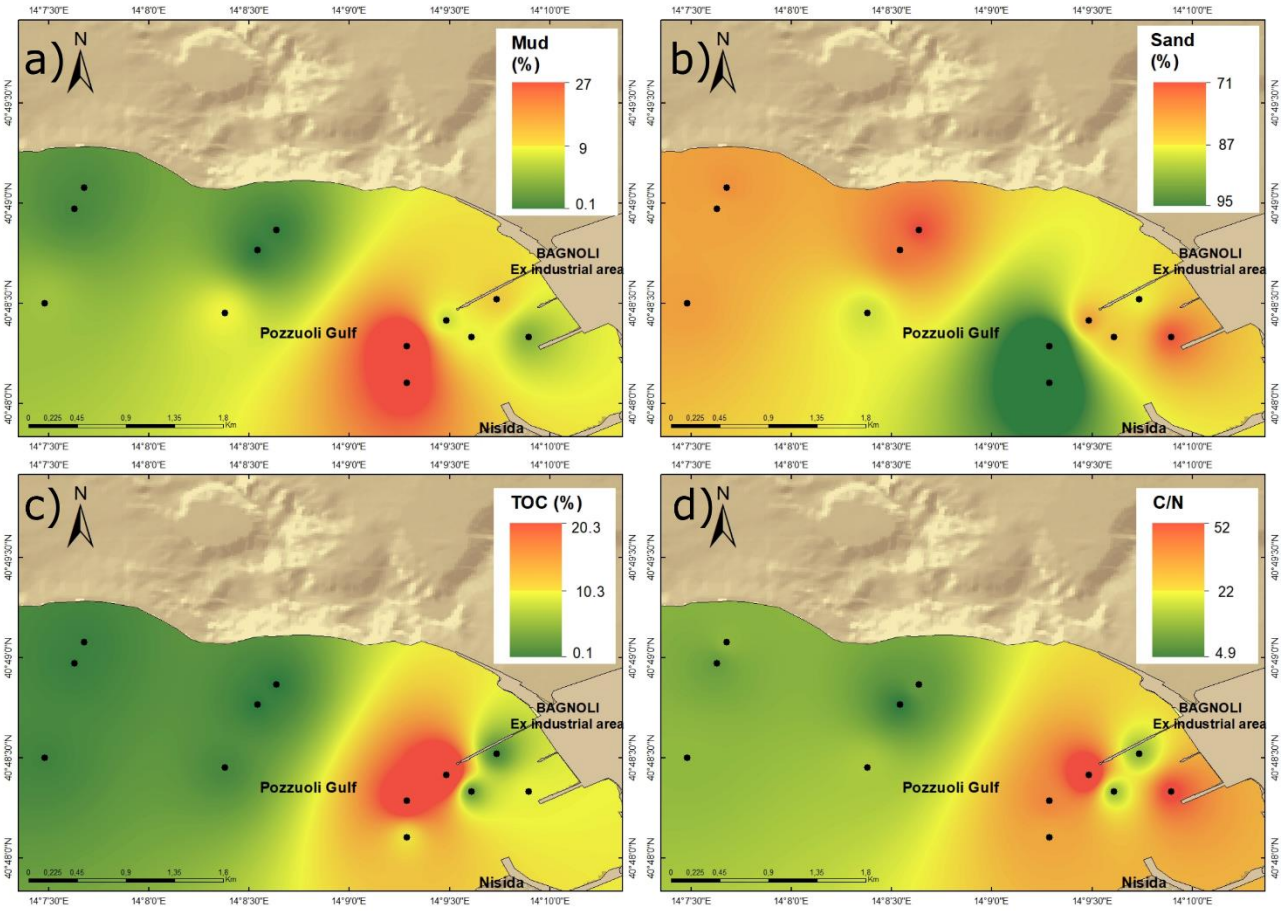

Figure 2.2. Spatial plots of a) mud content (%); b) sand content (%); c) total organic carbon (TOC) (%); and d) C/N ratio.

In Bagnoli, the detected concentrations of selected elements (i.e., As, Hg, Pb, and Zn) were above the ERM and the ERL in several stations. In particular, As and Hg concentrations were higher than the ERL at 8 stations (Table S2.1), whereas Pb showed concentrations up to 3 times higher than the ERM in the entire internal area (B3 and B4 transects; 6 stations) and above the ERL at the other 5 stations (Table S2.1). The concentration of Zn was two times higher than the ERM at 6 stations along the transects B3 and B4, and higher than the ERL at the other 4 stations (Table S2.1).

The mC_d showed very low values along transects B1 and B2, whereas the highest values were found along transects B3 and B4 (3.98 and 4.14, respectively) at 40-m depth (Fig. 2.3e). The *PLI* varied from 0.61 to 1.22 (Fig. 2.3f). All stations along transects B3 and B4 showed *PLI* values greater than 1, and the highest values were associated with the deepest stations. Based on the Q-mode CA, two main clusters (I and II) and two subclusters (IIa and IIb) could be identified (Fig. S2.1). Cluster

I was represented by stations along transects B1 and B2, whereas Cluster II groups stations belonged to transects B3 and B4. Sub-cluster IIa includes all shallower stations (i.e., 10- and 20-m water depth), whereas sub-cluster IIb only stations at 40 m.

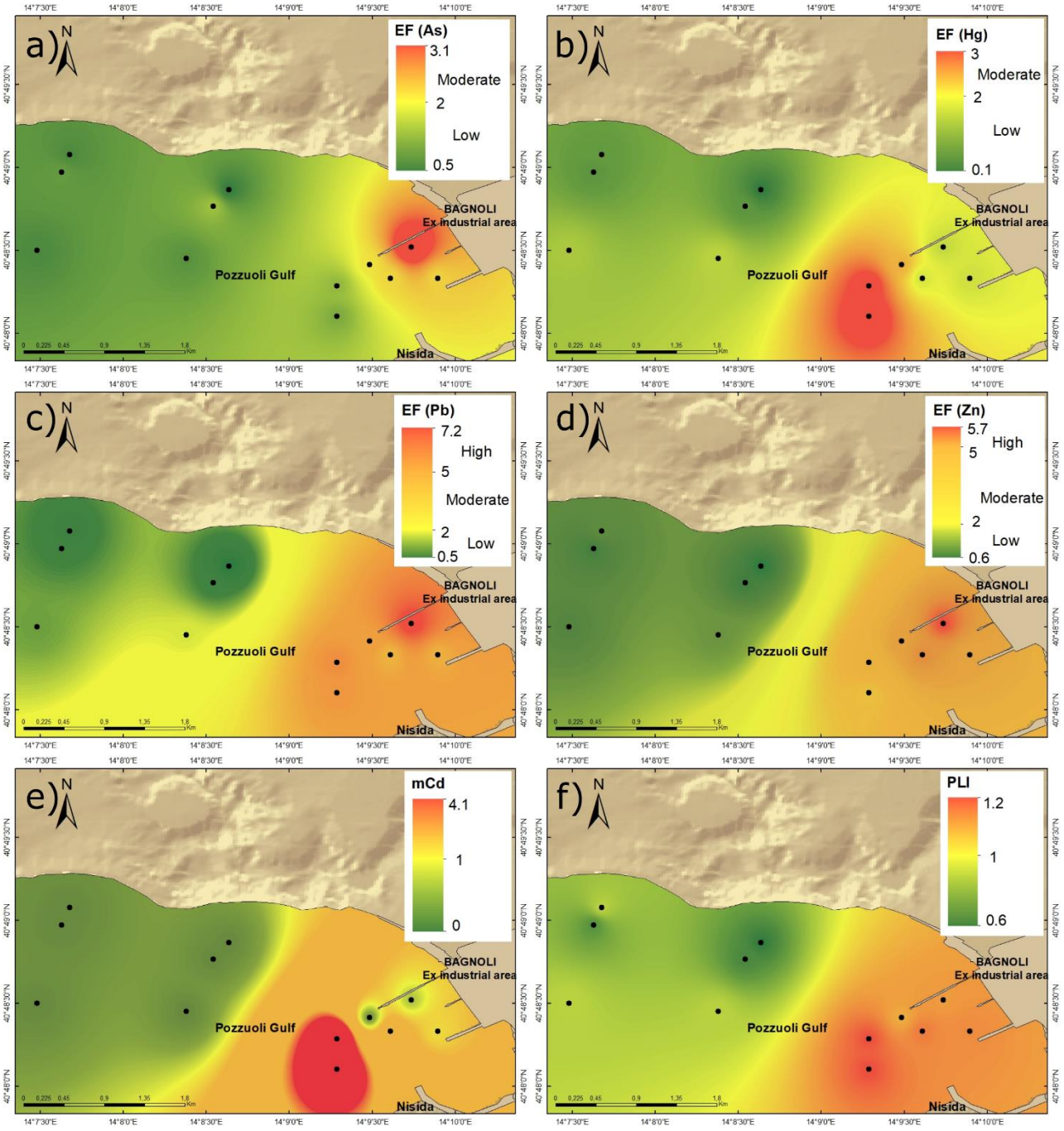

Figure 2.3. Spatial plots of a) enrichment factor of As; b) enrichment factor of Hg c) enrichment factor of Pb; d) enrichment factor of Zn; e) modified contamination degree (mCd); and f) pollution load index (PLI).

2.4.2. Benthic foraminifera

2.4.2.1 Morphological dataset

Overall, 57 species (4 agglutinated, 6 porcelaneous, and 47 hyaline) belonging to 36 genera were identified. The specific richness (S) values ranged between 11 and 30 (18.4, on average) with relatively higher values along external transects B1–B2 (19.7, on average) than along B3-B4 (17.1, on average). The H values (1.66–2.76) showed a clear difference between transects B1–B2 and B3–B4; in particular, the lowest values of H were recorded in stations along transects B3 and B4 (Table S2.5).

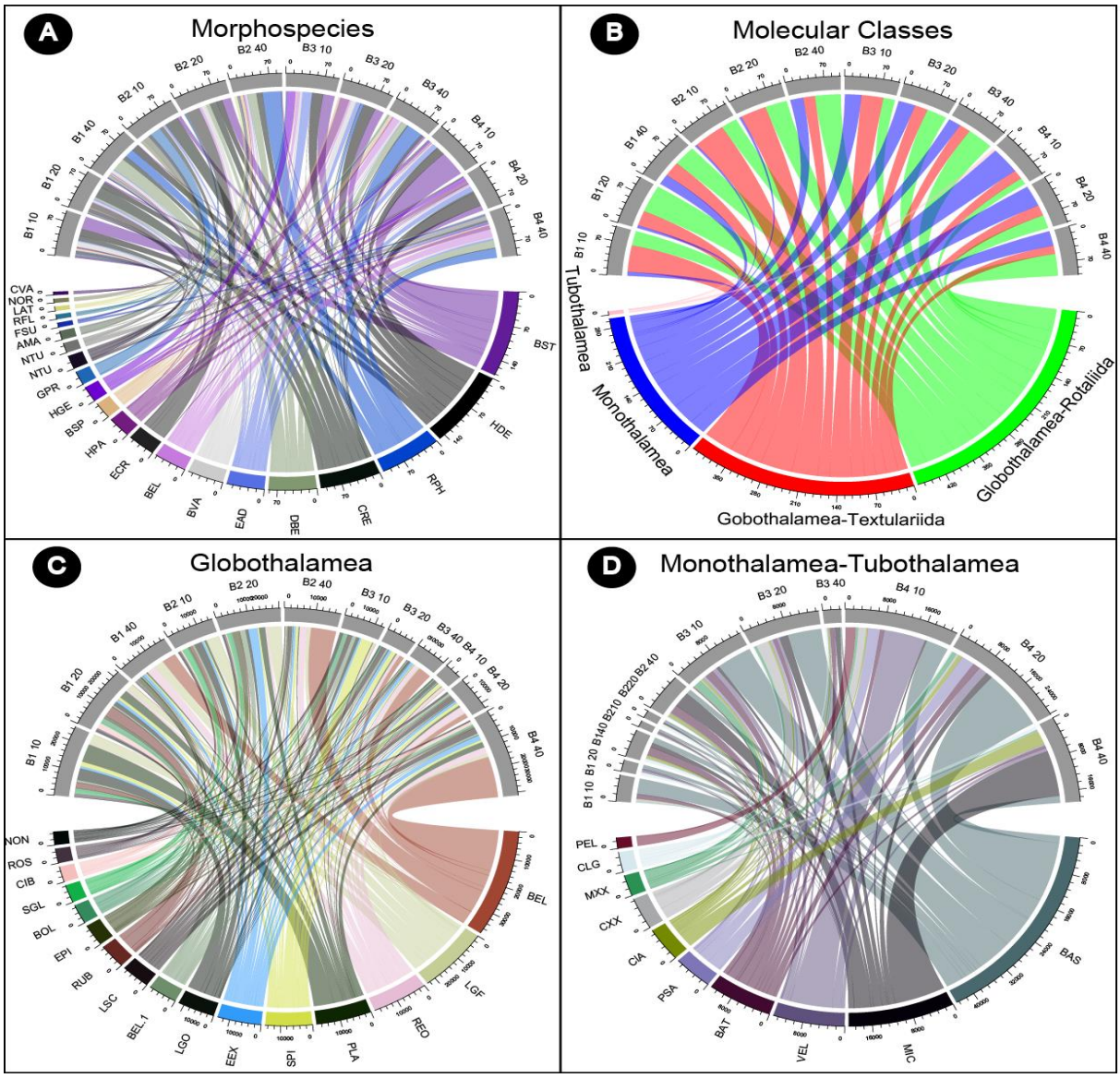

Figure 2.4. Chord diagram based on a) morphospecies and the eDNA dataset: b) molecular classes; b) Globothalamea; and d) Monothalamea-Tubothalamea; the top part shows the stations, whereas the lower part refers to morphospecies and MOTUs. A complete list of abbreviations is reported in Table S2.9.

The most abundant (%) species were *Bolivina striatula* (14.2% on average), *Haynesina depressula* (12.3% on average), *Rectuvigerina phlegeri* (9.3% on average), *Cibicidoides refulgens* (9.0% on average), *Discorbinella berthelotiana* (7.2% on average), *Elphidium advenum* (5.6% on average), *Bolivina variabilis* (5.4% on average). Some taxa, namely *B. striatula, H. depressula, E. advenum, B. elongata, H. pacifica*, and *H. germanica* exhibited a higher abundance at stations along transects B3 and B4 compared to those of B1 and B2, whereas an opposite trend was found for *C. refulgens, D. berthelotiana, E. crispum, G. praegeri, R. bradyi*, and *A. mamilla* (Fig. 2.4a).

2.4.2.2 eDNA dataset

The total number of raw sequences was 17,857,602, from which 5,112,227 were retained in the downstream analysis after stringent quality filtering. Overall, 12,400 MOTUs were produced by the VSEARCH clustering algorithm. This number was reduced to 1134 by removing MOTUs represented by less than 100 reads and combining the MOTUs assigned to the same morphospecies. Among them, 1061 were unassigned, whereas 44 MOTUs were represented by the multichambered calcareous or agglutinated Globothalamea, 27 MOTUs by single-chambered, organic-walled, or agglutinated Monothalamea, and only two MOTUs by Tubothalamea. The number of reads per sample (i.e., the pooled replicates per station) varied from 320178 to 597844. The richness (S) ranged between 426 and 751 (567, on average), with higher values along external sites (583, on average) than along transects B3 and B4 (552, on average) (Table S2.6). The Shannon-Weaver (H; 3.1-4.8) showed a clear difference between transects B1–B2 (4.45) and B3–B4 (3.89). The highest values of D and the lowest values of H and J were associated with the stations along transects B3 and B4 transects.

The assigned MOTUs were mostly represented by monothalamous taxa. The most common (%) monothalamous species were *Bathysiphon* sp. (1.1% on average), *Micrometula* sp. (0.5% on average), *Vellaria* sp. (0.4% on average), *Bathysiphon* (0.3% on average), *Psammophaga* sp. (0.2% on average), and *Cylindrogullmia alba* (0.2% on average), whereas the most common MOTUs

assigned to Globothalamea were *Bulimina elongata* (0.8% on average), *Reophax* sp. (0.4% on average), *Spiroplectammina* sp. (0.3% on average), *Liebusella goesi* (0.2% on average), *Planorbulinella* sp. (0.2% on average), *Buliminella elegantissima* (0.2% on average), *Leptohalysis scotti* (0.2% on average), *Epistominella* spp. (0.1%), *Cibicidoides* (0.08 % on average) and *Rosalina* sp. (0.07% on average) (Fig. 2.4b). The most abundant (>1 %) unassigned MOTUs, in order of decreasing reads, were 2 (6.9% on average), 1(5.8% on average), 0 (5.8(% on average), 7 (2.6% on average), 8 (2.4% on average), 4 (2.3 % on average), 6 (1.6% on average), 33 (1.3 % on average), 39 (1.3 % on average), 3 (1.1 % on average), 15 (1.1% on average), 34 (1.1 % on average) and 5 (0.6% on average). The change in diversity indices values with respect to the transects B1–B2 and B3–B4 was also reflected in the taxonomic composition of foraminiferal assemblages in terms of MOTUs. Accordingly, the transects B1–B2 showed a higher relative abundance (5.7% B1–B2 *vs*. 4% B3–B4) of MOTUs assigned to Textulariida, whereas those belonging to Monothalamea exhibited a higher relative abundance (1.4% B1–B2 *vs*. 3.5% B3–B4) along transects B3–B4 located in front of the former industrial site (Fig. 2.4b). MOTUs assigned to Globothalamea did not exhibit significant changes across transects, but a clear increase in their abundance was related to depth (Fig. 2.4c). Indeed, some MOTUs (i.e., *Bathysiphon* sp., *B. elongata*, *Micrometula* sp., *Reophax* sp., *Spiroplectammina* sp., *Vellaria* sp., *L. scottii*, *Psammophaga* sp., *C. alba*, *Eggerelloides*, and Monothalamea Clade A) showed a higher number of reads in stations at transects B3 and B4, whereas an opposite trend was found for Textulariida, Rotaliida, *L. goesi*, *Planorbulinella* sp., *Rosalina* sp., *B. elegantissima*, *Cibicidoides*, and *Glabratellina* sp. (Fig. 2.4c,d).

2.4.3. Relationship between environmental parameters and benthic foraminifera

Mantel's test showed a significant positive correlation ($r = 0.7$; p-value < 0.001) between the molecular and morphological dissimilarity matrices. In the PCA, the first two axes explained ~90.6% of the total variance (Fig. 2.5). The environmental parameters and geochemical indices were strongly

related to axis 1. On the basis of the PCAs, *PLI*, mC_d, TOC, C/N, and mud, were strongly related to the first axis that can, therefore, be interpreted as the environmental stress (ES) component.

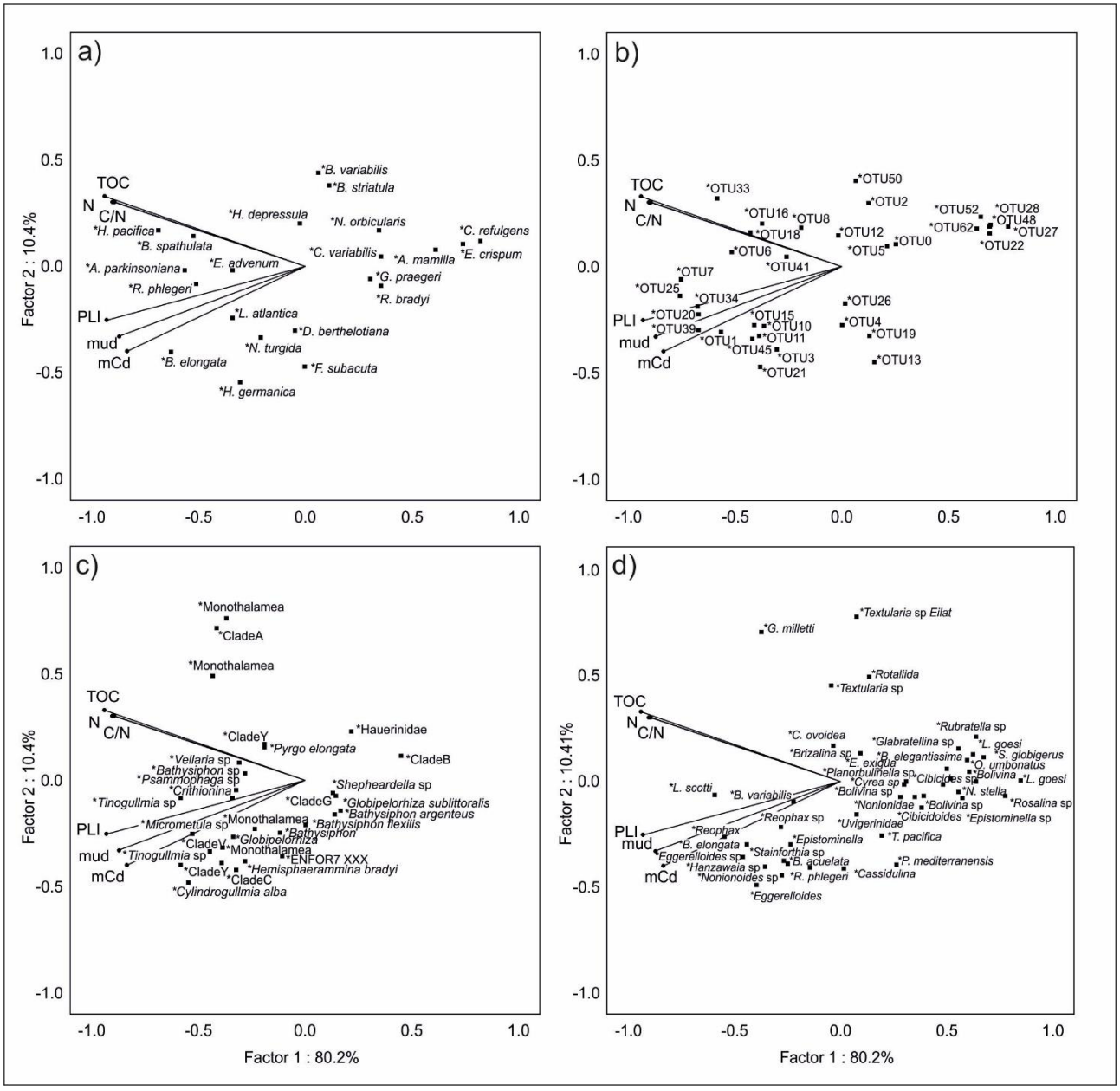

Figure 2.5. PCA diagram based on environmental parameters and a) morphospecies, b) unassigned OTUs > 5%, c) assigned Monothalamea, and d) assigned Globothalamea. Secondary variables are marked with an *.

Some morphospecies (i.e., *B. elongata, N. turgida, H. pacifica, B. spathulata*, *A. parkinsoniana*, *R. phlegeri*, and *E. advenum*) were negatively related to first component (Fig. 2.5a). An opposite trend was found for *E. crispum*, *C. refulgens*, *A. mammilla*, *C. variabilis*, *R. bradyi*, and *G. praegeri*. The unassigned MOTUs (i.e., 7, 25, 34, 20, 39, 1, 6, and 33) and MOTUs assigned to Monothalamea

(i.e., *Tinogullmia* sp., *Micrometula* sp., *C. alba, Vellaria* sp., *Psammophaga* sp., *Bathysiphon* sp., and Clade V) and Globothalamea (i.e., *L. scottii, Reophax, B. elongata, Eggerelloides* sp., *Nonionoides* sp., and *Stainforthia* sp.) were negatively related to the first component (Fig. 5b–d). On the other hand, the unassigned MOTUs (i.e., 52, 62, 28, 48, 27, and 22) and MOTUs assigned to Monothalamea (i.e., Clade B, Clade G, *Globipelorhiza sublittoralis*, *Shepheardella* sp., and *Bathysiphon argenteus*), Tubothalamea (Hauerinidae), and Globothalamea (i.e., *L. goesi*, Textulariida, *O. umbonatus*, *Rosalina* sp., *Epistominella* sp., *Cibicidoides* and *Cibicides* sp.) were positively related to the first component (Fig. 2.5b–d).

2.4.4 Biotic indices

The exp(H'_{bc}) based on morphospecies varied from 26.7 (station B1–20) to 8.2 (station B1–10) (Table 2.2). EcoQS ranged between excellent and poor, without showing a clear trend in the study area. For FSI, TSI-Med, and Foram-AMBI, the percentage of assigned species to EGs was higher than 80%. The FSI values varied from 2 to 9.1, with higher values at stations along transects B1–B2 (5.9 ± 2.0%) than the ones along B3–B4 transects (2.9 ± 0.6%). EcoQS varied from excellent and moderate in transects B1–B2 and from moderate to poor in B3–B4 (Table 2.2). The values of TSI-Med varied from 4.2 to 79.8%, with markedly higher values (50.1 ± 22.5%) along transects B3 and B4 than transects B1 and B2 (42 ± 21%) (Table 2.2). EcoQS varied from good to poor along transects B1 and B2, whereas it was persistently bad along transects B3 and B4. The Foram-AMBI ranged from 0.35 to 2.4 with a similar trend of TSI-Med. The relative EcoQS ranged between excellent and good in transects B1–B2 and good in B3–B4 (Table 2.2). Because this result overestimated the EcoQS in the study area, the new boundary classes (Foram-AMBI*) proposed by Parent (2019) were considered (Table 2.1). On the basis of the new boundary classes definition, EcoQS ranged from excellent to good along transects B1 and B2 and from good to moderate along transects B3 and B4 (Table 2.2).

Indexes	exp(H'bc)	FSI	TSI-Med	Foram-AMBI	Foram-AMBI*	g-exp(H'bc)*	g-Foram-AMBI*	g-Foram-AMBI-MOTUs*	Sum of score/indexes	Interpretation
B1_10	12.8	4.2	47.5	1.5	1.5	93.6	1.8	1.3	4/7	disagreement
B1_20	26.7	7.3	19.7	0.7	0.7	80.8	1.9	1.9	3/7	disagreement
B1_40	14.2	4.6	44.9	1.2	1.2	57.5	4.1	1.8	1/7	partial
B2_10	8.2	9.1	4.2	0.4	0.4	121.9	1.5	0.4	6/7	partial
B2_20	8.7	6.0	30.8	1.0	1.0	117.3	2.2	1.1	4/7	disagreement
B2_40	17.6	3.9	48.5	1.6	1.6	61.7	5.1	2.8	2/7	partial
B3_10	10.4	3.0	67.4	2.1	2.1	56.5	4.9	3.7	0/7	full
B3_20	9.8	2.0	72.6	2.2	2.2	37.1	5.6	4.9	0/7	full
B3_40	11.0	3.1	63.9	2.1	2.1	21.8	5.4	5.5	0/7	full
B4_10	9.0	2.2	79.8	2.4	2.4	58.5	5.6	4.8	0/7	full
B4_20	15.6	3.3	64.7	1.8	1.8	63.7	5.4	3.8	1/7	partial
B4_40	11.2	3.6	57.1	1.7	1.7	81.1	5.2	4.5	1/7	partial
Spearman's rho correlation to ES	-0.05	**0.83**	**-0.79**	**-0.82**	**-0.82**	**0.69**	**-0.86**	**-0.95**	Full: 4/12 - Partial: 5/12 - Disagreement: 3/12	Full: 33.3% - Partial: 41.7% - Disagreement: 25%
p. level	0.880	0.001	0.001	0.001	0.001	0.013	0.000	0.000		

Table 2 2. Ecological quality status calculated on the selected indices (see Table 2.1 for categorization). Spearman's rho correlation coefficients between indices and environmental stress (ES that is the scores of PCA1) are also reported. Bold values p. <0.05. The sum of the score agreement (acceptable: high or good EcoQS scored as 1 and not acceptable:

moderate-to-bad EcoQS scored as 0) is reported with the interpretation of the agreement (i.e., full 0/7 or 7/7, partial 1/7, 2/7, 5/7 or 6/7, and disagreement 4/7).

The g-exp(H'_{bc}) (i.e., based on eDNA) varied from 21.8 (station B3–40) to 121.9 (station B2–10) with comparatively much higher values in transects B1–B2 (88.8 ± 27) than B3–B4 (53.1 ± 21) (Table 2.2). EcoQS varied from excellent and moderate in transects B1–B2 and from moderate to bad in transects B3–B4. Two g-Foram-AMBI were calculated: the first was based on only assigned MOTUs (g-Foram-AMBI), whereas the second one (g-Foram-AMBI-MOTUs) considered all MOTUs regardless of their assignment (Tables S2.7–8). The g-Foram-AMBI and g-Foram-AMBI-MOTUs varied between 1.5 (station B2–10) and 5.6 (stations B3–20 and B4–10) and 0.4 (station B2–10) and 5.5 (station B3–40) (Table 2.2). For g-Foram-AMBI, EcoQS varied from good and bad in transects B1–B2 and from poor to bad in transects B3–B4. For g-Foram-AMBI-MOTUs, EcoQS varied from excellent to moderate in transects B1–B2 and from moderate to bad in B3–B4 (Table 2.2). These two indices were significantly and positively correlated (r= 0.92, *p*-value < 0.001). They showed a clear trend towards higher values in all sites in front of the former industrial plant, where values were constantly higher than 3.7 and 4.9 for g-Foram-AMBI and g-Foram-AMBI-MOTUs, respectively.

Spearman's rho matrix of correlation highlighted the significant correlations between *PLI* and all ecological indices, except for exp(H'_{bc}) (Fig. 2.6). Similarly, TOC had a significant correlation with all different indices except for exp(H'_{bc}). In particular, the Foram-AMBI, TSI-Med, g-Foram-AMBI, and g-Foram-AMBI-MOTUs were positively correlated with *PLI* (r= 0.76, 0.75, 0.83, 0.78, respectively) and TOC (r= 0.87, 0.85, 0.97, 0.91, respectively). On the other hand, FSI and g-exp(H'_{bc}) were negatively correlated to *PLI* (r= -0.74 and -0.51, respectively) and TOC (r= -0.90 and -0.74, respectively) (Fig. 2.6). Indeed, the ecological indices were plotted and correlated to the ES (Fig. 2.7 and Table 2.2). All ecological indices, except exp(H'_{bc}), were significantly correlated to the ES. The highest correlations were found between the ES and g-Foram-AMBI (r=-0.95) and g-Foram-AMBI-MOTUs (r=-0.86) (Table 2.2).

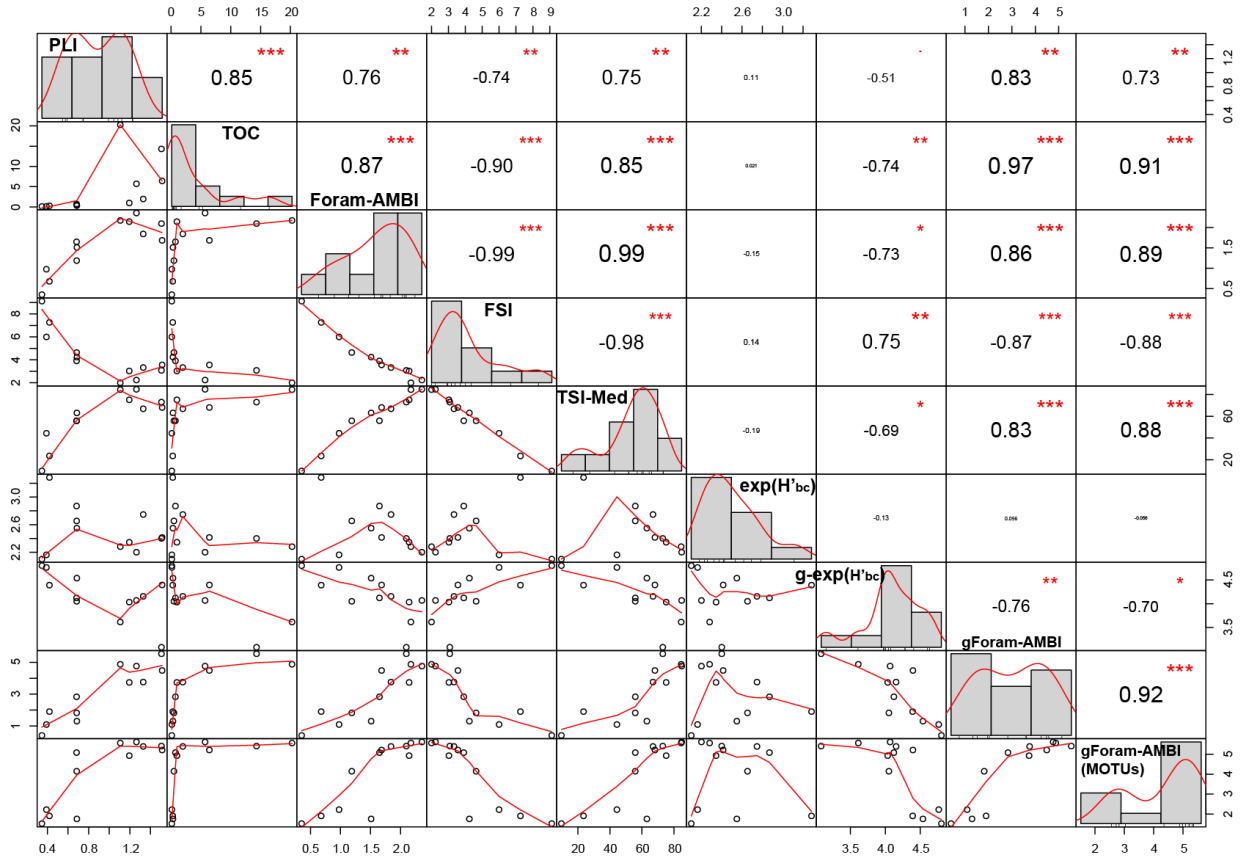

Figure 2.6. Spearman's rho matrix of correlation between environmental parameters (i.e., PLI and TOC) and biotic indices (i.e., Foram-AMBI, FSI, TSI-Med, exp(H'bc), g-exp(H'bc), g-Foram-AMBI, and g-Foram-AMBI MOTUs). The distribution (histogram) of each variable is shown on the diagonal. On the bottom of the diagonal, the bivariate scatter plots with a fitted line are displayed. On the top of the diagonal, the Rho values and the relative p-values are provided. Significance levels are reported as stars: 0.001, 0.01, 0.05, 0.1, 1 <=> "***", "**", "*", ".", " ".

2.5. Discussion

2.5.1 Environmental characterization of the SIN of Bagnoli

On the basis of our geochemical analyses, very high concentrations of several PTEs (i.e., As, Hg, Pb, and Zn) were identified in the Bagnoli area, particularly in front of the former industrial plant. The spatial distribution of As, Hg, Pb, and Zn matched well with previous assessments in the area (i.e., Romano et al., 2009, 2018; Trifuoggi et al., 2017; Sprovieri et al., 2020). The distribution of *PLI* values indicated a low level of pollution in the area corresponding to transects B1 and B2 (Fig. 2.2). Values above 1 have been constantly found along transects B3 and B4, defining the area as polluted (i.e., Jahan and Strezov, 2019). The mC_d distribution highlights a clear separation between

the northern area (transects B1 and B2), where a low degree of contamination occurs, and the stations along the transects B3 and B4 characterized by a low to high (B4 at 40 m) mC_d. The separation is also supported by the Q-mode CA. The pollution level appears to be influenced by the distance from the ex-industrial area and depth (i.e., increasing toward the deeper stations) (Fig. 2.2). This increase can be ascribed to the sediment characteristics, such as mud and organic matter contents (Savvides et al., 1995). In fact, the highest values of mC_d and *PLI* recorded at 40 m of depth, between the two piers, are probably linked to the higher content of mud and organic matter that are capable of adsorbing PTEs. The C/N ratio is commonly used as a proxy to distinguish the source of organic matter in marine environments (Gordon and Goni, 2003), where values higher than 20 are likely associated to a terrestrial source of organic matter (Meyers, 1994). In the study area, the C/N ratio was extremely high in the marine sediments, particularly in all stations along transects B3 and B4 40 m depth in front of the Bagnoli ex-industrial area (B3 and B4 transects), suggesting a probable terrestrial carbon input and/or a significant contamination by hydrocarbons (with a highly unbalanced C/N ratio).

Following the PCA score plot representing the ES (Fig. 2.7a), it is clear that the most stressful conditions occur in the area in front of the former industrial plant (i.e., B3 and B4 transects), and the stations that are, therefore, most polluted are B3–20, B3–40, and B4–40 m. On the other hand, the lowest ES was found in the northern area (B1 and B2) with the highest score values at shallower stations (i.e., 10 and 20 m). The marine sediments along transects B3 and B4 are affected by the continental source of pollution from the former plant area. Indeed, the trace elements are mobilized from the Bagnoli plain (i.e., ex-plant soils) and transported westward toward the deeper sea sediments along an axis that is parallel to the northern pier (Trifuoggi et al., 2017; Sprovieri et al., 2020). This process ultimately promotes the accumulation of PTEs at 40-m-water-depth stations at transects B3 and B4. Although the northern area (transects B1 and B2) was identified as relatively low to not polluted, minor contamination input may affect the marine sediments due to a secondary current circulation from the former plant toward the NW (Sprovieri et al., 2020). According to this model,

sediments of the transects B1 and B2 at a 40-m depth could also be affected by the same source of contamination of transects B3 and B4 but to a lesser extent.

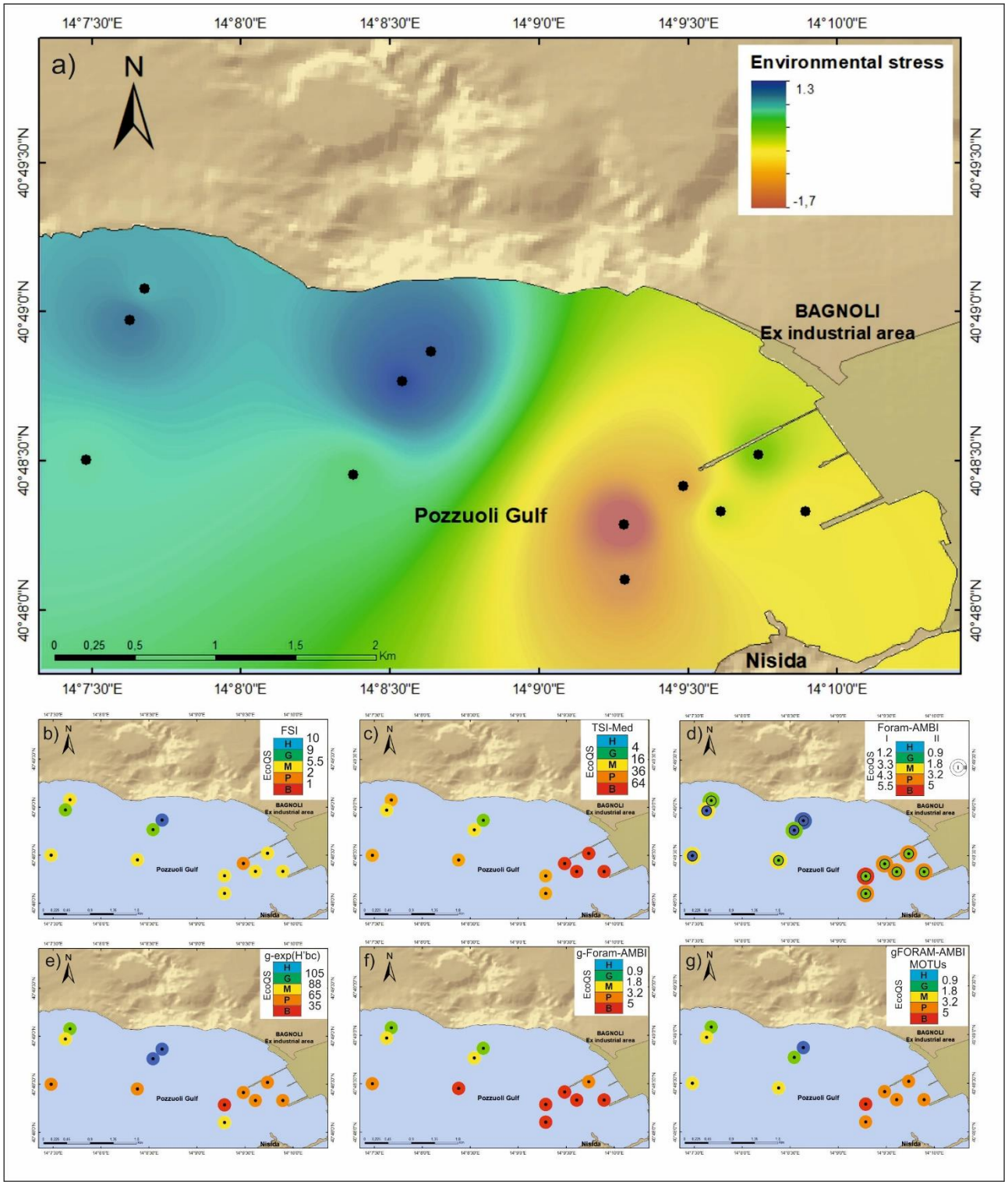

Figure 2.7. Spatial plots of a) environmental stress (ES) based on PCA first axis scores, b) Foram Stress Index (FSI), c) Tolerance Stress Index (TSI-Med), d) Foram-AMBI, e) g-exp(H'bc), f) g-Foram-AMBI, and d) g-Foram-AMBI MOTUs. The ecological quality status categorizations are also reported following Table 2.1. Two categorizations I and II are provided for Foram-AMBI based on Borja et al. (2003) and Parent (2019), respectively.

2.5.2 Foraminiferal metabarcoding vs. morphology

2.5.2.1 Congruent trend of diversity metrics

The clear separation between the B1–B2 transects (low- to unpolluted) and B3–B4 ones (highly polluted) based on environmental parameters (Fig. S2.1) was also reflected in benthic foraminiferal assemblages of both the molecular and morphological datasets. Accordingly, lower values of diversity (i.e., H and S) were recorded in front of the former industrial site that results as the most polluted area. A decrease in morphospecies' foraminiferal diversity is commonly associated with stress conditions (i.e., unstable physico-chemical parameters of water, oxygen deficiency, pollution) (e.g., Alve, 1995). Similarly, a lowering of MOTUs diversity has been associated with deteriorating environmental quality in response to fish farming (Pawlowski et al., 2014a; Pochon et al., 2015), gas and oil drilling activities (Laroche et al., 2016, 2018), and gas platforms (Cordier et al., 2019; Frontalini et al., 2020). In our study, the decrease in diversity values identified in the morphological dataset was also recognized in the molecular one that it is also more evident. In particular, the more pronounced reduction of diversity (i.e., exp (H'_{bc})) in the molecular dataset can be ascribed to the higher number of MOTUs compared to the number of morphospecies in the morphological one. In fact, the molecular dataset includes soft-shelled (i.e., naked monothalamids) species that are commonly neglected in the traditional morphological approach as well as small-size taxa (i.e., <63 µm) that are mostly overlooked (Pawlowski et al., 2014b).

2.5.2.2. Foraminifera as bioindicators

Similar to previous studies in the area (e.g., Bergamin et al., 2003, 2005; Romano et al., 2008, 2009), a limited number of living specimens was found and most of them in the finer fraction (i.e., 63–125 µm). This observation can likely be ascribed to the prevailing high-pollution conditions. It is worth mentioning that differently from the previous studies (based on total assemblages), the present

investigation was only based on living specimens, providing reliable information about local ecological conditions at the moment of the sampling.

The relative abundances of some morphospecies and assigned and unassigned MOTUs varied in relation to the pollution gradient. In fact, some morphospecies (i.e., *B. elongata, N. turgida, H. pacifica, B. spathulata, A. parkinsoniana, R. phlegeri*, and *E. advenum*) appeared to be tolerant to environmental stress. All these taxa except *A. parkinsoniana* and *E. advenum* were identified as opportunist (i.e., from first to third order) (Jorissen et al., 2018). On the other hand, some taxa (i.e., *E. crispum, C. refulgens, A. mammilla, C. variabilis,* and *R. bradyi*) showed a more sensitive behavior in accordance with their assignment to the sensitive ecological group in Jorissen et al. (2018).

Monothalamea appeared to be more abundant at the more polluted stations, whereas an opposite trend was observed for Globothalamea, particularly for Textulariida (Fig. 2.4b). Some Monothalamea (i.e., *Tinogullmia* sp., *Micrometula* sp., *C. alba*, *Vellaria* sp., *Psammophaga* sp., *Bathysiphon* sp., and Clade V) and Globothalamea (i.e., *L. scottii*, *Reophax*, *B. elongata*, *Eggerelloides* sp., *Nonionoides* sp., and *Stainforthia* sp.) were positively related to the stress gradient and were, therefore, identified as tolerant species (Fig. 2.5). The MOTU assigned to *Leptohalysis scotti* was found to be well adapted to impacted conditions (i.e., enriched sediment) of fish farming (Pawlowski et al., 2014a; Pochon et al., 2015). The same MOTU was revealed to be related to finer sediment fractions (i.e., silt, clay, and mud) (Frontalini et al., 2020) where oxygen levels were likely lower. Moreover, even in the traditional morphological approach, *L. scotti* has been included as a first- (Jorissen et al., 2018), second- (Bouchet et al., 2018b), and third-order opportunist (Parent et al., 2021). Similarly, the MOTU assigned to *Vellaria* sp. has been reported to be well adapted to impacted conditions (Pawlowski et al., 2014a; Pochon et al., 2015) and high concentrations of Hg (Frontalini et al., 2018). A higher abundance of the MOTU assigned to *Psammophaga* sp. has been documented near fish farms (i.e., Pawlowski et al., 2014b) and associated to moderately organic-enriched sediment (Pochon et al., 2015). Higher read numbers of the MOTU assigned to *Bathysiphon* sp. have been found close to an oil drilling site (Laroche et al., 2016). The MOTU assigned to *Micrometula* sp. has been associated

to lower organic enrichment and with a preference to oxic conditions (Pawlowski et al., 2014a; Pochon et al., 2015). Similarly, the morphospecies *Micrometula hyalostriata* has been found in sites with low TOC and high bottom-water oxygen concentrations, and this species has, therefore, been identified as sensitive (Bouchet et al., 2018b). In contrast, in the morphological approach, *Micrometula* spp. including *M. hyalostriata* and *Micrometula* sp. has been assigned to the first-order opportunists (group V) (Fossile et al., 2021). The morphospecies *Bulimina elongata* has also been identified as an opportunistic taxon (Jorissen et al., 2018). The morphospecies *Cylindrogullmia alba* is reported in environments with high-to-low TOC and bottom-water oxygen concentrations and identified as an indifferent species (Bouchet et al., 2018b).

Other MOTUs belonging to Monothalamea (i.e., Clade B, Clade G, *G. sublittoralis*, *Shepheardella* sp., and *B. argenteus*), Tubothalamea (Hauerinidae), and Globothalamea (i.e., *L. goesi*, *O. umbonatus*, *Rosalina* sp., *Epistominella* sp., *Cibicidoides*, and *Cibicides* sp.) show a more sensitive behavior. Most of these taxa have been rarely found in previous eDNA metabarcoding studies, and a comparison of their ecology and driving factors is, therefore, limited. Interestingly, the MOTU assigned to *Epistominella* spp. has been found to be more prevalent at a high-flow (sandy) site (Pochon et al., 2015); hence, it matches well with its higher abundance at B1 and B2 transects that present, comparatively, coarser grain size and lower organic enrichment. On the other hand, the MOTU assigned to *B. argenteus* was found to be more common at moderately impacted low-flow sites (Pochon et al., 2015). Given that the ecological behavior of these MOTUs was compared to the morphospecies, and most of the morphospecies belonging to *Rosalina* and *Cibicides* genera have been regarded as sensitive species and, therefore, assigned to group I (Jorissen et al., 2018), *Liebusella goesi* has been recognized as a tolerant taxon (Bouchet et al., 2018b).

Despite the different taxonomic composition of the metabarcoding and morphology assemblages, some congruent trends can be identified (Fig. 2.5). This identification is supported by the significant positive correlation (i.e., Mantel's test) between the molecular and morphological datasets, suggesting a clear and similar shift in the two dissimilarity matrices (i.e., foraminiferal turnover) in

the study area. In particular, *B. elongata* is placed in the same PCA position (i.e., negative values of PCA1), suggesting a clear match in its ecological behavior in the morphological and molecular dataset. *Nonionoides turgida* (morphological dataset) and *Nonionoides* (molecular dataset) showed a highly similar trend as did, to some extent *R. phlegeri*. Moreover, *R. bradyi*, *C. refulgens*, *C. variabilis* (morphological dataset), and *Cibicides*, *Cibicidoides*, and *Rosalina* sp. (molecular dataset) showed a highly congruent pattern towards positive values of PCA1.

2.5.3 Assessing the ecological quality status of Bagnoli based on benthic foraminiferal biotic indices

All the biotic indices computed for both morphological and molecular datasets displayed congruent trends with the ES (Fig. 2.7a and Table 2.2). In fact, lower EcoQS values were found in the area in front of the former industrial site (i.e., stations along B3 and B4 transects) (Fig. 2.7b–e). All these indices except exp(H'bc) exhibited a significant Spearman's rho correlation to *PLI*, TOC, and the ES (Fig. 2.6 and Table 2.2). The diversity-based index exp(H'_{bc}) was successfully applied to assess the EcoQS in different marine settings mostly in transitional environments (Bouchet et al., 2012; Bouchet et al., 2018a; Dijkstra et al., 2017; Francescangeli et al., 2016; S. dos S. de Jesus et al., 2020). However, controversial results have also been provided in previous environmental characterizations (El Kateb et al., 2020). On the contrary, the g-exp(H'_{bc}) based on foraminiferal eDNA showed a significant negative correlation to *PLI*, TOC, and ES. This association can be ascribed to the higher number of taxa (i.e., MOTUs) and "specimens" (i.e., reads) compared to the morphological dataset. Indeed, naked and small-size foraminifera that are commonly overlooked in dry-picked morphology-based assessments are retained in the eDNA approach (Pawlowski et al., 2014b). The application of metabarcoding provides a more holistic view of foraminiferal diversity (He et al., 2019: Frontalini et al., 2020).

The recent advances in the foraminiferal morphospecies' assignments to ecological groups (EGs) (Alve et al., 2016; Jorissen et al., 2018; Bouchet et al., 2021) significantly facilitate the implementation of the sensitive-based indices (FSI, TSI-Med, Foram-AMBI). The Foram-AMBI may

indeed suffer from a lack of foraminiferal assignments to EGs, invalidating its effectiveness when the percentage of assigned species is lower than 80% (Borja and Muxika, 2005). For instance, in the Gulf of Gabes (Tunisia) (El Kateb et al., 2020) and in the Gulf of Manfredonia (Italy) (Fossile et al., 2021), the assessment of the species was often under this threshold. On the contrary, in our study, the percentage of assigned species for FSI, TSI-Med, and Foram-AMBI was always > 80%, providing reliable ecological quality assessments.

For evaluating the EcoQS, one of the key aspects is not only the choice of metrics but also the definition of appropriate class boundaries (i.e., categories) for each metric. Boundary-setting is one of the most critical steps in the design of assessment methods because it defines the target values for environmental management (Birk et al., 2012). The EcoQS based on g-exp(H'_{bc}) fits particularly well with the ES in the area (Fig. 2.7) as well as with the categorization for the definition of the EcoQS. The class boundaries of Foram-AMBI were derived from the AMBI, a well-known biotic index based on macrofauna (Borja et al., 2003), Table 2.1). However, if the same macrofaunal categories are applied, the EcoQS of the study area results in excellent (i.e., in the area away from the industrial plant) to good (in correspondence of the former plant) (Fig. 2.7). Similar controversial results have been reported in the assessment of the EcoQS in the Gulf of Manfredonia (Italy) (Fossile et al., 2021). It is evident that a redefinition of boundaries is urgently required in order to optimize the application of Foram-AMBI in biomonitoring. In light of this issue, we follow the new categorization of Parent (2019) (Tables 2.1 and 2.2). On the basis of this new categorization, the EcoQS varied from moderate to high (Fig. 2.7). In particular, the area in front of the former industrial plant exhibited an EcoQS ranging from good to moderate that matches much better with those values computed from TSI-Med as well as of the molecular dataset (i.e., g-exp(H'_{bc}), g-Foram-AMBI, and g-Foram-AMBI-MOTUs). The g-Foram-AMBI and g-Foram-AMBI-MOTUs evidenced critical ecological conditions (poor-bad) in the stations with the highest degrees of pollution (Fig. 2.7) that also match well with the EcoQS derived from g-exp(H'_{bc}). The comparison of EcoQS (acceptable or not acceptable) resulting from the different biotic indices suggests the lowest percentages of agreement for Foram-AMBI with

the traditional classes and all other ecological indices, whereas the highest agreement was found between g-Foram-AMBI and all the other indices. When the Foram-AMBI with the traditional classes was removed, EcoQS of the stations results in full agreement in 4 out of 12 stations (about 33%) and partial agreement in 5 out of 12 stations (ca. 42%) (Table 2.2).

2.6. Conclusions

Innovative foraminiferal eDNA metabarcoding was used to assess the EcoQS in the highly polluted SIN of Bagnoli and compared to more traditional morphology-based biomonitoring. Geochemical and statistical analyses identified the area in front of the former industrial plant as the most polluted. Significant changes in both morphological and molecular datasets were associated with environmental stress (i.e., high trace elements and TOC levels) and were well spatially defined (i.e., in front *vs*. away from the former industrial plant). Similarly, the selected ecological indices inferred from both morphological and molecular datasets strikingly and congruently resulted in a clear separation following the environmental stress gradient. The molecular indices (i.e., g-exp(H'_{bc}), g-Foram-AMBI, and g-Foram-AMBI-MOTUs) reliably identified moderate-to-bad EcoQS in the polluted area and good-to-high EcoQS in the area more distant to the former plant, particularly those sites at a shallower water depth (i.e., 10 and 20 m). The morphology-based Foram-AMBI appeared to register the overall trends of EcoQS efficiently, but this approach did seem to overestimate the EcoQS if the traditional class boundaries were considered. The congruent and complementary trend between morphological and molecular biotic indices further support the application of foraminiferal metabarcoding in routine biomonitoring to assess the environmental impacts of heavily polluted marine areas.

___Personal contribution: Morphological foraminifera analysis, maps interpolation, geochemical indexes calculation, analysis of results, MS writing, reviewing, graphical contribution___

Chapter III

3. Encapsulated in sediments: eDNA deciphers the ecosystem history of one of the most polluted European marine sites

Published in **Environment International** in January 2023.

Barrenechea Angeles, I., Romero-Martínez, M., Cavaliere, M., Varrella, S., Francescangeli, F., Piredda, R., Mazzocchi, M.G., Montresor, M., Schirone, A., Delbono, I., Margiotta, F., Corinaldesi, C., Chiavarini, S., Montereali M.R., Rimauro, J., Parrella, L., Musco, L., Dell'Anno, A., Tangherlini, M., Pawlowski, J., and Frontalini, F., 2022**.** Encapsulated in sediments: eDNA deciphers the ecosystem history of one of the most polluted European marine sites. Environment International, Volume 172, 107738, ISSN 0160-4120, https://doi.org/10.1016/j.envint.2023.107738.

3.1. Introduction

The increasing human impacts and the concurrent threat on the environmental resources at both global (i.e., climate change) and local (e.g., pollution, overexploitation) scales have led to defining the current Epoch as the Anthropocene (Lewis and Maslin, 2015). The deterioration of environmental conditions is widespread in marine environments, particularly in coastal ecosystems that represent the main global economic assets in terms of ecological services (Costanza et al., 1997; Keyes et al., 2021). The impact on coastal marine ecosystems has pervasive consequences by leading to species extinction (Barnosky et al., 2011; Dirzo et al., 2014), impairing the ecological functions (Obura et al., 2021), and losing ecosystem goods (Worm et al., 2006). In the light of it, the monitoring of marine

biodiversity changes at different spatio-temporal scales is becoming a priority tool for planning conservation strategies at the international level (Dornelas et al., 2014; Danovaro et al., 2020).

The emerging omics technologies (e.g., metagenomics) have recently offered a new perspective for understanding the impact of anthropogenic activities on biodiversity (Carraro et al., 2020). The environmental DNA (eDNA) has revolutionized the detection of species and found applications in biodiversity assessment and biomonitoring (Kelly et al., 2014; Cordier et al., 2021). Specifically, the application of eDNA metabarcoding improves the capability to simultaneously capture various biological components encompassing multiple trophic levels (Djurhuus et al., 2020). Indeed, the analysis of ancient eDNA preserved in sediment (*sedaDNA*) enables the reconstruction of the present-day to past biological communities and paleo-environmental conditions (Pedersen et al., 2015; Brown and Blois, 2016; Capo et al., 2021). In lakes sediments, prokaryote communities (cyanobacteria) were targeted to evaluate temperature rise and eutrophication effects (Monchamp et al., 2017), while changes in the composition of micro-eukaryotic communities allowed to follow anthropogenic impacts in Alpine lakes (Keck et al., 2020). Until now, only few studies have been conducted on sediment cores collected in marine coastal environments. Siano et al., (2021) showed anthropogenic effects around the Bay of Brest in the last 5000 years based on microbial eukaryotes community, while Armbrecht et al., (2022) targeted phytoplankton to track harmful algal blooms over ~9000 years off the East Australian coast. These studies allow for the comprehension of the effects of human activities on biodiversity over time and the definition of reference conditions (e.g., baseline or pre-industrial). However, both studies focused on a single marker that altogether prevents a holistic comprehension of community shifts or diversity changes and hampers the observation of their potential interactions.

In this work, we investigated changes in biodiversity and community composition spanning from prokaryotes to multicellular organisms, through a multi-markers metabarcoding approach. Our *sedaDNA* multimarker data consistently reveal a five-phase variation of the paleo-community that perfectly matches with the anthropogenically-induced environmental changes as supported by the

historical archives and geochronology in one of the most polluted European (Armiento et al., 2022; Sprovieri et al., 2020), likely worldwide, marine sites of Bagnoli-Coroglio (Italy; Fig. S3.1). The bay and hinterland area of Bagnoli-Coroglio have a long-lasting legacy of environmental impacts emerging from a complex interplay of anthropogenic activities (i.e., urbanization, industry, polluted-sediment disposal, land-use, coastline, and water-circulation changes) (Bertocci et al., 2019). The first industrial activities started to develop in the first decades of 1900 and reached their production peak in the late 1960s-early 1970s (Cavaliere et al., 2021). The site hosted the second-largest Italian steel factory (Ilva/Italsider), active till the early '90s (Trifuoggi et al., 2017), as well as asbestos (Eternit) and concrete (Cementir) factories. Due to the concentrations and hazardousness of pollutants, and their impacts on the ecosystem and human health, the area was declared a contaminated Site of National Interest (SIN) in 2000 (Law 388/2000). Today, Bagnoli-Coroglio is a large brownfield area, with marine sediments and benthic assemblages still intensively impacted by metals and polycyclic aromatic hydrocarbons (PAHs) (Ausili et al., 2020; Gambi et al., 2020; Tangherlini et al., 2020).

3.2. Methods

3.2.1. Core collection and processing

The AB01 sediment core (110 cm in length) was collected at 55 m water depth in the Bay of Bagnoli (Gulf of Pozzuoli, Tyrrhenian Sea; 40° 48.150' N, 14° 08.913' E) (Fig. S3.1) on December 5th, 2018, with an SW-104 corer Carma®, equipped with a liner of 10.4 cm in diameter. After collection, the core was transported to the laboratory, sliced through extruder equipment at 1 cm resolution discarding the outermost centimeter in contact with the liner, to avoid smearing effects downcore. Sediment layers were sliced using sterile spatulas, photographed, weighed and the color was scored following Munsell Soil Chart. For the first 41 cm and starting from the top layer (0-1 cm= layer #1), odd layers were used for grain size and chemical analyses, while even layers were used for

biological analyses and organic matter (OM) characterization (Table S3.1). Samples for eDNA metabarcoding were collected by cutting the central portion of each layer with a disposable, sterile petri dish (diameter 5 cm) and placed in 5 ml cryovials (two biological replicates for eukaryotes and two replicates for prokaryotes), frozen in liquid nitrogen and stored at -80°C

3.2.2. Grain size analyses

Each core sediment sub-sample (odd layers) was washed with deionized water, then disaggregated using 1% sodium metaphosphate, and analyzed by a laser particle size analyzer (Helos KF SympaTEC). Grain-size results from the top core to 40-41 cm sediment layer are reported as a volume percentage of sand and mud (as silt and clay fractions) against the correspondent age, accordingly to the sediment core dating described below.

3.2.3. Radiometric analyses and geochronology

Gamma spectrometry analyses were performed on 20 g geometry of slightly ground sediment samples to determine ^{210}Pb and ^{226}Ra activities. Calibration, quality checks, and measurement procedures have been described in Delbono et al. (2016). The excess ^{210}Pb ($^{210}Pb_{ex}$) activity was calculated as the difference between the total ^{210}Pb and the fraction in equilibrium with the parent radionuclide ^{226}Ra. Mass depth (g cm^{-2}) was used to account for the compaction of the sediment layers. The Constant Rate of Supply (CRS) model (Appleby and Oldfield, 1978) was applied to determine the age of each layer of the sediment core, assuming a CRS of unsupported ^{210}Pb. The ^{210}Pb dating was validated and extended over several centuries using information taken from ^{226}Ra activities. In fact, the ejected sediments by Vesuvius volcanic activities are marked by a high ^{226}Ra concentration (Voltaggio et al., 2004), and its recent historical activity (1631-1944) is well-known and continuous (Scandone et al., 2008) giving a series of well-recognized time-markers: in the AB01 sediment core, ^{226}Ra peaks due to Vesuvius eruptions in 1944, 1906 and 1822 were identified (Armiento et al., 2022).

3.2.4. Chemical analyses

Sediment samples were transferred to the laboratory in polyethylene high-density (PEHD) containers at a temperature of 4°C, where the phases of pre-treatment and analysis for metals and PAHs were performed. A detailed description of analytical procedures is reported in Armiento et al. (2020). Briefly, after extraction by microwave-assisted acid digestion of the samples, metals (Cd, Cu, Cr, Hg, Pb, and Zn) analytical determinations were carried out, according to the EPA 6020b method, by inductively coupled plasma-mass spectrometry (ICP-MS, Agilent 7800) except for Hg that was analyzed by atomic absorption spectrometer (AMA-254) according to EPA 7473 method. PAHs were extracted by an Accelerated Solvent Extractor (ASE 200 Dionex) and the analytical determination was carried out according to EPA 8270D method with the Agilent 7890A-5975C GC-MS system.

3.2.5. Organic matter

Sediment samples were dried in an oven (60°C) and subsequently ground and homogenized. Sub-samples were then weighed (~10–20 mg) in silver capsules and treated with increasing HCl concentration solutions (v/v 8%, 18%, and 25%) to remove the inorganic carbon fraction (carbonates) completely. Total organic carbon (TOC) and total nitrogen (TN) were analyzed using a Thermo Electron Flash Elemental Analyzer (EA 1112).

3.2.6. Prokaryotic metabarcoding

Total DNA was extracted in two replicates from 1 g of selected sediment layer (i.e., 1-2, 5-6, 9-10, 13-14, 17-18, 25-26, 27-28, 53-54) by using the DNeasy PowerSoil Kit (QIAGEN©, Düsseldorf, Germany) following manufacturer's instructions. The amount of DNA isolated was estimated by the absorbance at 260 nm and the purity by 260/280 and 260/230 nm ratios, by a NanoDrop spectrophotometer (ND-1000 UV-Vis Spectrophotometer; NanoDrop Technologies, Wilmington, DE, USA). The amplification of 16S rRNA V4-V5 regions (~410 bp) was performed using 515F-Y

forward and 926R reverse primers (Parada et al., 2016). Libraries were prepared from each sample by pooling three PCR replicates and sequencing was performed with all libraries on a single Illumina MiSeq flow cell by LGC Genomics GmbH (Berlin, Germany).

The raw reads were filtered low-quality base calls (<30 Phred score) using the QIIME2 (Bolyen et al., 2019). Primer sequences were discarded using Cutadapt (Martin, 2011) using default parameters. Sequence reads were error-corrected, merged and amplicon sequence variants (ASVs) were identified using DADA2 with --trunc-len-f 272 and --p-trunc-len-r 192 (Callahan et al., 2016). ASVs were taxonomically classified using VSEARCH (Rognes et al., 2016) against the SILVA database (release 138) created trimming to the amplified region. Taxonomic information was used to remove eukaryotic, chloroplast and mitochondrial-related sequences before subsequent analyses. To reduce analytical biases due to different sequencing depths among samples, the ASV table was randomly subsampled to the same number of sequences (13600). This normalized table was subsequently converted to a phyloseq class object in R for further analysis (McMurdie and Holmes, 2013). The same dataset was utilized to construct a table within the microeco package (Liu et al., 2021), which was then used as an input for a LefSe analysis (Segata et al., 2011) which allows assessing the differences in assemblage composition across the historical periods identified. The raw data is available from the Sequence Read Archive public database under the accession number: PRJNA822883.

3.2.7. Eukaryotes, foraminiferal and metazoan metabarcoding

For each sediment layer, 5 g of sediment was extracted using the DNeasy® PowerMax® Soil kit (QIAGEN©, Düsseldorf, Germany) following the manufacturer's instructions. All eDNA extractions and manipulations were performed to avoid cross-contamination between samples and contamination by modern eDNA. Three genetic markers, commonly used in eukaryotic biodiversity surveys (Frontalini et al., 2020; Lanzén et al., 2021; Pawlowski et al., 2021), were used to obtain a wide range of marine organisms. Eukaryotes, foraminifera, and metazoans were targeted by amplifying the V9

region of 18S rRNA (~150 bp) with 1389F - 1510R primers (Amaral-Zettler et al., 2009), 37F region of 18S rRNA (~190 bp) with s14F1- s15 primers (Pawlowski and Lecroq, 2010), and mitochondrial cytochrome oxidase 1 gene (~390 bp) with mlCOIintF and dgHCO2198 primers (Leray et al., 2013), respectively. Eight nucleotides were attached to the 5' extremity of primers to allow the multiplexing of samples (Esling et al., 2015). Primer sequences and PCR programs are detailed in Table S3.2. Per sediment sample, three replicates and one control (blank) were performed and checked on 1.5% agarose gels. The triplicates were merged and the amount of DNA was quantified for the pool and its PCR control using high-resolution capillary electrophoresis with the QIAxcel system (QIAGEN©, Düsseldorf, Germany). The PCR products were equimolarly pooled into one 1.5 ml tube per marker and were purified using the High Pure PCR Product Purification kit (Roche Molecular Systems©, Basel, Switzerland). The final DNA concentration of pools was quantified using QubitTM HS dsDNA (Invitrogen, Thermo Fisher Scientific, Massachusetts, U.S.) kit. The libraries were prepared using the TruSeq® DNA PCR-Free Library Preparation Kit (Illumina©, California, U.S.) and then quantified by qPCR using the Kapa library quantification kit (Kapa Biosystems, Massachusetts, U.S.) for Illumina platform. Paired-end sequencing was performed on a MiSeq instrument (Illumina©, California, U.S.). We used the v2 kit with 300 cycles for V9 and foraminiferal amplicons and the v3 with 500 cycles for COI amplicons. The bioinformatic analysis was performed using SLIM software (Dufresne et al. 2019). The raw sequencing data were demultiplexed with the module DTD. We performed DADA2 (Callahan et al., 2016) with the pseudo-pool option to filter the low-quality sequences, trim the primers, merge the paired-end reads and remove the chimeras. This DADA2 module produced ASV sequences and count tables. We applied a LULU (Frøslev et al., 2017) curation on all markers datasets to filter PCR and sequencing errors or intra-individual variability as recommended in (Brandt et al., 2021). Taxonomic assignments for the representative ASV-LULU V9 sequences were performed using standalone blast in the blast + suite (Camacho et al., 2009) against PR2 database version 4.14.0 (Guillou et al., 2013) integrated with some private references sequences from diatoms strains. Assignments with a similarity of <90% and query coverage >90 bp

were removed and assignments at the species level were manually checked. Taxonomic assignments for ASV-LULU foraminiferal sequences were done using VSEARCH (Rognes et al., 2016) at 95% similarity against our local database. The ASV-LULU COI sequences were taxonomically assigned using blast+ against the NCBI database with 95% similarity and a query coverage of >230 bp. The raw data from foraminifera, COI and V9 sequencing are available on the Sequence Read Archive public database under the accession number: PRJNA824838.

3.2.8. Benthic foraminifera morphology

Benthic foraminifera were analyzed from 20 samples in the sediment fraction > 125 µm, where possible at least 300 specimens were picked. The taxonomical identification largely followed Cimerman and Langer (1991), Sgarella and Zei (1993) and Milker and Schmiedl (2012).

3.2.9. Ecological indexes

3.2.9.1. Metazoan gAMBI and Foram-AMBI indices

For marine macrofauna, we applied gAMBI index, an adaptation based on the genetic metazoan data of the AZTI's Marine Biotic Index (AMBI; Borja et al., 2000). The gAMBI values were calculated using AMBI Index Software v6.0 (Borja and Muxika, 2005) where a list of macrofaunal taxa with their ecological values is included (http://ambi.azti.es; Species List v. Dec2020).

To evaluate the Paleo-EcoQS based on benthic foraminifera, the Foram-AMBI (Jorissen et al., 2018), an adaptation of the AMBI macrofauna (Borja et al., 2000) was calculated.

3.2.9.2. MicrogAMBI and prokaryotes indices

Based on the prokaryotic taxa encountered in the different sediment layers, the microgAMBI was calculated following Aylagas et al. (2017). Putative indicator taxa of the ecological quality were identified based on their relationships with the pollution index as the probability of toxicity m-ERM-

q (Kowalska et al., 2018; Long et al., 2000) by linear model regression analysis (lm) performed in R (R Core Team, 2013).

3.2.10. Statistics

For each group, the Shannon Weiner (H') alpha diversity was calculated. Taxa relative abundances were used to group layers (i.e., years) by using a constrained hierarchical clustering analysis (HCA) along the core depth. A similarity tree was produced using the Euclidian distance. Coniss (Grimm, 1987) was used as the clustering method. The analysis was performed using the package vegan (Oksanen et al., 2007) and rioja (Juggins, 2022) in RStudio. A Spearman's Rho correlation was used to identify significant relationships between environmental variables (i.e., PLI, PAHs, TOC, C/N, TN, Mud) and the diversity of the main taxonomical groups. A biological and environmental (BIO-ENV) analyses (Clarke and Ainsworth, 1993) were performed to detect the best subset of environmental variables with maximum (rank) correlation with morphological and molecular groups. This procedure finds the correlation (Spearman's Rho) between community dissimilarities (based on Bray-Curtis matrix) and environmental distances (Euclidian matrix), and for each size of subsets provides the best result. Canonical Correspondence Analyses (CCAs) were performed to observe the relationships between the environmental parameters and the assemblage turnover of main taxonomical groups. Data analyses were performed using the R software (3.6.3) and following packages: "vegan", (Oksanen et al., 2007), "PerformanceAnalytics" (Peterson et al., 2014) and "lattice", (Sarkar, 2008).

3.3. Results

3.3.1. The geochemical signature of the pollution history at the Bagnoli-Coroglio SIN

The analysis of the AB01 sediment core provides a high-resolution (4.6 yr cm^{-1}), continuous, complete, and well-constrained (i.e., ^{210}Pb and ^{226}Ra) record for the reconstruction of paleo-

environmental changes in the Bagnoli-Coroglio SIN in the last ~190 years (Fig. 3.1 and Table S3.1) (Armiento et al., 2022).

The geochemical profiles highlight a progressive increase in the concentrations of inorganic (i.e., trace elements as underlined by the Pollution Load Index (PLI) and organic (i.e., Polycyclic Aromatic Hydrocarbons: PAHs) pollutants as well as in the quantity (i.e., TOC) and quality (i.e., C/N) of the OM at the very beginning of the 20th century (i.e., 1901) and a marked peak in the period 1954-1992 (Fig. 3.1, Tables S3.3-S3.4). The PLI record reveals moderately polluted conditions since 1921 that turns from highly to extremely highly polluted in 1944 up to 1990. A similar pattern is observed in the total concentration of PAHs whose origin is mostly pyrogenic (i.e., Anthracene to Anthracene plus Phenanthrene> 0.1, Fig. S3.2).

The TOC trend shows a progressive increase since 1916, with a peak between 1954 and 1992. Based on the C/N values that are persistently >19, a terrigenous origin of the OM has been inferred (Meyers, 1994). However, the significant increase of C/N in the 1960-1987 interval suggests a higher input of carbon of terrestrial origin, possibly resulting from the "*Colmata a Mare*" that corresponds to the disposal of contaminated soil between the two piers in 1962-1967 to enlarge the industrial area and/or from contamination by hydrocarbons (i.e., PAHs with a highly unbalanced C/N ratio).

3.3.2. Community composition shifts from past to present

The HCAs based on community changes in multimarker *sedaDNA* datasets and foraminiferal morphospecies consistently identified five main groups corresponding to different time intervals related to the development and exploitation of the area based on historical archives (Fig. 3.1). These stepwise temporal phases were defined as pre-industrial (1827-1851), initial industrial phase and land-use change (1851-1911), developing industrial phase (1911-1950), maximal industrial expansion (1950-1992), and post-industrial/partial decommission (1992-2016) (Fig. 3.1). These findings were supported by the CCAs analyses. They showed that layers deposited before 1911 (i.e., the pre-industrial and the beginning of industrialisation phases) were mostly associated to mud and

lowest contaminations (i.e., negatively correlated to PLI, PAHs and TOC). In contrast, layers deposited during the industrial peak and the post-industrial phases were related to the highest values of PLI, PAHs, TN, TOC, and C/N. The detailed analysis of community changes for different groups along the vertical profile of the sediment is presented below.

The prokaryotic metabarcoding analysis showed that the ASVs belonging to *Bathyarchaeia* accounted on average for 13.5% of the prokaryotic assemblage, followed by *Anaerolineaceae* (on average, 7.9%), and *Aminicenantales* (on average 4.8%). However, the relative abundance of the prokaryotic taxa changed in relation to the analyzed sediment layers corresponding to different historical periods (Fig. S3.3). In particular, LefSe analysis showed that several taxa (considering all taxonomic levels from phylum to species) were associated with one or more temporal phases (Fig. S3.4a); at the Family level, we found that groups such as Aminicenantales, Woesebacteria, Thermoflexaceae were associated with early stages of industrialization (with Aminicenantales representing ca. 6% of the assemblages at pre-industrial and initial industrial phases), while others, like Thermoanaerobaculaceae (ca. 4%), Flavobacteriaceae (2%), Woeseiaceae (2%), Rhodobacteriaceae, Cyclobacteriaceae, Deslfobulbaceae, were more represented in the post-industrial phase (Fig. S3.4b).

The eukaryotic metabarcoding data revealed clear temporal faunal turnover when considering the major groups of multi- and unicellular organisms (Fig. 3.2). The eukaryotic assemblage was dominated by seagrasses (*Posidonia oceanica*) in the oldest layers (1832-1851). A clear DNA signature of *P. oceanica* persisted until the beginning of the industrial phase (up to 1911). A similar temporal trend was also detected for terrestrial plants, whose signature almost disappeared after 1911 (Fig. 3.2). The plant DNA signatures were progressively replaced by those of microbial eukaryotes (protists) from 1860 to 2003 and metazoans from 2007 to 2013. The CCA analysis showed that before 1911 (i.e., the pre-industrial and the beginning of industrialisation phases), the layers clustered and were related with mud, whereas layers from the industrial peak and the post-industrial phases formed a group that was mainly related to PLI, PAHs, TN, TOC, and C/N (Fig. S3.5a). The BIO-ENV

analysis identified PLI, PAHs and mud as the environmental factors affecting the most the eukaryotes communities and PLI and mud for seagrasses and terrestrial plants communities (Table S3.5).

The dramatic shift in the paleo-community composition observed at the beginning of the industrial period (i.e., after 1911) was also detected within protists (Fig. 3.2). The CCA analysis revealed a separation of layers before, during and after industrialisation (Fig. S3.5b). Like other eukaryotes, protists before the industrial period were more influenced by mud, whereas after this period strongly by PLI, PAHs, TN, TOC, and C/N. The protist diversity showed a strong negative correlation with these environmental parameters (Fig. S3.6). Indeed, among them, PLI and PAHs were revealed to be the most important parameters in explaining these community changes (Table S3.5). Before 1911, the protist assemblage was highly diversified, represented by free-living (Dinophyceae) and parasitic (Syndiniales) dinoflagellates, Apicomplexa, ciliates, diatoms, and Rhizaria (Radiolaria, Foraminifera, and Cercozoa). A remarkable decrease in the abundance of cercozoans and radiolarians (dominated by planktonic spumellarians and nassellarians), as well as Apicomplexa, was observed after 1911 (Fig. 3.2). From 1921, the protist community was dominated by Dinophyceae, mainly including genera known to produce resting stages (e.g., *Protoperidinium*, *Scrippsiella* and other taxa belonging to the family Thoracosphaeraceae, *Gymnodinium*) (Fig. S3.7). Among other groups, diatoms represented a rather constant percentage of the protist assemblage. They were markedly dominated by planktonic taxa that produce resting stages, among which the genus *Chaetoceros* was retrieved all along the core, while *Biddulphia*, *Skeletonema* and *Thalassiosira* became abundant after the main industrialization (i.e., after 1954) (Fig. S3.8). From 1967, an increasing abundance of ciliates was also detected. The CCAs based on dinoflagellates and diatoms provided a clear separation of layers in pre- and industrial periods (Fig. S3.5c-d). During the industrialization phase and after, dinoflagellates and diatoms showed an opposite relationship with environmental variables and diversity. The diversity of dinoflagellates was negatively correlated with PLI, TN and mud, whereas the diversity of diatoms was positively correlated with PLI, PAH, TOC, TN, C/N and negatively with mud (Fig. S3.6). The BIO-ENV analysis revealed that PLI and PAH were amongst the most important

parameters shaping the dinoflagellate and diatom assemblages. Mud was also a very influential factor for diatoms (Table S3.5).

A community composition shift after 1911 (beginning of industrial phase) was also observed in benthic foraminifera analyzed with both molecular and morphological approaches (Fig. 3.2). Before 1911, the foraminiferal assemblages inferred from *sedaDNA* data were dominated by monothalamids and representatives of taxonomically non-identified environmental clades. In 1911, a small number of reads corresponding mainly to one ASV was identified. Since 1967, buliminids and other calcareous globothalaminids were continuously present. In the morphological dataset, the most abundant species were *Valvulineria bradyana, Cassidulina carinata*, *Rosalina bradyi*, *Ammonia parkinsoniana, Gavelinopsis praegeri,* and *Lobatula lobatula*. The abundance of *C. carinata* showed a marked increase between 1911 and 1921 (from 8 to 20%) that was associated with a lower abundance of *A. parkinsoniana* (1880-1997), *Textularia pala* (1911-1990), *L. lobatula* (1921-2001), *Cibicides refulgens* (1901-2013) and *Nonionella turgida* (1954-2013). *Bulimina elongata* exhibited a significant increase after 1954 (Fig. 3.2, Table S3.5). There is a difference between pre and industrial layers in CCA analysis in molecular and morphology foraminiferal assemblages (Fig. S3.5e-f). On overall, the environmental factors that influenced the most foraminifera were PLI (molecular data) and TOC (morphology data) (Table S3.5). The diversity of benthic foraminifera was negatively correlated to PLI, PAHs, TN, TOC, and C/N for the morphological dataset, whereas an opposite trend was found in the molecular one (Fig. S3.6).

.

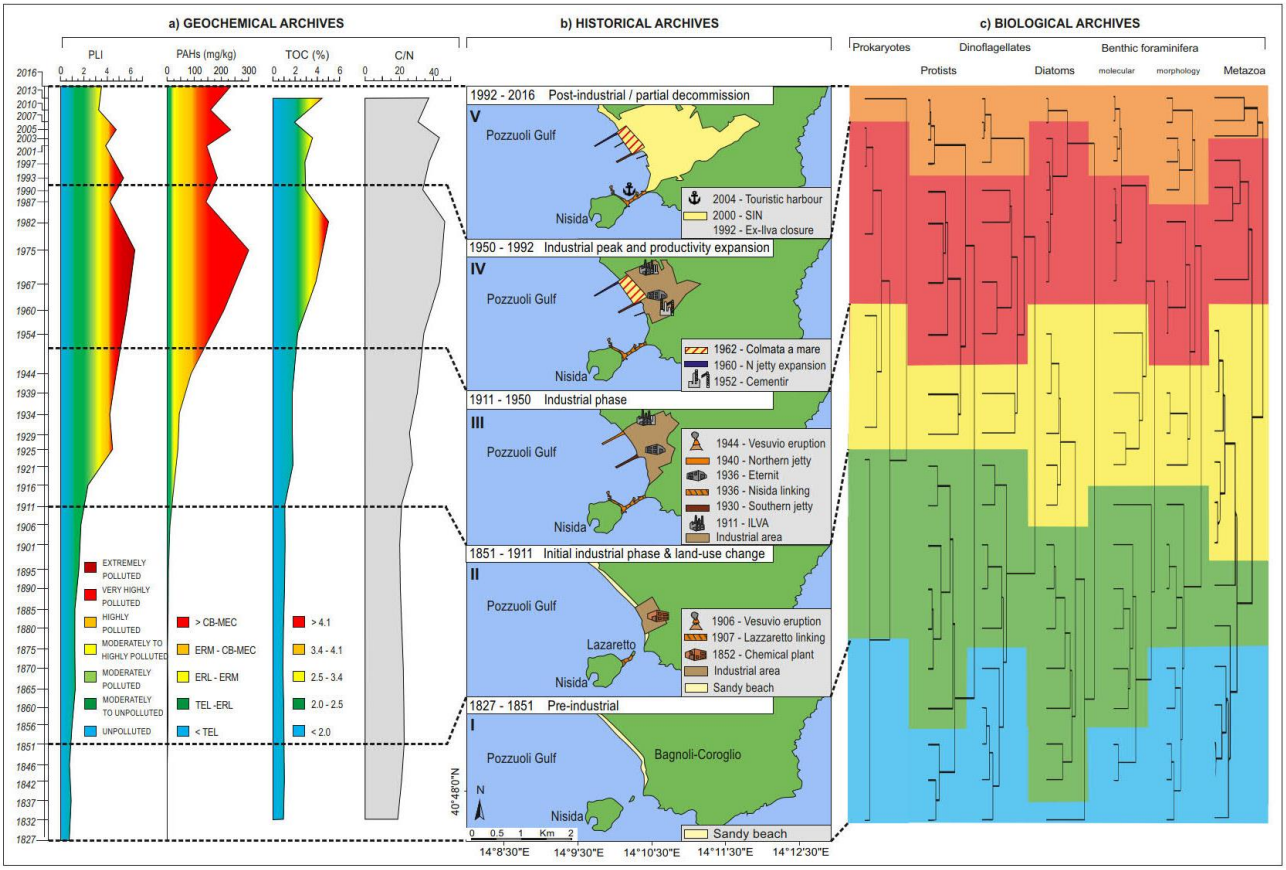

Figure 3.1 Geochemical, historical and biological archives. Plot of selected geochemical proxies (PLI: Pollution Load Index; PAHs: Polycyclic Aromatic Hydrocarbons, TOC: Total Organic Carbon; C/N: carbon-nitrogen ratio). Classification of PLI after Zhang et al. (2011) with modification, sediment quality guidelines for PAHs (TEL: threshold effect level; ERL: effects range low; ERM: effect range median; CB-MEC: Consensus Based - midrange effect concentration) after Burton (2002) and TOC after Bouchet et al. (2018a). Historical archives with significant human-induced changes and activities. Hierarchical Cluster Analyses (HCAs) based on prokaryotes, protists, dinoflagellates, diatoms, benthic foraminifera (molecular and morphological) and metazoa. The colour-shaded areas over HCAs denote the stepwise temporal phases along the AB01 core in the Bagnoli-Coroglio SIN (Gulf of Pozzuoli, Tyrrhenian Sea), namely I: Pre-industrial (1827-1851; blue), II: Initial industrial phase & land-use change (1851-1911; green), III: Industrial phase (1911-1950; yellow), IV: Industrial peak and productivity expansion (1950-1992; red) and V: Post-industrial/partial decommission (1992-2016; orange).

Similar changes were also observed in the metazoan community, although their timing was slightly different. Older layers corresponding to pre-industrial and initial phases clustered together and were positively correlated with mud, whereas layers from post- and industrial peak tended to be negatively related with PLI, PAHs TN, TOC, and C/N (Fig. S3.5g), also supported by the correlation analysis (Fig. S3.6). The BIO-ENV analysis identified PAHs, mud and TOC as the most important parameters influencing the metazoan communities changes (Table S3.5). Encrusting metazoans

(ascidians, sponges) were constantly observed until 1911. After 1911, the encrusting and colonial ascidians were replaced by epibenthic and solitarian ascidiaceans that also disappeared after 1954 (Fig. 3.2). The sequences of mainly planktonic Hydrozoa decreased throughout the core and almost disappeared in 1939. The most recent layers (i.e., 1997-2013) were mainly dominated by burial polychaetes (Annelida), whereas Crustacea were dominant in the phase of heavy industrialization (1967-1990).

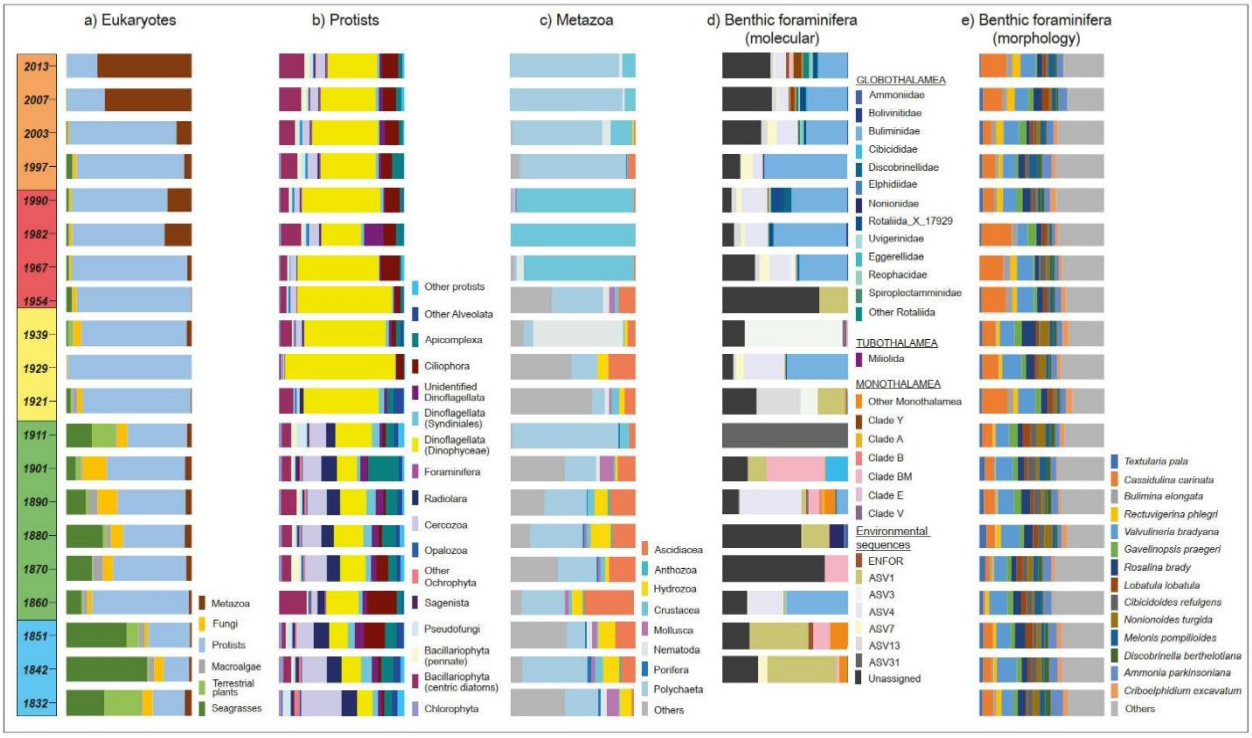

Figure 3.2. Paleo-community composition shift. Eukaryote, protists, metazoa, and benthic foraminifera (molecular and morphological) composition changes along the AB01 core in the Bagnoli-Coroglio SIN (Gulf of Pozzuoli, Tyrrhenian Sea) inferred from multimarker sedaDNA data from 1827 to 2013. The different colours over the ages refer to the main phases (I: blue; II: green; III: yellow; IV: red and V: orange) as identified in Figure 1.

3.3.3. Changes in diversity and ecological indices

The faunal turnovers were accompanied by changes in alpha-diversity (H') and ecological indices (Fig. 3.3 and Table S3.6). From 1832 to 1921, relatively higher diversity values were identified for protists and dinoflagellates, and morphospecies of foraminifera. A similar trend between 1954 and 1967 was observed for metazoan diversity, while the opposite was instead found for prokaryotes,

diatoms, and foraminifera. *Posidonia oceanica* meadows were consistently identified from 1832 to 1911 when it substantially disappeared along with terrestrial plants. This dramatic event was associated with a clear shift in foraminiferal assemblage dominated by epiphytic species and replaced by infaunal ones after 1911 (Fig. 3.2 and Table S3.6). Encrusting metazoans followed a similar trend showing higher percentages in the pre-industrial and partly in the early industrial phases, except in 1939.

The microgAMBI values increased progressively from the oldest sediment layer to the recent ones with the highest values (3.5) corresponding to the period from 1967 to 1990 and then slightly decreased. These values allowed us to classify ecological quality status (EcoQS) conditions from good/moderate in 1901 to mostly poor in 1967-1990 (Fig. 3.3 and Table S3.6). A similar trend was found for the probability of toxicity (i.e., m-ERM-q) with a marked peak in 1967. The abiotic factors explaining the changes in prokaryotic diversity were mud, C/N, TOC and TN (Fig. S3.6). Foram-AMBI showed a clear increasing trend from 1911-1922 to 1982-1990 and a shift from good-moderate to moderate EcoQS. A similar trend was also found for gAMBI values based on macroinvertebrate molecular data with two relevant peaks pointing to bad EcoQS in 1921 and 1967. Overall, the gAMBI mostly classified the EcoQS as excellent up to 1901 and moderate-to-bad afterwards (Fig. 3.3 and Table S3.6).

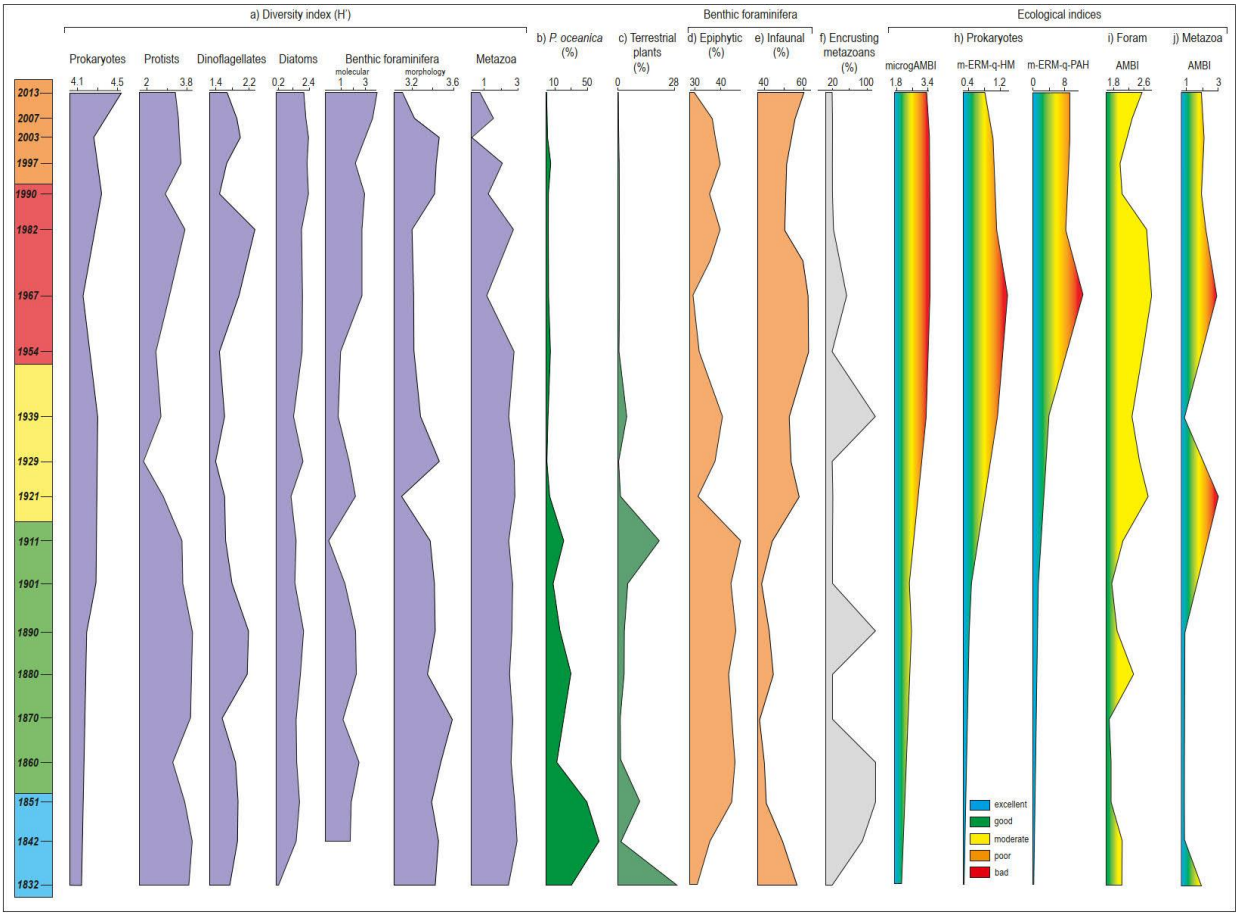

Figure 3.3. Changes in diversity and ecological indices. Diversity (H') plots of prokaryotes, protists, dinoflagellates, diatoms, benthic foraminifera (molecular and morphological) and metazoa coupled with relative abundance of *Posidonia oceanica*, land plants, epifaunal and epiphytic foraminifera and encrusting metazoa percentages. Ecological indices for prokaryotes (microgAMBI, m-ERM-q-HM, and m-ERM-q-PAHs), foraminifera (Foram AMBI) and metazoa (AMBI) are also plotted. The different colour over the ages refer to the main phases (I: blue; II: green; III: yellow; IV: red and V: orange) as identified in Figure 3.1.

3.4. Discussion

The fluctuations of geochemical proxies, the *sedaDNA* records, the alpha-diversity (H') and ecological indices observed in the AB01 sediment core over two centuries reflect the ecosystem changes in the history of the area resulting from anthropogenic activities. The HCAs multimarker *sedaDNA* records consistently reveal a five-phase evolution of the area that perfectly matches with the anthropogenically induced environmental changes as supported by historical archives and other sources (Figs. 3.1 and 3.2). The environmental changes have not only resulted from contamination of the site but also from the geomorphological changes resulting from the expansion of the production

site (i.e., reclaiming the area between the two piers "*Colmata a Mare")* and those that modified water circulation and sediment deposition (e.g., Lazzaretto and Nisida linking, piers' construction) (Fig. 3.1). Taken together, these anthropogenic activities led to a concurrent modification of the biological communities from prokaryotes and protists to higher plants and metazoans, impacting their diversity and ecological indices. The five phases of the ecological transformation of the area are discussed below.

Anthropogenic activities as demonstrated in Siano et al., (2021) and in this study led to irreversible shifts in biological communities. In our study all trophic levels were impacted from prokaryotes and unicellular eukaryotes to higher plants and metazoans. As a result, their diversity and ecological indices were altered.

3.4.1. Phase I (1827-1851)

Until the Industrial Revolution, the Bagnoli-Coroglio plain was a marshy back-barrier as supported by geomorphological evidence and the presence of palustrine sediments (Ascione et al., 2021) (Fig. 3.1-b). Moreover, biotic and abiotic values inferred an unpolluted environment. Agriculture was the main activity and the whole area was characterized by a few residential constructions and some touristic resorts along the beach, where thermal springs were just discovered. The lowest values of both organic and inorganic contaminants are recorded in this phase together with the highest diversity values of different biological communities (i.e., protists, dinoflagellates, foraminifera, metazoa). All ecological indices (e.g., AMBIs and m-ERM-q) inferred excellent and good conditions. This finding indicates pristine environmental conditions, the ecosystem baseline with insignificant anthropogenic impacts. The most evident signature in our records is the very high relative abundance in this phase of higher plants and more importantly of the seagrass *P. oceanica* (Fig. 3.2).

3.4.2. Phase II (1851-1911)

From the mid-1800 to the beginning of the 20th century, a long sequence of anthropogenic interventions has deeply modified the natural landscape of the area. This period shows not significantly changes in biological composition and remains an environment almost unpolluted. The initial projects for settling the industrial district at Bagnoli plain dated back to 1852, when the glasswork Melchiorre - Bournique and the chemicals plant Lefevre went into operation (Cirillo et al., 2022) (Fig. 3.1-b). In 1907, the tuff reef of Lazaretto was linked to the Island of Nisida (Fig. 3.1-b). In 1905, the Ilva/Italsider company set up the construction of one of the largest Italian steel plants that started its production in 1911.

The environmental parameters and paleo-community records do not show any substantial change during Phase II still reflecting good environmental conditions with minor variations imputable to early urbanization and land-use changes. These data match well the information deriving from the historical archives and the mapping of benthic community where *P. oceanica* meadows were indeed recorded between 10 and 30 m depth up to the first decade of the pre-industrial period (1910) in front of the Bagnoli-Coroglio industrial area (Porzio et al., 2020). However, the signature of *P. oceanica* decreased in this period paralleled by a reduction of terrestrial plants, whose signature almost disappeared after 1911 (Figs. 3.2 and 3.3). This was probably due to a change in land use of the area where orchards were progressively replaced by buildings for workers (ca. 2000 people in 1910 and 4000 in 1918 at Ilva/Italsider) in the expanding industrial area (Selvaggio, 2015). This phase, as compared to the subsequent ones, was characterized by higher abundances of parasitic taxa, mainly Syndiniales (parasites of dinoflagellates, radiolarians, ciliates) and Apicomplexa (parasites of metazoans) (Fig. 3.2), which may be related to the presence of specific hosts and further indicates a marked change of the community composition in the area.

3.4.3. Phase III (1911-1950)

This period marks the beginning of the industrial phase. Pollutants concentration start to increase and notable changes in biological composition were observed. The environmental ecological status

turned from unpolluted to polluted. In 1927, a factory for the production of blast furnace cement was built, and three years later, a pier was constructed for loading finished products and receiving coal and iron ores from vessels (Fig. 3.1-b). In 1936, the Island of Nisida was completely linked to the mainland by a 700-m-long strip of land that modified water circulation dynamics and the sedimentological pattern in the Gulf of Pozzuoli (Fig. 3.1-b). In 1936, a plant to produce asbestos (Eternit) started its activity and in 1940 a northern jetty was built. The enlargement of the factory continued till 1943, when the Second World War interrupted plant operations up to 1946. In this period, a marked contamination started with an overall increase of mostly inorganic chemicals (i.e., PLI) pointing to moderately-to-highly polluted conditions. PAHs started to increase with concentrations higher than the Effect Range-Low (ER-L) and, at the end of the Phase III, even higher than Effect Range-Median (ER-M). The extreme concentrations of PAHs (up to 87,000 μg g^{-1} d.w.) and their predominantly pyrogenic origin were also reported along with short cores in the beaches surrounding the former industrial plant (Passaro et al., 2020).

These changes are accompanied by radical paleo-community shifts in *sedaDNA* archives, namely the disappearance of *P. oceanica*, and important turnovers in the communities of protists and metazoans. *Posidonia oceanica* is an ecosystem engineer species endemic to the Mediterranean Sea that forms dense meadows in areas characterized by clean and clear waters (Marbà et al., 2014). The disappearance of this habitat-forming species was accompanied by a drastic decrease of epiphytic (i.e., plant-dwelling) foraminiferal taxa as well as of encrusting animals such as ascidians (*Botryllius* sp.) and sponges (Fig. 3.2). It can be reasonably hypothesized that the disappearance of *P. oceanica* was related to the construction of the connection between Lazaretto and the mainland in 1906 that altered the hydrodynamics of the area markedly and led to the deposition of finer sediments (silt and clay) leading to higher water turbidity and ultimately to reduced photosynthetic activity. However, grain-size data of AB01 sediment core show only minor variations in the sediment fine fractions (silt and clay) after 1906 (Fig. S3.9). According to Porzio et al. (2020), the massive hydrocarbons (i.e., PAHs) released in this area could contribute to *P. oceanica* disappearance. The changes in water

circulation could also explain a remarkable decrease of planktonic radiolarians, while the modification of the seabed could have led to the replacement of encrusting and colonial ascidian by epibenthic and solitarian ascidiaceans after 1911. In Phase III, considerable changes are observed in the protist community, with a decrease in diversity (Fig. 3.3) and a shift in its composition. Lower relative abundances of parasitic dinoflagellates (Syndiniales), Apicomplexa, Radiolaria, and Cercozoa were compensated by a marked dominance of Dinophyceae, mainly including taxa known to produce resting cysts (Figs. 3.2 and 3.3).

Many of these changes reflect a worsening of the environmental conditions triggered by the beginning of industrial activities. Overall, a reduction in diversity of eukaryotes, protists and foraminifera is associated with the beginning of the industrial activities in 1911 and becomes particularly evident during the maximum expansion of the industrial phase (i.e., 1920-1980) (Fig. 3.3). The increase in Foram-AMBI and microgAMBI, proxies for estimating the EcoQS, is associated with the increase of OM (i.e., TOC and C/N) and reliably follows its patterns. Indeed, this shift in the quantity (i.e., TOC) and possibly the quality (i.e., C/N) of OM strongly matches with the decrease of epiphytic foraminiferal species that are affected by the enhanced OM availability (i.e., higher TOC) with a more refractory origin (i.e., higher C/N). On the other hand, the concurrent increase of infaunal (i.e., organisms living within the sediment) taxa perfectly reflects the enhanced OM availability at the seafloor.

3.4.4. Phase IV (1950-1992)

This period defines the peak of the industrial phase and is mainly reflected by the highest level of contamination with highly-to-extremely highly polluted conditions based on PLI (Fig. 3.1-a). In addition, biological disturbances occur and are reflected in diversity (H') and ecological indices changes. In 1952, the Cementir started its production of concrete and the '60s marked the production peak of steel reaching up to $2x10^6$ tons yr^{-1} and involved ca. 5400 workers at Ilva/Italsider. Between 1962 and 1964, a large amount of contaminated soil from the industrial area was used to enlarge the

industrial area by filling the gap between the two piers and creating the so-called "*Colmata a mare*". In the '70s with 7698 workers at Ilva/Italsider, the steel production started to decrease, in 1985 the Eternit ceased its asbestos production and the steel factory permanently closed in 1992 (Fig. 3.1-b). The highest level of contamination (i.e., PLI and PAHs) was recorded between 1960 and 1987.

The ecological indices associated with prokaryotes, namely m-ERM-q-HM and -PAHs, clearly evidence an increasing trend and a marked peak in 1967 (Fig. 3.3). The Phase IV is also characterized by the worst EcoQS equally indicated by AMBI of prokaryotes, foraminifera, and metazoans, with a marked peak in 1967, in response to the enhanced OM availability. Despite the increase in C/N ratio suggesting a terrestrial origin of OM, the absence of higher plants record based on *sedaDNA* suggests an overall decrease over time of terrestrial inputs that implies a strong contribution of PAHs to the increase of C/N values (Meyers, 1994; Rumolo et al., 2011). In Phase IV, the protist community is still characterized by the marked dominance of cyst forming dinoflagellates as in Phase III (Fig. 3.2). The remarkable abundance of these free-living heterotrophic and mixotrophic dinoflagellates can reflect a change in the trophic structure of the community. Alternatively, it could indicate a specific response of these unicellular organisms to the high concentration of pollutants in the sediments and the overlying water column. The transition between free-living motile stages to non-motile resting cysts occurs in the deeper layers of the water column, close to the sediments (Brosnahan et al., 2017) and it has been shown that high concentrations of heavy metals and PAHs are related to an increase of cyst production (Dale, 2001; Horner et al., 2011; Triki et al., 2017). The Phase IV was characterized by a marked reduction of metazoan diversity starting from 1954 (Fig. 3.3). The delayed response of metazoans compared to planktonic protists might be associated with the higher sensitivity behaviour of the latter to water chemical and physical variations that allow them to respond to changes rapidly. It might be speculated that the time lag response of metazoans is also linked to their higher position in the marine trophic web.

3.4.5. Phase V (1992-2016)

After the dismantling of the site started between 1994 and 2000 the Bagnoli-Coroglio area was included in the SIN list by the Italian Government, highlighting the threat to human health and the need to apply a remediation program (Ausili et al., 2020; Morroni et al., 2020; Romano et al., 2004). In the early 2000s, the first remediation projects were planned but the complete remediation has not been completed (Fig. 3.1-b). This post-industrial phase shows an overall reduction of contamination, though PLI and PAHs still remain high, and a concurrent increase of diversity indices values. Metazoans dominated in the most recent layers (2013 and 2007) and were mainly represented by polychaetes that are currently abundant in the sandy bottom of the Bay of Bagnoli-Coroglio (Fasciglione et al., 2016; Morroni et al., 2020).

3.5. Conclusion and future perspectives

The present study provides the first holistic insight into the ecosystem changes that occurred in one of the most polluted marine coastal areas during the last two centuries. In the absence of long-term ecological studies of coastal communities, paleogenomics offers a unique opportunity to reconstruct past changes in biodiversity by linking them to environmental change and increased anthropogenic pressure. The investigation of *sedaDNA* allows us to retrospectively identify a five-stage stepwise evolution in the prokaryotic and eukaryotic communities, demonstrating how the industrial pollution and land-use changes have deeply modified their natural equilibrium. The site was characterized by seagrass meadows and high eukaryotic diversity until the beginning of the 20th century. Then, the ecosystem completely changed, with seagrasses and associated fauna as well as diverse groups of planktonic and benthic protists being replaced by low diversity biota dominated by dinophyceans and infaunal metazoan species. The *sedaDNA* approach enables to disentangle the multi-level cascade effects of industrialization, bringing to light the pre-industrial reference conditions and showing that after 20 years of decommissioning, the good ecological conditions have not fully recovered yet.

From the future perspective, it is important to highlight that paleogenomics is not only a tool for recording past ecosystems but might also help in assessing the recovery of degraded coastal marine ecosystems. Our metabarcoding approach is universally applicable. It is based on standardized and widely available protocols. It could be applied to any other polluted sites, as long as the reference database for local fauna and flora, especially the bioindicator taxa, is available. The open question is whether it is possible to recover the reference conditions revealed by paleogenomics. In the case of Bagnoli Bay, the ecosystem changes might be irreversible. The return to pristine conditions would require reintroduction of *Posidonia* meadows, which might be difficult if not impossible. However, in other less polluted sites, it might be still possible to conduct remediation actions that would lead to the recovery of preindustrial conditions. In such cases, the investigation of sedimentary DNA archives is highly recommended as this is the only way to obtain a holistic overview of the past biodiversity and ecosystem changes.

___*Personal contribution: Morphological foraminifera analysis, bibliographic review, maps creation, figures creation, analysis of results*___

Chapter IV

4. Paleoenvironmental Impact: the Morphometric Variation of Benthic Foraminiferal Species in Bagnoli-Coroglio SIN (Site of National Interest)

4.1. Introduction

The industrial activities, started worldwide in the mid of 1800, have always been one of the primary sources of chemical contamination of aquatic and terrestrial environments. Since pollutants tend to accumulate in sea sediments, which can be considered as the final sink of contamination due to their tendency to adsorb contaminants in the finest fractions (Li et al., 2000), the plants that operate in coastal areas have a particularly strong impact on the marine ecosystems.

Benthic foraminifera, single cell organisms, have hard tests (i.e., shells) often preserved in the sediment forming fossil assemblages (Klootwijk et al., 2020). This characteristic makes them a reliable proxy for paleoenvironmental reconstructions (i.e., Alve, 1991; Hayward et al., 2004; Scott et al., 2005). Because of their short life cycle, they quickly reflect changes of the abiotic factors (i.e., chemical-physical parameters) in their assemblages in terms of morphology and diversity. Therefore, they have been widely used as proxies for assessing the anthropogenic impact in marine environments (Alve et al., 1995; Bouchet et al., 2007; Bouchet et al., 2012; Francescangeli et al., 2020) as well as to characterize changes in the environmental conditions (e.g., climate changes, nutrient concentration) of a marine ecosystem (Alve et al. 2009). Variations of test sizes are proved to be linked to changes of environmental parameters (i.e., environmental disturbances) in both planktonic and benthic foraminifera assemblages (Abramovich and Keller, 2003; Falzoni et al., 2018). Decreases in size have

been interpreted as a synonymous of environmental stress in many investigations (i.e., McKinney, 1990; Ferraro et al., 2020), defining the dwarfism (i.e., Lilliput Effect) as globally associated with past environmental perturbations also related to smaller extinction events (Urbanek, 1993). Abnormalities (i.e., deformities and dwarfism) in benthic foraminiferal assemblages have been related to low O_2 values, high Polycyclic Aromatic Hydrocarbons (PAHs) and Potentially Toxic Elements (PTEs) concentrations (Peréz-Cruz and Machain-Castilho, 1990: Samir and El Din, 2001: Armynot du Châtelet et al., 2004: Vilela et al., 2011).

Another marine organism commonly used as bioindicators of the ecological status of a marine ecosystem is the *Posidonia oceanica*. Thanks to its ecological role, sensitivity to stress and widespread distribution, the Mediterranean endemic *P. oceanica* has been chosen by the European Union within the Water Framework Directive (WFD, 2000/60/EC) as a Biological Quality Element to classify water bodies (Pergent-Martini et al., 2005).

Marine biomonitoring studies are often based on "recent" sediments (i.e., regarding the last 20 years), while the anthropogenic contamination has been affecting the actual ecosystems for decades. Therefore, in marine paleo-contamination assessments, the baseline conditions should be referred to the period before the industrialization, indeed to the sediments deposited before the 1860 (Dale et al., 1999; Alve et al., 2009). In this scenario, the analysis of sea sediment cores and the variation of its ecological communities is a great tool to distinguish the effects of pollution from the natural background and to evaluate the consequences of pollution on the marine ecosystem (Alve, 1991; Pergent-Martini, 1998) Cobelo-Garcia et al, 2003).

The Italian Government has recognized as Sites of Nation Interest (SINs) certain areas where the anthropogenic contamination is causing an environmental risk and, therefore, a remediation programme is needed to restore the area (www.isprambiente.gov.it). The Bagnoli-Coroglio SIN hosted the second largest Italian steel factory (Trifuoggi et al., 2017). The former Bagnoli industrial district operated from the beginning of the XX century till the early '90s critically affecting the

geochemistry and the morphology of the coastal environment of the Gulf of Pozzuoli (Molisso et al., 2020). Many surveys (i.e., Damiani et al., 1987) established a high degree of anthropogenic contamination due to PAHs, generated from coal and oil combustion, and PTEs. Others found the foraminiferal communities extremely affected (Bergamin et al., 2005) and a bad Ecological Quality Status (EcoQS) (Cavaliere et al., 2021) in the area.

In this research, it has been analysed the temporal morphometric variations of benthic foraminiferal assemblages in a core collected in the Gulf of Pozzuoli in proximity of the highly polluted coastal area of the Bagnoli-Coroglio SIN. The analysis on the sizes of tests were performed on two target species (i.e., *Rosalina bradyi* and *Valvulineria bradyana*) with different ecological behaviour. The historical foraminiferal records were also integrated with the variations of contamination due to PTEs and PAHs in the marine sediment along the core, as well as the temporal variation of the relative abundance of *P. oceanica*.

The aims of this study are: i) assessing the benthic foraminiferal response to the paleo-environmental stress due to the anthropogenic contamination; ii) understanding the correlations between the chronological information about Bagnoli industrial district and the temporal morphometric variations of the target species; iii) describing the effects of the anthropogenic impact on the marine ecology during the last 150 years.

4.2. Study area and historical changes

The Bagnoli coastal area is located in Campania region, in the western sector of the city of Naples (Southern Italy) (Fig.4.1). It faces the Tyrrhenian Sea in the eastern part of the Gulf of Pozzuoli.

The geomorphology is flat and the geology of the area is volcanic. In fact, Bagnoli plain belongs to Campi Flegrei caldera, a volcanic field where the volcanic activity, started 200 kyr, has produced ignimbrite and tuff emissions, hydrothermal and seismic activity (Barberi et al. 1984; Di Vito et al., 1987; Troise et al. 2007; Del Gaudio et al. 2010) originating around 50 craters within the caldera (Fig. 4.1).

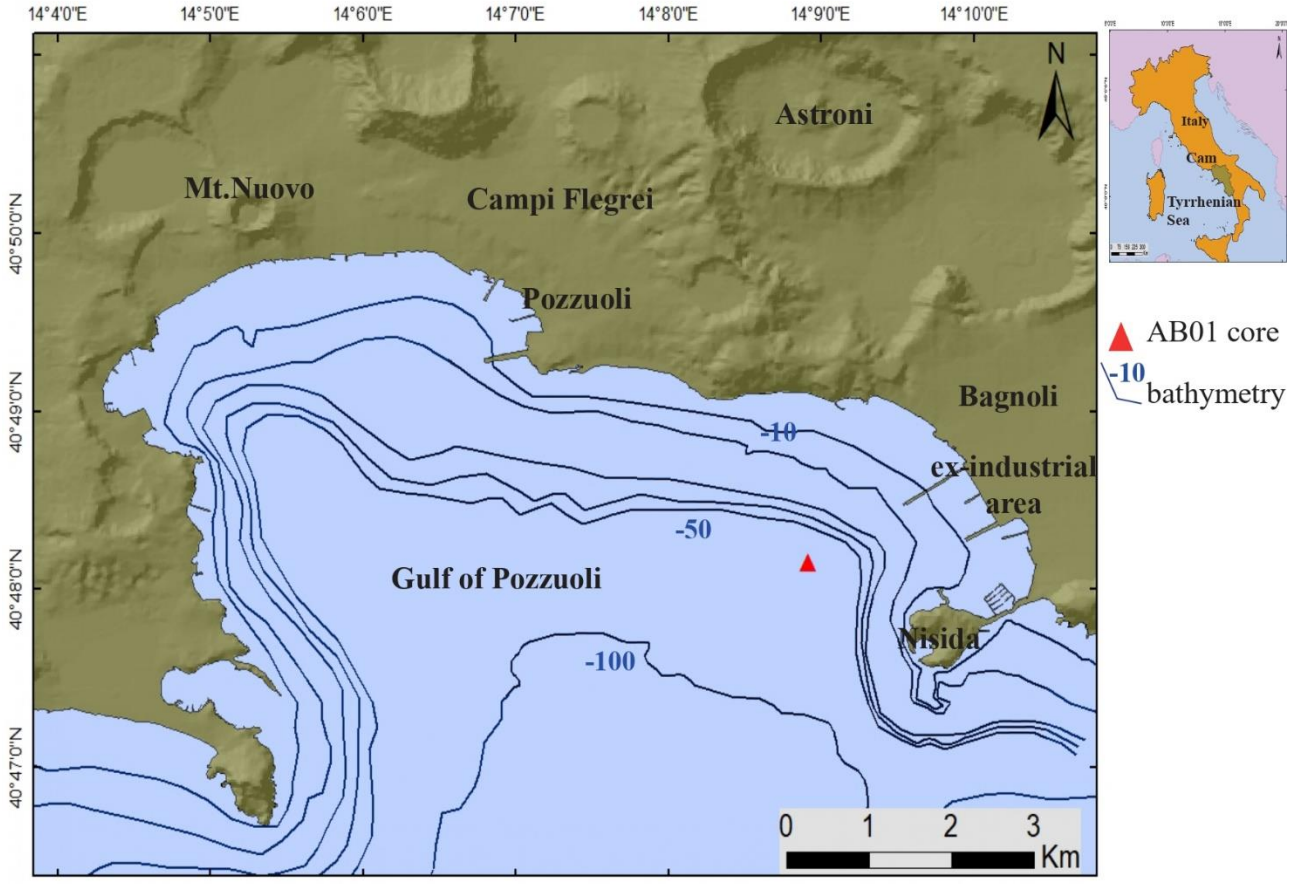

Figure 4. 1 Study area. Location of the Bagnoli-Coroglio SIN within the Campi Flegrei Caldera. Geographical coordinates referred to the World Geodetic System 1984 (WGS-84).

During the Roman Age, the strong urbanisation occurring in Campi Flegrei led the Pozzuoli town to become one of the most important harbour of the Roman Empire.-Till the XIX century, Bagnoli was a rural area, with cultivated lands and recreative structures along the sandy beach, where several thermal springs occurred (Cirillo et al., 2016).

With the Industrial Revolution time, thanks to its geomorphologically features, the plain of Bagnoli was chosen to host an industrial district and the urbanisation of the city of Naples started to spread toward west. Since then, the coastal landscape has been markedly altered. In 1907, the glasswork Melchiorre - Bournique and the chemicals plant Lefevre started their production and the rocky reef of Lazaretto was linked to the Island of Nisida (Fig. 4.2). A steel plant of the ILVA company was inaugurated in 1910 and in 1930 a long pier was constructed. The Island of Nisida was bridged to the mainland in 1936, affecting the local hydrodynamic of water circulation in the whole

Gulf (Fig. 4.2). The enlargement of the factory continued (in 1952 the concrete plant of Cementir was built), leading the industrial district to a 2km^2 extension in 1954 (Fig. 4.2). Between 1962 and 1964, the industrial area was enlarged of roughly an extra 2 km^2 toward offshore, dumping highly contaminated soil between the two piers (area named *Colmata a mare*).

The decrease of steel demand and production caused the end of any industrial activity between 1985 and 1992, when the former ILVA was closed down and later dismissed.

In 2000, the Italian Government declared the Bagnoli-Coroglio area (the brownfield plus the adjacent sea sediment) as a SIN (Site of National Interest) (Romano et al., 2004; Ausili et al., 2020). In 2004, the industrial buildings were almost completely dismantled (Fig. 4.2) and different remediation programmes were proposed. Nevertheless, the remediation has never been completed (Fig. 4.2).

High concentrations of hydrocarbons and trace elements (i.e., Cu, Fe, Hg, Mn, Pb, and Zn) were diffusely detected in soils and sea sediments constantly during the surveys conducted in the past 30 years (Damiani et al., 1987; Romano et al., 2009; Arienzo et al., 2017). The contamination, clearly linked to the activity of the former plant, affects the sea sediment especially between the two piers at 40-60 metres of depth, along an incised valley who runs toward West from the *Colmata a mare*, where the pelitic component of the sea sediment influences adsorption processes (Albanese et al., 2010; Sprovieri et al., 2020).

Paleoenvironmental studies of the area (Romano et al., 2018) highlighted a marked increase in contamination since the first decades of the last century. Many ecological monitoring programmes have found that anthropogenic contamination also affects the ecological marine fauna in the Bagnoli-Coroglio SIN. The former plant pollution has been correlated to a negative response of foraminiferal assemblages observed in low density and diversity and reduced mean size of certain species (Bergamin et al., 2005) as well as abnormal specimens found (Romano et al., 2008).

4. Materials and methods

4.1. Sampling and samples treatment

The AB01 core (40° 48.150' N, 14° 08.913' E) was collected in the Gulf of Pozzuoli in December of 2018. The core was collected at 55 metres of depth and 1.7 km SSW from the Bagnoli area coastline in a location chosen to well characterize the impacted zone. The total length of the AB01 core was of 58 cm. Once collected, the AB01 core was subdivided in 1 cm thick layers for a total of 40 layers. At alternating intervals, a total of 18 layers was chosen for the geochemical-geochronological analysis, while the other layers, collecting 50 mL of each sample, were considered for foraminiferal, ecological analysis and organic matter characterization. Each aliquot was wet weighted and the main physical characteristics were also noted.

More information about the sampling procedure and samples treatment can be found in the *Chapter 3.2.1.Core collection and processing* of the present thesis.

4.2. Core analysis

4.2.1. Geochemistry and geochronology

Information about the geochronology and geochemical analysis of the core can be found in the *Chapter 3.2.3 Radiometric analyses and geochronology* and *3.2.4 Chemical analysis* of this thesis.

To summarize the degree of contamination in a single parameter, the Pollution Load Index (*PLI*) (Tomlinson et al., 1980) was calculated with equation (4.1):

$$PLI = \sqrt[n]{Cf_1\ Cf_2 \dots Cfn} \quad (4.1)$$

where n is the number of PTEs considered, and C*f*i is the Contamination Factor (Cf) of the element considered, calculated standardizing the concentration of the element to the background of the same element as expressed in equation (4.2):

$$Cf = \frac{[element]i}{[element]background} \quad (4.2)$$

Local background concentrations chosen are based on different studies in the Campi Flegrei and Bagnoli area (Damiani et al., 1987; Cicchella et al., 2005; De Vivo and Lima, 2008) and reported in Table S2.1. PLI classification, based on Zhang et al., 2011, is reported in Table S.2.2. PAHs concentrations are compared with the threshold declared by the Italian Government (D.Lgs. 152/06), which establishes the threshold of intervention of 100 mg/kg for industrial and commercial soils. The PAHs concentrations were also compared with the limits expressed by Sediment Quality Guidelines (SQGs) (Burton, 2002; McGrath et al., 2019). In particular, to the effect range low (ERL) (3.5 mg/kg of PAHs) (Burton, 2002), which indicates values below which effects are not likely observed (Long et al., 1995), and to the effect range median (ERM) (23.5 mg/kg of PAHs) (Burton, 2002), which express concentrations of a pollutant above which toxic effects are commonly observed (ICRAM-APAT 2007; McGrath et al., 2019).

For the organic matter characterization, sediment samples were dried in an oven (60 °C) and subsequently ground and homogenized. Sub-samples were then weighed (~10–20 mg) in silver capsules and treated with increasing HCl concentration solutions (v/v 8%, 18% and 25%) to completely remove the inorganic carbon fraction (carbonates). Total organic carbon (TOC) and total nitrogen (TN) were analysed using a Thermo Electron Flash Elemental Analyzer (EA 1112) calibrated with acetanilide (C_8H_9ON, elemental composition: 71.09% carbon and 10.36% nitrogen) standards. The results were expressed in percentage of dry weight.

4.2.2. Benthic Foraminifera – Morphometric analysis

For the foraminiferal morphological analysis, 20 samples were considered. After gently washing 50 mL of the samples through a 63-μm sieve to eliminate mud particles, residues were oven-dried at 40°C overnight and around 300 foraminifera specimens (280 on average) for sample were dry picked in the > 125 μm sediment fraction. The picked specimens were placed in microslides for microscopic observations, executed using an optic microscope. Tests were compared to Cimerman and Langer

(1991), Sgarrella and Moncharmont Zei (1993), and Milker and Schmiedl (2012) for the taxonomical classification of benthic foraminifera species. Two target species, *Rosalina bradyi* and *Valvulineria bradyana*, were chosen among the most abundant ones in order to represent two different ecological behaviours and stress tolerance based on Barras et al. (2014), where, the *R. bradyi* is considered as a stress-sensitive species, while the *V. bradyana* is described as a stress tolerant species (Bergamin et al., 1999).

The high-resolution tests images were acquired using the Carl Zeiss™ AxioVision Rel. 4.8.2 Software. The measures of both species were executed using the same software.

The overall trends of sizes variations were plotted applying a moving average, calculating the average between three consecutive values to smooth the raw trend.

All the plots expressing the temporal variations of the ecological and diversity indexes were performed using the software STATISTICA 13.5.

4.2.3. Posidonia oceanica

Information about the *Posidonia oceanica* abundance calculation can be found in the *Chapter 3.2.7. Eukaryotes, foraminiferal and metazoan metabarcoding.* The relative abundance of *P. oceanica* was calculated as percentage among the whole eukaryotic communities.

4.4. Results

4.4.1. Temporal changes in contamination

The dating model applied to the core allowed to calculate an accurate geochronological reconstruction, with average intervals of around 5 years between each sample. The bottom core (42 cm of depth) was dated back to 1820 whereas the top was dated back to 2016. The sedimentation has been regular over the whole period with an average rate of 0.2 cm/ year.

The temporal variations of the PTEs concentrations observed vary considerably. Almost every PTEs considered (Cd, Cr, Cu, Ni, Pb and Zn) occurred with the same trend, ranging between the minimum values reached in the second half of 1800 (0.16 mg/kg; 14.3 mg/kg; 23.97; 0.39; 82 and 74 mg/kg respectively) and the maximum ones (2.69 mg/kg; 56.42 mg/kg; 115.32 mg/kg; 2.77 mg/kg; 648 mg/kg and 1224 mg/kg respectively) reached in 1975. Hg concentrations showed a different trend, with the maximum concentration occurring in 1925. Similarly, the PLI exhibited lower values (around 1) till the 1905 (unpolluted to moderately polluted), when a marked increase occurred till 1975 (maximum value = 6.8) leading the area to be very highly polluted. After then and till 2016, an overall decrease of PLI is observed, although the values (on average 4.4) kept being classified as moderately to highly polluted/ highly polluted (Fig.4.2).

Total PAHs concentration occurred with a very similar trend, ranging from 0.5 mg/kg in 1846 to 301.6 mg/kg in 1975. It is important to highlight that the increase of PAHs started from the 1944, slightly later than the PLI. From 1880, PAHs values started to be above the ERL, and from 1925 their concentrations were higher the ERM. All the layers from the 1950 to the most recent one contained PAHs in concentrations higher than the industrial threshold of intervention (D.Lgs. 152/06) (Fig. 4.2).

The TOC concentrations range between 1.12% (in the 1870) and 4.95% (in the 1982) (on average 2.2%). The maximum value is found in the 1982, while the minimum one in the 1870. Overall, TOC concentrations show low values till the 1911(values below the 1.5%), followed by a marked increase between the 1921 and the 2013, with values constantly close or above 2%. C/N ratio ranges between 18.9 (in the 1832) and 46.5 (1982). Its temporal variations exhibit a very similar trend, with minimum values (average below 30) between the core bottom and 1929, and maximum values found in the upper section (between 1939 and 2013), where the average increases to 37.4.

4.4.2. Morphometric and ecological variations

The relative abundance of *R. bradyi* in the total assemblage was around 5.9%. 391 tests of *R. bradyi* were measured overall (on average 21.7 tests for each sample). The minimum abundance found was 14 (in 1975), while the maximum 34 (in 1939). The tests sizes ranged between 0.13 mm to 0.69 mm (on average 0.263 mm). Maximum average values in tests size occurred between 1870 and 1901 (0.3 mm), while the minimum average ones (0.23 mm) were found in 1975 and 2007. Overall, a decrease of tests size was observed from 1911 to the most recent layers (Fig. 4.2).

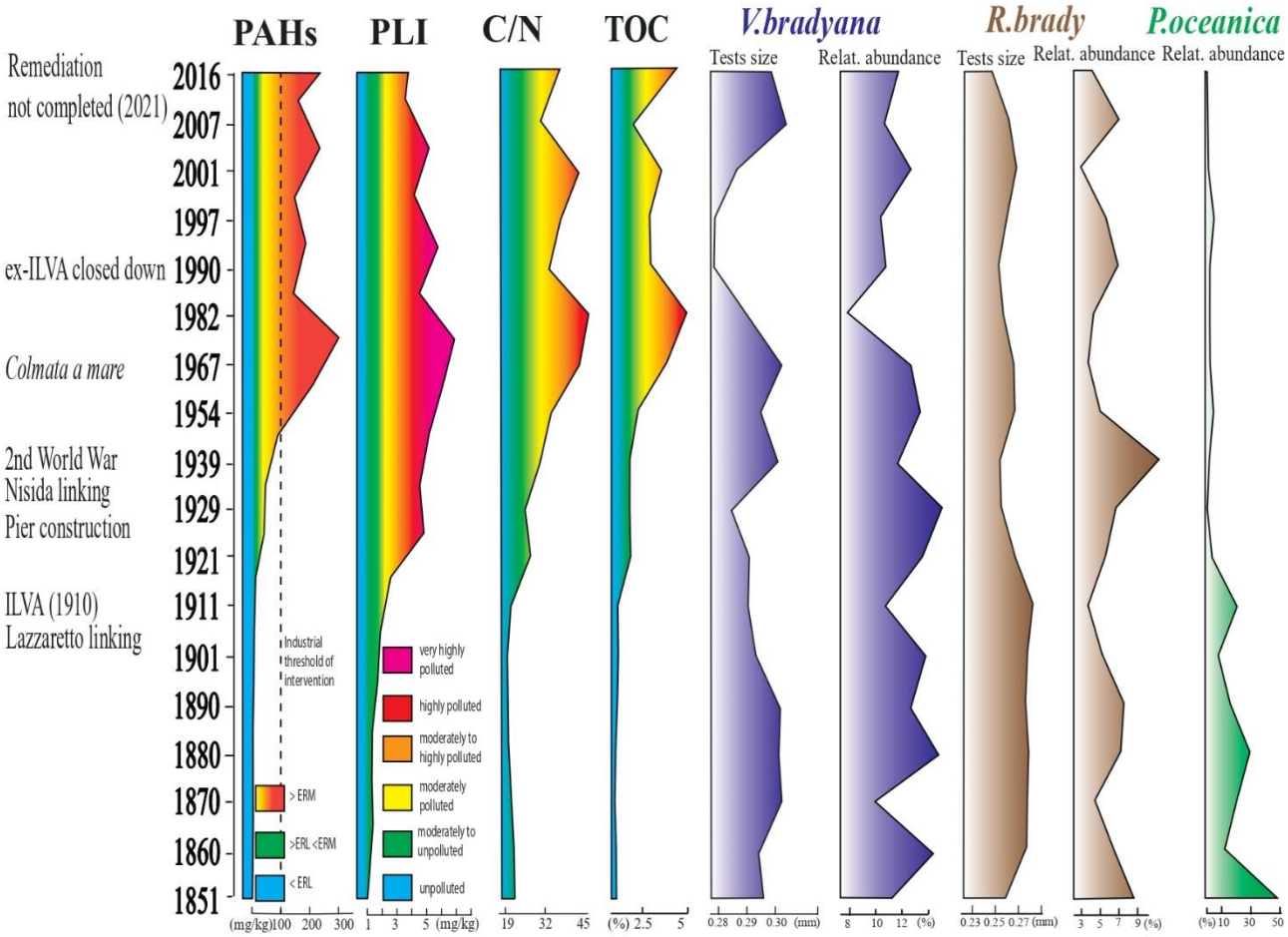

Figure 4.2. Abiotic (PAHs, PLI, C/N, TOC) and biotic (*V. bradyana and R. bradyi* relative abundance, tests size and *P. oceanica* relative abundance) factors temporal variations.

The relative abundance of *V. bradyana* in the total assemblage was around 12.1%, making this species the most abundant within the whole foraminiferal assemblages. 563 tests were measured overall (on average 31.2 tests for each sample). The minimum abundance was 16 (in 1975) and the

maximum 43 (in 1929). The tests sizes ranged between 0.11 mm to 0.55 mm (on average 0.294 mm). Maximum average values occur in 1870 and 1939 (0.31 mm), while the minimum was found in 1990. As general trend, *V. bradyana* tests sizes showed two marked lowest peaks, one in 1929 and another one between 1975 and 2001, with tests reduced by up to 0.02 mm (Fig. 4.2).

Posidonia oceanica relative abundance along the core was also calculated. The layer where it is most abundant is related to the bottom of the core (1851). After then, a first steep decrease led its abundance from around 50% to values ranging between 7% and 29% (in the layers between 1860 and 1911). A second marked decline started in 1921 and continued till 2016. In this interval, the abundance dropped to values below 5%, with some layers where the *P. oceanica* was almost completely disappeared (values < 1%) (1929, 2003 and 2016). Overall, two distinct phases were observed for *P. oceanica* temporal variations. A first one, from 1851 to 1911, when the abundance was high or relatively high, and a second one, from 1921 to the uppermost layer, with disappearance or low abundance of *P. oceanica.*

4.5. Discussion

4.5.1. Morphometric variations vs. chronological events

According to the geochemical analysis, a severe organic and inorganic contamination has been affecting the sea sediment in Bagnoli area since 1921. Sea sediments are contaminated of trace elements and PAHs with concentrations greater than those that are a risk to humans and ecosystems. Sea sediments along the core dated between 1960 and 1982 show the highest pollution of both trace elements and PAHs. The *Colmata a mare* can indeed be clearly considered as the most impacting event happened during the Bagnoli industrial era. Although a slight decrease in contamination after 1985, the high pollution due to PTEs and hydrocarbons found also in the most recent layers (last 20 years) suggests that the pollutants has not been diluted but it continued to accumulate in the sediments also after the plant decommission (Fig. 4.2). The environmental stress between the 1960 and the most

recent layer is also due to the TOC concentrations, which shows an enrichment trend very similar to the temporal variations of the pollutants.

The sedimentological feature and the geographical location have made the sediments of the AB01 core an optimal spot where the contamination could have been accumulating since the first plants activities. The groundwater system existing in Bagnoli plain caused a direct westward flow of trace elements and PAHs. Aquifers waters crossing the brownfield carried pollutants to the Gulf of Pozzuoli seawater firstly and secondary to sea sediments. The silty texture of the sediments at 50-60 metres of depth promoted adsorption phenomena of toxic particles on finest grains.

A strong relation between trace elements contamination and *P. oceanica* abundance has been observed (Fig. 4.2). Particularly, the *P. oceanica* disappearance in 1921 could be linked to the increase of Hg contamination due to the industrial activity. *P. oceanica* has been proved to be particularly accurate in assessing the present and past effect of Hg contamination (Pergent-Martini, 1998) since it tends to accumulate the element in its tissues taking it from the seawater. The bioaccumulation process makes this species able to "memorize" Hg contamination over the decades. In the SIN of Bagnoli-Coroglio this process could be responsible of the regression of *P. oceanica*, particularly considering that the Hg concentration starts to exceed the ERM (1.3 mg/kg) in 1916, reaching its peak in 1925. Although an overall lowering of contamination is registered after then, the concentrations do not decrease below the ERM till 2016. As many authors suggested, the disappearance of *P. oceanica* could not be related only to the PTEs contamination (Ward 1989; Pergen et al., 1995) but also to the other events that affected the marine ecosystem in the Bagnoli area. The linking of Nisida Island to the mainland happened in 1936, but already partially started in 1907 with the linking of Lazzaretto with Nisida Island, would have probably altered the hydrodynamics and sedimentary process of the Gulf of Pozzuoli, increasing the turbidity and lowering the oxygenation of the bottom waters, contributing as well to the decrease of the *P. oceanica* in the area (Fig. 4.2).

Interestingly, *R. bradyi* tests size variation over time shows a trend similar to the temporal variation of *P. oceanica* abundance (Fig. 4.2). Due to its ecological behaviour (i.e., epiphytic), *R. bradyi* tests size could have been affected directly by the sudden decrease of seagrass, which have a structural role in the lifecycle of epiphytic foraminifera, and less by the sediment contamination.

Valvulineria bradyana, an infaunal benthic foraminifera, is commonly known to be an opportunistic species that can tolerate low O_2 environments. Its high dominance in the total benthic assemblages along the core is an interesting signal typical of a high organic matter and low oxygenated environment (Bergamin et al., 1999). *Valvulineria bradyana* present a "delayed" stressed phase respect to *R. bradyi* with a period when it shows smaller tests ranging between 1975 and 1992. The effects of a change in the environmental conditions are also reflected on its relative abundance, which drastically reduces by the 40% in 1982 (from 12.6% in 1967 to 7.8 % the minimum value, in 1982) (Fig. 4.2). The ecological behaviour of *V. bradyana* could explain its tests sizes variation trend. The nature of the organic matter plays an important role in lifecycle of infaunal species such as the *V. bradyana.* In the Bagnoli marine area, the organic matter has mainly a terrestrial origin (Cavaliere et al., 2021), particularly at 40-50 metres of depth in the AB01 core location. The organic matter received by the benthic communities in this area has probably been always abundant, originated from the inland groundwater flow. These conditions, causing a low O_2 environment, favoured the infaunal species proliferation. *Valvulineria bradyana* response to paleo-stress, showed in reduction of tests size and abundance in the '60s, would be explained by a change in the organic matter input contribution. In fact, for distinguishing the source of organic matter in marine environments, the C/N ratio is often used as a great proxy (Gordon and Goni, 2003). Ratio values higher than 20 are often considered to be relative to a terrestrial source of organic matter (Meyers, 1994). In the Bagnoli area, the input is balanced (i.e., marine and terrestrial) till the 1921, when the organic matter origins start to be prevalently terrestrial. After the *Colmata a mare* ('60s), the organic matter enrichment is very high and the input turns into totally terrestrial. High concentrations of hydrocarbons are directed toward the sea sediments from the contaminated former-plant soils just discharged along the Gulf of

Pozzuoli coastline. The marked decrease in tests dimensions and abundance for *V. bradyana* could be linked to its ecological responses to the toxicity effects of hydrocarbons and to an extreme contribute of terrestrial organic matter.

Overall, chemical contamination in Bagnoli area has significantly altered the marine ecosystem following temporally and chemically different patterns. Firstly, from the 1925, the water pollution due to trace metals contamination (i.e., Hg) affected the *P. oceanica* and the epiphytic benthic communities species, and secondly, in 1962-1964, after the Colmata a mare, the sediment contamination, mainly due to PAHs, affected the infaunal species. Although the plant decommission and the remediation projects, the ecological and geochemical background conditions are far from being restored.

4.6. Conclusions

The organic (i.e., PAHs) and inorganic (i.e., trace elements) contamination has been affecting the Bagnoli area for the last 100 years. The contamination and the other human interventions (Nisida linking) have altered the marine ecosystem equilibria, causing the disappearance of certain species (i.e., *P. oceanica*) and stressed living conditions for others (*V. bradyana* and *R. bradyi*). In particular, the stressed conditions are registered by the benthic foraminifera communities also as temporal variations in abundance and tests sizes. The differences between the tests size variations trends strictly depend as well on the ecological behaviour of the species. Benthic foraminifera confirmed to be a great proxy for evaluating detailed temporal variations in environmental and ecological factors of a marine area.

____Personal contribution: Morphometric foraminiferal analysis, bibliographic review, figures creation, analysis of results, MS writing___

Chapter V

5. Paleoenvironmental changes in the Gulf of Gaeta (central Tyrrhenian Sea, Italy): a perspective from benthic foraminifera after dam construction

Submitted to **Water** (Special Issue Research on the Aquatic Species Biodiversity and Morphology) in January 2023.

M. Cavaliere, V. Scipioni, F. Francescangeli, L. Ferraro and F. Frontalini

5.1. Introduction

Benthic foraminifera are single-celled organisms commonly used as environmental tool in biomonitoring programmes of coastal and estuarine sedimentary environments (e.g., Frontalini et al., 2014; Armynot du Châtelet et al., 2018; Francescangeli et al., 2021; Cavaliere et al., 2021). Because of their abundance, diversity, sensitivity to environmental changes (e.g., variations in organic matter, pollutants, water and sediment physical parameters), as well as their fossilizable tests (i.e., shells), they have been widely used to investigate short- and long-term paleoclimatic variations and in paleoenvironmental reconstructions (Hayward et al., 2010; Francescangeli et al., 2018). The investigation of sediment archives (i.e., cores) allows us to read the historical environmental variations resulting from natural climatic fluctuations and antrophic activities over time (e.g., Alve et al. 2009; S. dos S. de Jesus et al., 2020; Barrenechea Angeles et al., 2023). In the Anthropocene Epoch, foraminiferal-base proxies have record the dramatic signature of anthropogenic impact on

modern ecosystems, distinguishing background (i.e., pre-impacted) from human-induced conditions (e.g., Alve et al., 2009; Francescangeli et al., 2016; da Silva et al, 2022).

Marine coastal areas receiving loads of continental sediments are strongly related to the human activities (e.g., vegetation or land use change, human settlement and industry) such that they can be registered in the sedimentary records (Horrocks et al., 2007). Indeed, rivers' mouths are complex environments, where complex interactions between the fresh and marine waters take place (MacDonald et al., 2013; Horner-Devine et al., 2015). Riverine waters have therefore a strong impact on the marine areas nearby the mouth that represents possible contamination pathways to oceans. In this scenario, monitoring the fluvial inputs (i.e., water and sediments) in terms of quality and quantity is crucial to understand the dispersal mechanisms of sediments, nutrients and pollutants and their effects on the surrounding marine and estuarine environments (Wright, 1977; De Pippo et al., 2003). Indeed, changes in the coastal ecosystems are also driven by constructions of dams that can unbalance the natural discharge of sediment.

The Tyrrhenian Sea, with a high sedimentation rate, represents a key area for assessing paleo-climatic and -environmental changes over the last centuries (Budillon et al., 2005; Sacchi et al., 2009; Lirer et al., 2013, 2014). In particular, the sedimentary records of Gaeta Gulf (Campania Region, south-western Tyrrhenian Sea) have been deeply investigated (e.g., Bonomo et al., 2016; Margaritelli et al., 2016; Di Rita et al., 2018; Misuraca et al., 2018). Correlating multi-proxy data and historical archives, Margaritelli et al. (2016) recognized several climatic intervals in the last five millennia. During the last centuries, palynological analyses have revealed clear shifts of vegetation patterns in the coastal inland of the Gulf of Gaeta due to paleoclimate changes (Di Rita et al., 2018). However, the area has also experienced an increase in human activities with deforestation and the development of agricultural activities (e.g., farming, field harvesting, ornamental species culturing).

During the last years, the waste disposal management turned into a dramatic issue in the Campania Region. Illegal discharges of industrial and urban waste have been documented in continental and marine environments, including illegal dumping and burning of toxic waste (D'Alisa et al., 2015,

Legambiente, 2014). The impact events and the common burns of industrial residuals made the Campania Plain be known as Terra dei Fuochi (Land of Fires), with toxic compounds possibly migrating from soils to groundwater, rivers and estuarine and coastal environments. Moreover, the increase of agricultural activities in Campania has caused a high input of pesticides and fertilizers in aquatic environments with a consequent deterioration of the water quality (Triassi et al., 2022).

The present research aims at implementing the outcomes of previous studies in the Gulf of Gaeta by focusing on the response of benthic foraminifera to historical human-induced changes in the last ca. 300 years. Our reconstruction ranges between the 1686, late period of the Little Ice Age (ca. 1250 –1850), to the Modern Warm Period (ca. 1950 CE–present). Furthermore, the effect of land-use change on benthic foraminiferal communities will be carefully investigated during this temporal interval.

5.2. Study area

The Gulf of Gaeta (Tyrrhenian Sea) is located in the central part of the Tyrrhenian Sea, the deepest basin in the western Mediterranean Sea (Astraldi and Gasparini, 1994). The gulf is bordered by the Aurunci Mounts and the Roccamonfina volcano (Radicati di Brozolo et al., 1988) in the northern sector, by the Apennine fold-and-thrust belt in the eastern sector and by the Neapolitan volcanic complex in the southern sector (de Alteriis et al., 2006) (Fig. 5.1).

The geomorphological and geophysical features of the Gulf of Gaeta are strongly connected to the Volturno River and its discharge (40 m^3s^{-1}). The Volturno River is the longest river in southern Italy (ca. 175 km of length) and its catchment basin (ca. 1550 km^2) includes territories of Campania, Molise and Lazio regions (Iermano et al., 2012). The last sector of the Volturno River crosses the Campanian plain, flowing till the town of Castel Volturno, where its mouth is located. The Gulf of Gaeta seafloor can be described as a typical continental shelf characterized by the alluvial plains of the Volturno and Garigliano Rivers. The Quaternary clastic and volcanic deposits prograde gradually

westward, deepening sharply at 120 metres of depth (De Pippo et al., 2003; de Alteriis et al., 2006; Misuraca et al., 2018).

In the Gulf of Gaeta, the water circulation is characterized by the interactions between a cyclonic vortex with the superficial and intermediate waters (De Pippo et al., 2003; Bonomo et al., 2014). Similar to the overall Tyrrhenian circulation, two seasonal currents influence the coastal circulation in the Gulf of Gaeta as well as coastal morphology, and submerged morphostructures (Moretti et al., 1977; Sorgente et al., 2020).

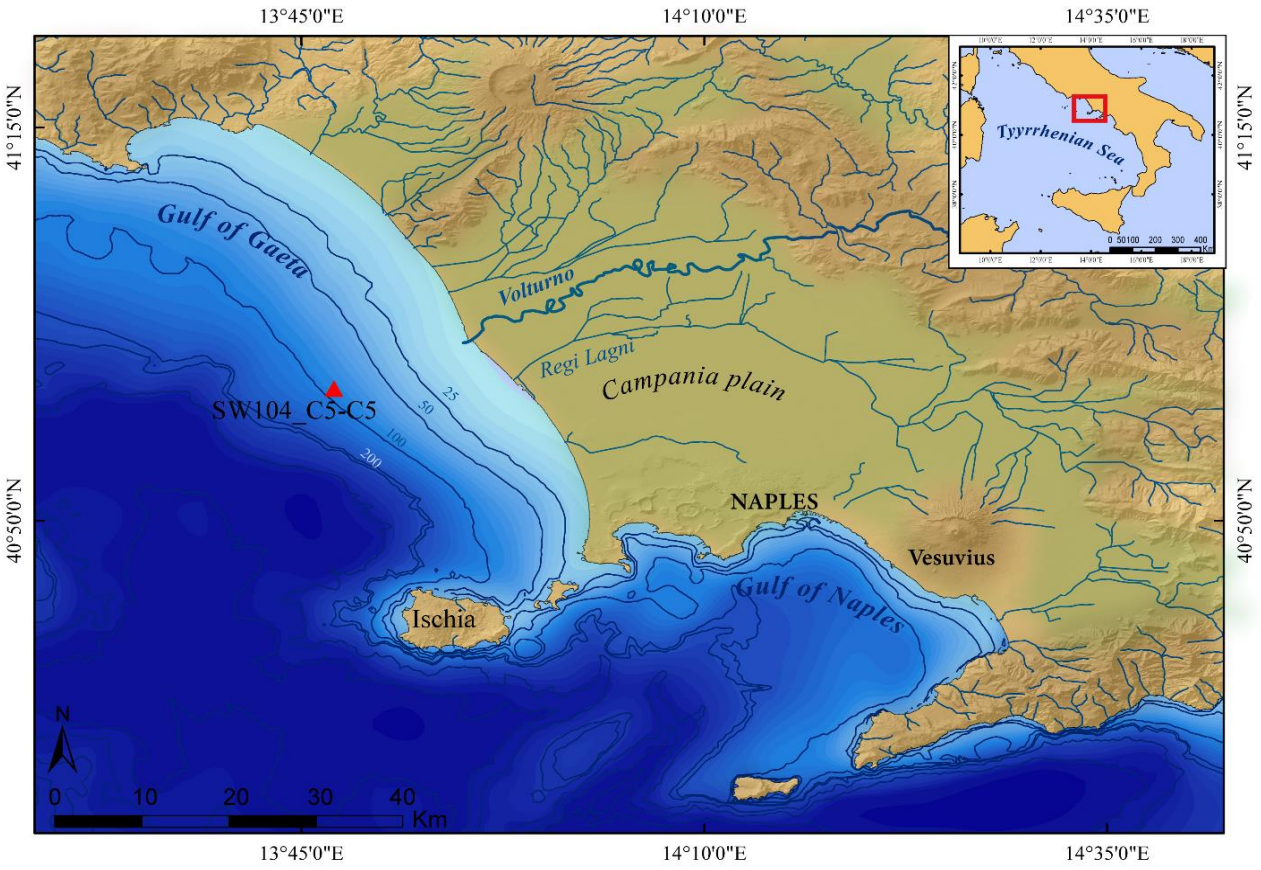

Figure 5. 1. Location map of the Gulf of Gaeta in Southern Italy and SW104_C5 core site.

Humans have been exploiting the volcanic and fertile soils of Campania and Lazio since the Palaeolithic (Nava et al., 2007). First historical humans' settlement in the area is documented back to the 9th century BC. Greek and Roman colony established in the coastal plain of the Volturno River

between 200 years BC 500 years AC, while during the Middle Age, several different kingdoms controlled the area. The last one, the Spanish domination, lasted till the 1860, when the region became part of Italy. Since a few decades ago, the Campania Plain was characterized by a marshy and palustrine environment (Ruberti et al., 2018). The first remediation actions started in the XVI century under the Borbone Kingdom. The Regi Lagni, a complex network of artificial drainage channels, was built over the last 400 years to make the backwater flowing toward the sea. The articulated interventions lasted till the 1950. Important artificial interventions took placed along the Volturno River with the dams' constructions. Between the 1909 and 1916, the first dam of Sorgente di Capo Volturno was built in the uppermost part of the river. Between the 1953 and 1958, the Traversa di Ponte Annibale was also built around Capua. Overall, in the last century several human interventions occurred over the river for hydraulic energy exploitation and agricultural purpose. Nowadays, agriculture is the most important activity in the Campanian plain, with intensive and wide areas covered by permanent orchard and olive groves.

The Volturno Plain-Regi Lagni area between the provinces of Naples and Caserta is densely populated area and falls within the Regional Interest Priority Site "Litorale Domizio-Agro Aversano" characterized by a strongly urbanization, intensive agricultural activities and, in the last decades, by an unknown number of illegal activities (Rezza et al., 2015). Several studies have investigated the quality of Volturno River waters and sediments by assessing the microbiological and chemical discharges (Mancini et al., 1994; Parrella et al., 2003; Montouri et al., 2020-21). The contamination of the Volturno River is mainly due to polychlorinated biphenyls (PCBs), organochlorine pesticides (OCPs) and polycyclic aromatic hydrocarbons (PAHs) (total amount discharged yearly is 87.1 kg /year, 19.7 kg/year and 3158.2 kg/year respectively) produced by vehicle traffic, agricultural waste and combustion processes (Montouri et al., 2020).

5.3. Materials and Methods

5.3.1. Core sampling and geochronology

The 108 cm long-core SW104-C5 sea sediment was collected in 2013 at 93 meters of water depth in the Gulf of Gaeta, 13 km offshore the Volturno's mouth (40°58′24,993″N, 13°47′03,040″E) (Fig. 5.1).

The geochemical analyses of the sea sediments were carried out at the ISMAR-CNR of Bologna. The ^{210}Pb and ^{137}Cs were used for establishing the geochronology of the core. The bottom of the core was dated back to 1686 AC. More details about the aging model and geochronology techniques of the core can be found in Margaritelli et al. (2016).

5.3.2. Benthic foraminiferal analysis

For the benthic foraminiferal analysis, twenty-three sediment samples were chosen at ca. 4.3 cm intervals corresponding to 14.2 yrs., in order to well represent the whole temporal sequence between 2013 (uppermost layer) and 1686 (bottom layer). In the laboratory, sediment samples were gently washed with tap water, through a 63 μm mesh sieves, and dried at 40°C. About 300 specimens were dry-picked from the fraction > 125 μm and placed in plastic microslides for morphological identification. Benthic foraminiferal species were taxonomically identified following the works of Sgarrella and Moncharmont Zei (1993) and Milker and Schmiedl (2012). The current nomenclature was double checked the database the World Register of Marine Species (Hayward et al., 2022). At each core interval, the relative abundance, the species richness (S), the Shannon Index biased correct (H'_{bc}) (Chao and Shen, 2003), the Equitability (J) and the enhanced Benthic Foraminifera Oxygen Index (EBFOI) were calculated. The EBFOI is a modification of the BFOI introduced by Kaiho (1994) to improve the estimation of dissolved oxygen contents in the sediment (Kranner et al., 2022). We used the equation (5.1) that considers suboxic indicators to the Kaiho equation applicable when oxic indicators are present (Kranner et al, 2022):

$$EBFOI = 100(O/(O + D + S/2) \quad (5.1)$$

where O, D and S are the sum of oxic, dysoxic and suboxic indicators at each interval. The oxic requirements of benthic foraminiferal species (i.e. oxic, dysoxic or suboxic) were attributed following previous literature shortcoming (e.g., Jorissen 1992, 2018; Sgarrella and Moncharmont Zei, 1993; Altenbach et al., 1999; Fontanier et al., 2002; Frezza et al., 2011; Kranner et al., 2022). The following oxygenation concentration thresholds and relation of oxygenation are considered for EBFOI: 100 to 50 high oxic, 50 to 0 low oxic, 0 to -40 suboxic, -40 to -50 dysoxic, -55 anoxic.

The packages "Entropy" (Hausser and Strimmer, 2014) and "vegan" Oksanen et al. (2016) in RStudio were used to determine S, E and $H'_{bc.}$ The package "rioja" (Juggins, 2022) was used to plot vertical temporal profiles.

5.3.3. Statistical analysis

The relative abundances of benthic foraminiferal species were grouped using a constrained hierarchical clustering analysis (HCA) along the core depth (i.e., years) and a similarity tree was produced using the Euclidian distance. Coniss was used as the clustering method (Grimm, 1987). The analysis was performed using the package "vegan" (Oksanen et al., 2016) and the plot produced by the package "rioja" (Juggins, 2022) in RStudio.

The maps were made using the software ArcMap 10.5 (Esri). The geographic review of the area was based on different historical maps (Annali delle Bonificazioni – Anno I – 1858; Istituto Geografico Militare, 1914; Satellite Imagery, Google Earth, 1990).

5.4. Results

5.4.1. Diversity indices and species abundance variations

Based on the available geochronology, a mean sedimentation accumulation rate of 0.30 cm/year was calculated, defining an age of 1922 AC at 50 cm from the surface and 1686 at 99 cm from the surface.

A total of 77 species, belonging to 43 genera, were recognized. The benthic foraminifera abundance and the relative abundance for each species recognized was reported in the Table S5.1. The S values ranged between 20 (in 1876) and 37 (1936) without a clear trend. The H'_{bc} values spanned between 2.5 (1876) and 3.1 (1950) and were relatively constant over time. A similar trend was exhibited by the J, which varied between 0.80 in 1936 and 0.88 in 1989 (Fig. S5.1).

The most abundant species (relative abundance on average > ~5%) were *Valvulineria bradyana* (10.7 %), *Bulimina gibba* (10.6 %), *Cassidulina carinata* (9.5%), *Hyalinea balthica* (7.47%), *Melonis barleeanum* (6.8%), *Spiroplectinella wrighti* (6.1%), *Bulimina marginata* (5.5%), *Uvigerina mediterranea* (4.8%0), *Melonis pompilioides* (2.8%), *Elphidium crispum* (2.2%) and *Uvigerina peregrina* (1.9%) (Fig. 5.2) (Table S5.1). *Valvulineria bradyana* showed an overall decreasing percentage along the core, with a maximum of 21.0% in 1853 and a minimum of 3.3% in 1989 (Fig. 5.2). *Bulimina gibba* abundance exhibited an increasing trend till 1928 and a steady drop from 1942 to 2013 with minimum and maximum values of 2.0% and 28.4% set at 1823 and 1928, respectively (Fig. 5.2). *Cassidulina carinata* presented an increasing trend in the lower part of the core then it decreased till 1958 when the abundance rose up again till 2013. The highest abundance (16.7%) was registered in 1853, while the lowest ones (4.3%) in 1735 (Fig. 5.2). *Elphidium crispum* displayed an overall constant abundance till 1950, when it drastically dropped and remained low till 2013. *Bulimina marginata* presented a decreasing trend up to 1936 then its abundance increased (Fig. 5.2). *Uvigerina peregrina* exhibited constantly very low values from the bottom of the core till 1936 (Fig. 5.2). A similar trend was observed for *Uvigerina mediterranea* (Fig. 5.2).

5.4.2. Changes in the benthic foraminiferal composition

The HCA showed a clear separation of the samples in two main clusters (cluster I: 1686-1913 and cluster II: 1918-2013) (Fig. 5.3a). Cluster II can be further sub-divided in two sub-clusters (sub-cluster II a: 1918-1950; and sub-cluster II b: 1958-2013) (Fig. 5.3). The Cluster I (1686-1913) was characterized by relatively higher abundances of *V. bradyana, C. carinata, M. barleeanum, B. marginata, M. pompilioides,* and *E. crispum* (Fig. 5.2) than in Cluster II. A significant increase in abundance of *B. gibba, B. alata, B. nodosaria* and *U. peregrina* was observed in the sub-cluster IIa (1918-1950). Compared to the Cluster I, a decrease of *V. bradyana, C. carinata, H. balthica, B. marginata, M. pompilioides* and *G. subglobosa* were observed in sub-cluster IIa (Fig. 5.3a). In the sub-cluster IIb (1958-2013) an increase in abundance of *C. carinata, H. balthica, B. marginata, U. mediterranea, B. nodosaria, G. subglobosa* and *U. peregrina* occurred. At the same time, there was a further decrease in abundance of *V. bradyana, B. gibba,* and *M. pompilioides,* while *E. crispum* is absent (Fig. 5.3a).

The maximum value (47) of the EBFOI was recorded in 1823 and 1735, while the lowest one (19) in 1958 (Fig. 5.3b). On overall, the EBFOI exhibited relatively higher values (close to high oxic conditions) until 1913. Then, there was a decrease with lower values (low oxic conditions) lasting from 1918 to nowadays (Fig. 5.3b).

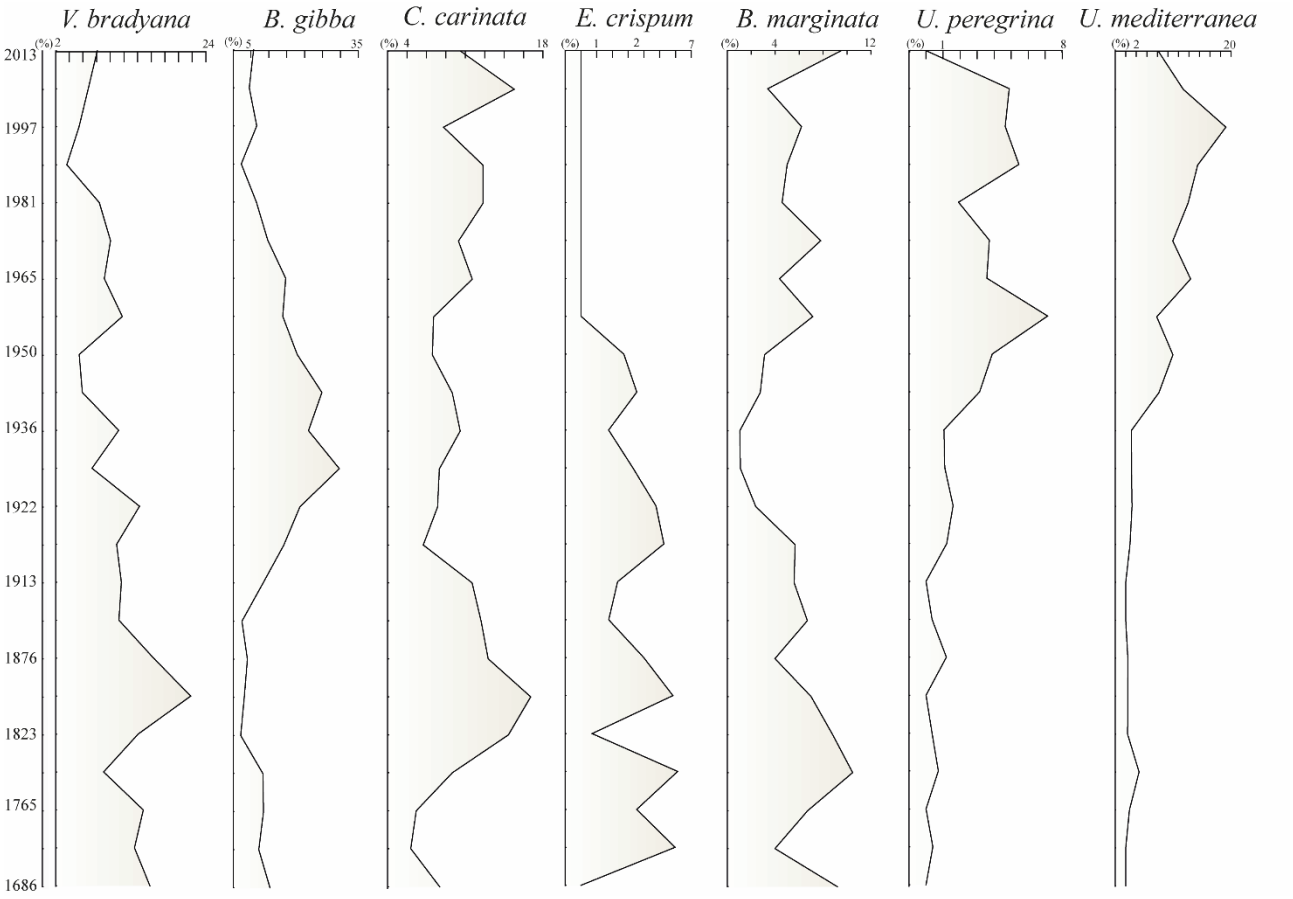

Figure 5. 2. Temporal relative abundance variations of selected benthic foraminiferal species.

5.4.3 Historical environmental changes

The analysis of historical maps of the study area revealed important information about the land use changes during different historical periods (i.e., 1858, 1914 and 1990). In the 19th century, the whole area was mainly covered by natural lands, with only a few residential areas (i.e., city of Caserta and the towns of Capua and Aversa) and a wide coastal area (Fig. 5.3c). At the end of the 20th century, natural lands remained only in the inner mountainous area. The whole plain was urbanized or used as cultured lands. The coastal area was reduced, and an intense loss of sandy beach was observed.

5.5. Discussion

The present study allows us to decipher the paleoenvironmental changes in the Gulf of Gaeta (Tyrrhenian Sea) during the last ca. 300 years using benthic foraminiferal assemblages as proxies for climatological and paleoecological variations. The severe changes in the land use during the last centuries in the Campania Region have been confirmed through the historical-cartographic review of the area that allows us to observe how the natural lands, which covered the main part of the Northern area of Campania till 1850, was completely converted into agricultural and residential areas during the Industrial Period (Fig. 5.3c). A crucial role in the Volturno River and Gulf of Gaeta ecological dynamics must be attributed to the dams' construction and the Regi Lagni reclamation. The reclamation was achieved by filling lowlands with alluvial materials from river waters that were canalized and diverted (Ruberti et al., 2018, 2022). Such interventions (i.e., reduction of wetlands) led to the urbanization of coastal area and also increased the amount of fine sediments transported toward the sea, the nutrients supply (i.e., organic matter) as well as the water turbidity (Incarbona et al., 2010).

Based on the HCA, three main phases (cluster and sub-clusters) corresponding to faunal turnovers are identified and their separations can be associated to the dam construction. Specifically, the two major faunal turnovers taking place at 1913-1918 and 1950-1958 well correspond to the building of the dams of Sorgente Capo Volturno (1909-1916) and Ponte Annibale (1953-1958) (Fig. 5.3a).

5.5.1. Natural conditions and the Regi Lagni reclamation

The 1686-1913 phase is mainly characterized by a high abundance of *V. bradyana, B. marginata,* and *E. crispum*. *Valvulineria bradyana* is a typical species of coastal terrigenous circalittoral and epibathyal muds (Blanc-Vernet, 1969). This taxon has been assigned to the group IV, the "second-order opportunists" by Jorissen et al. (2018), absent where the content of organic matter is low or moderate but very abundant where enrichment of organic matter occurs. This taxon is normally

favoured in a low O_2 environment and by high amount of organic matter (Bergamin et al., 1999; Capotondi et al., 2022). *Bulimina marginata* belongs to group III "third-order opportunists" and has been reported as widespread in circalittoral and bathyal muds deeper than 100 m (Sgarrella and Moncharmont Zei, 1993). Although the occurrence of dysoxic indicators, during this phase, the EBFOI has, on overall, high and constant values (close to high oxic conditions). Indeed, in the same interval we register the higher abundance of oxic indicators as *E. crispum* that is a sensitive species to organic enrichment and is commonly found in low-polluted sites (Jorissen et al., 2018).

These apparently controversial conditions can be explained by the mutual effect of human interventions and the overprint of climatic changes in the Mediterranean basin. In this period (1686-1913), the Volturno coastal plain experienced significant changes with the reclamation of swamp zones and the Regi Lagni intervention that was represented by historic drainage channels for rainwater and spring water toward the sea and modified the continental fluvial regime (Alberico et al., 2018). These hydraulic restorations started during the Borbone Kingdom but they have been completed in different stages up to the present day and from 1850 the reclamation proceeded with the use of landfill of lowland areas (Alberico et al., 2018). On a wider-climatic perspective, the present interval records the upper part of the Little Ice Age (ca. 1250 to 1850) and, in particular the Maunder event, a cold phase with reduced solar activity during the Little Ice Age (Margaritelli et al., 2016). Based on micropaleontological analyses, Margaritelli et al. (2016) revealed a shift of carnivorous and herbivorous planktonic foraminifera and the beginning of forest recovering (e.g., mixed oak forest and evergreen trees and shrubs) at 1850 (Di Rita et al., 2019).

This interval also covers an important phase the Industrial Revolution (1850-1950 sensu Margaritelli et al., 2016) typified along the studied core by an increase of warm-water-oligotrophic planktonic foraminiferal taxa (i.e., *Globigerinoides quadrilobatus* and *Globigerinoides ruber*) and the dominance of herbivorous–opportunistic planktonic foraminifera associated to more humid

climatic conditions. These wetter and warmer climate conditions were also supported by the pollen record (Di Rita et al., 2019).

5.5.2. The aftermath of the construction of the Capo Volturno dam

Beside the marked variations as previously along the water column and in the continental environment as revealed from the planktonic foraminiferal and pollen assemblages (Margaritelli et al. (2016), prominent changes took place in the sea bottom as supported by benthic foraminiferal assemblages from 1918-1950. In this interval, the benthic foraminiferal assemblages are in fact markedly different from the previous period, with a strongly increase of dysoxic indicators to the detriment of oxic indicators. *Valvulineria bradyana* is replaced by *Bulimina gibba* as dominant species. The latter belongs to group III ("third-order opportunists"), which includes species tolerant to the first stages of organic enrichment and absent where the enrichment is maximum. In this time interval, we also observed a rapid increase of other triserial taxa (e.g., *Uvigerina*). This phase also exhibits a decrease of the EBFOI. These changes can be ascribed to the construction of the Sorgente of Capo Volturno between 1909 and 1916 that might have increased the quantity of finer materials discharge by the Volturno River leading to development of lower oxygen conditions (Fig. 5.3b). Similarly, a foraminiferal turnover characterized by a significant reduction in abundances of *V. bradyana* and a strong increase of triserial taxa such as *U. mediterranea* and *B. aculeata* was set after 1920 in the Gulf of Salerno (Vallefuoco et al., 2012). That variation was related to enhanced availability of organic matter at the seafloor along with a strong reduction of sandy riverine materials and, ultimately, to the construction of a dam in the Sele river in 1934.

5.5.3. Changes associated with the Ponte Annibale dam

In the most recent period (1958-2013), there is a clear increase of *B. marginata, C. carinata, U. mediterranea, U. peregrina,* and *G. subglobosa*. *Uvigerina mediterranea,* classified in the group II (Jorissen et al., 2018), is particularly abundant at depths greater than 430 m, in bathyal muds (Sgarrella and Moncharmont Zei, 1993), while *U. peregrina* is classified in the group III (Alve et al., 2016). *Cassidulina carinata* and *B. marginata* are considered as opportunistic taxa (Jorissen et al., 2018). The ecological behaviour of these species would support an increase in the availability of organic matter (nutrients) and/or a decrease in oxygen content, mainly driven by the enhanced terrigenous discharge. In this period, we observe the higher dominance of dysoxic and suboxic indicators, and the persistent low percentage of oxic indicators. The shift in foraminiferal assemblages takes place between 1950-1958 that also exhibits the lowest value of EBFOI (Fig. 5.3b). These changes perfectly match the completion of the construction of the Ponte Annibale dam (i.e., 1953) that has been suggested to have reduced the river sediment supply to the coast (Alberico et al., 2018). Accordingly, it was documented a shoreline retreat (up to 28.3 m/yr) after the construction of the Ponte Annibale dam (1953) because of the decrease of sand supply to river mouth (Donadio et al., 2018; Ruberti et al., 2018). The EBFOI also evidences a phase from 1950 to 1980 with relatively low values of oxygen availability at the seafloor.

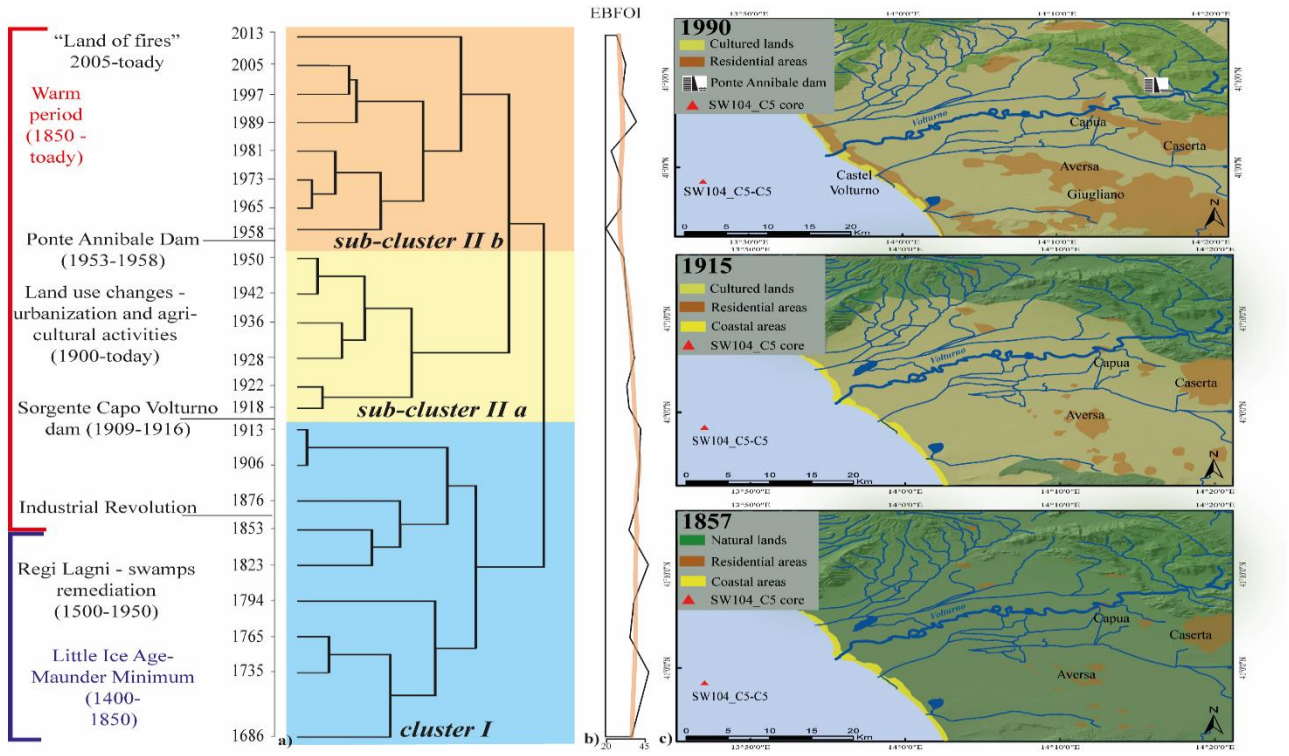

Figure 5. 3. Paleoclimate periods (blue and red from Margaritelli et al., 2016) and anthropogenic interventions. a) HCA (Hierarchical cluster analysis) based on benthic foraminiferal relative abundances; b) Enhanced Benthic Foraminifera Oxygen Index (EBFOI) temporal variations; c) Paleoenvironmental reconstruction and land-use change in 1857 (Annali delle Bonificazioni – Anno I – 1858. Pianta Generale del Bacino Inferiore del Volturno con la indicazione delle opere di strade e di canali eseguite dal Real Governo), 1915 (Istituto Geografico Militare, 1914, Cartografia 1:25000) and 1990 (Satellite Imagery, Google Earth, 1990)

This interval was also characterized by a significant increase in planktonic species as *Globigerinita glutinata* and *Turborotalita quinqueloba* (Margaritelli et al., 2016). These taxa have been reported to thrive in areas influenced by continental runoff and nutrient-rich waters, suggesting, on overall high surface productivity (Margaritelli et al., 2016). Similar to our findings, an increase of *B. aculeata* in the Gulf of Salerno (south Tyrrhenian Sea) suggests enhanced productivity but also suboxic or dysoxic conditions in pore and bottom waters (Vallefuoco et al., 2012; Lirer et al., 2014). Accordingly, these authors inferred a marked decrease of coarse-grained materials, which might have possibly changed the nutrient supply at the seafloor, as a consequence of dam construction in the central-southern Tyrrhenian coastal areas during the last century. This interval was also characterized by an intensive urbanization and particularly of cultivation of the continental area of the Gulf of Gaeta. In fact, pollen analyses revealed the dominance of *Pinus* reflecting extensive plantation of pine

forests. It was also suggested an overall of increase in cultivated plants, such as *Olea, Juglans, Vitis*, *Corylus*, Cannabaceae, and cereals, all considered anthropogenic pollen indicators, further supporting the exploitation of land for agriculture purpose (Di Rita et al., 2018, 2019).

5.6. Conclusion

The present study identifies three main intervals (i.e., 1686-1913, 1918-1950, and 1958-2013) based on variation of benthic foraminiferal assemblages in the Gulf of Gaeta. The first interval reflects mostly natural conditions with higher oxygen availability. However, it was difficult to distinguish at the seafloor the climatic overprint from human interventions such as the reclamation of marsh areas. Significant changes in the benthic foraminiferal assemblages and a lowering of the oxygen availability that were associated to the construction of the Sorgente of Capo Volturno between 1909 and 1916 that might have increased the quantity of finer materials discharge by the Volturno River. A further shift in the benthic foraminiferal assemblages and a lowering of oxygen availability took place between 1950-1958. These changes perfectly match the completion of the construction of the Ponte Annibale dam in 1953 that has been suggested to have reduced the sand supply to river mouth. This investigation reveals that dam construction unbalancing the sediment input and reducing the coarse sediment supply might determine significant alteration in the composition of benthic foraminiferal assemblages and further supports the capability of benthic foraminifera to record paleoenvironmental variations even induced by anthropization.

____*Personal contribution: Bibliographic review, visualization, analysis of results, MS writing*___

Chapter VI

6. Conclusions and future challenges

Marine pollution is increasingly damaging aquatic ecosystems, threatening our health and causing a severe impact to coastal and pelagic environments. The importance of developing the best scientific techniques to assess the human impact has become huge and compelling as also supported by the EU directive (i.e., WFD and MSFD). The 2030 Agenda for Sustainable Development established by the United Nations (United Nations, 2015) also highlights the importance to conserve and sustain marine environments (Goal number 14: Life below water) and to make cities safe and sustainable (Goal number 11: Sustainable Cities and communities).

6.1. State of the art and research impact

As discussed in this PhD thesis, the application of benthic foraminifera in biomonitoring offers an innovative and successful tool that can be applied to a wide range of environmental conditions and ecosystems.

The classic morphological based approach has been adopted together with the innovative eDNA metabarcoding in different researches, with reliable and complementary results. In this thesis, the congruences and agreement between the two approaches, based on the calculation of ecological indexes for each dataset (i.e., exp(H'bc) *vs*. g-exp(H'bc) or Foram-AMBI *vs*. g-Foram-AMBI), are discussed in *Chapter II* and *Chapter III* and provide compelling evidences on the suitability of the metabarcoding in EcoQS assessment and Paleo-EcoQS reconstruction.

Benthic foraminifera can be considered as effective bioindicators for their ecological behaviour, as well as for the flexibility of techniques and approaches that can be used. In fact, analysing their

assemblages in superficial marine sediment can identify areas with stress conditions and qualify in terms of EcoQS. This aspect is described in the *Chapter II* of this thesis, where the spatial distribution of abiotic and stressful factors (i.e., PLI, organic matter) are precisely correlated with the distribution of the ecological indices based on the living BF assemblages. This approach provides an instant picture of the marine area, useful for assessing the present EcoQS.

On the other hand, the ability of benthic foraminiferal tests to be preserved in the sediment record make them also as suitable example of bioindicator for evaluating temporal variations of ecological (i.e., Paleo-EcoQS) and environmental conditions. The investigations of temporal shifts in foraminiferal assemblages within the sedimentary record can help to make accurate paleoenvironmental reconstructions, highlighting changes in the last decades, possibly trying to relate them to environmental and anthropogenic interventions and establishing the background (i.e., reference) conditions. This approach has been described in the *Chapter III*, *IV* and *V* of this thesis. In *Chapter III*, the *sedaDNA* is for the very first time used along with the classic micropaleontological approach (and many other bioindicators), for the Paleo-EcoQS reconstructions that confirm the good congruence between these two approaches.

The recent publications (Dias and Sukumaran, 2023; Fajemila et al., 2022; Cao et al., 2022) confirm that the research community has a deep interest in the topics described in this PhD thesis, which offers a new scientific contribution that could have wider implications toward the international and sustainable development.

6.2. Future challenges

The innovations regarding the use of benthic foraminifera as bioindicator will be explored even more deeply in the future. It is likely that the revolutionary approach of the metabarcoding will have more and more importance in the next years. The recent advances in omic technologies (e.g., genomics, proteomics, metabolomics, and transcriptomics) can supply new tools and approaches for

understanding, at the molecular level, the effects of pollutants on biota. Accordingly, the molecular, biochemical, cellular, and physiological alterations (i.e., biomarkers) in a biological system can be used to detect the toxic effects of pollutants and can eventually be applied in environmental biomonitoring even as an early warning of stress. For instance, a recent research on foraminiferal biomarkers (i.e., proteins and enzymes) has provided evidences of the effects (i.e., oxidative stress) of Hg on *Amphistegina lessonii* (Ciacci et al., 2020).

The surprising applications of these unicell organisms continue to open new scientific way in environmental sciences and ecology. It is iconic how, through the complex and huge dynamics that rule the nature, a very small test containing a very simple organism can reveal so precious information regarding our present and our past. Sometimes, focusing on details can be worth for better understanding a wider picture.

References

Abramovich, S., Keller, G., **2003**. Planktonic foraminiferal response to the latest Maastrichtian abrupt warm event: a case study from South Atlantic DSDP Site 525A. Mar. Micropaleontol. 48, 225–249.

Albanese, S., De Vivo, B., Lima, A., Cicchella, D., Civitillo, D., Cosenza, A.. **2010**. Geochemical baselines and risk assessment of the Bagnoli brownfield site coastal sea sediments (Naples, Italy). Journal of Geochemical Exploration. 19-33. 10.1016/j.gexplo.2010.01.007.

Alberico, I., Cavuoto, G., Di Fiore, V., Punzo, M., Tarallo, D., Pelosi, N., Ferraro, L., Marsella, E., **2018**. Historical maps and satellite images as tools for shoreline variations and territorial changes assessment: the case study of Volturno Coastal Plain (Southern Italy). Journal of Coastal Conservation. 22, No. 5, 919-937.

Altenbach, A.V., Pflaumann, U., Schiebel, R., Thies, A., Timm, S., Trauth, M., **1999**. Scaling percentages and distributional patterns of benthic foraminifera with flux rates of organic carbon. Journal of Foraminiferal Research. 29, 173-185.

Alve, E., Hess, S., Bouchet, V.M.P., Dolven, J.K., Rygg, B., **2019**. Intercalibration of benthic foraminiferal and macrofaunal biotic indices: An example from the Norwegian Skagerrak coast (NE North Sea). Ecological Indicators 96, 107–115. https://doi.org/10.1016/j.ecolind.2018.08.037

Alve, E., Korsun, S., Schönfeld, J., Dijkstra, N., Golikova, E., Hess, S., Husum, K., Panieri, G., **2016**. Foram-AMBI: A sensitivity index based on benthic foraminiferal faunas from North-East Atlantic and Arctic fjords, continental shelves and slopes. Marine Micropaleontology 122, 1–12. https://doi.org/10.1016/j.marmicro.2015.11.001

Alve, E., Lepland, A., Magnusson, J., Backer-Owe, K., **2009**. Monitoring strategies for re-establishment of ecological reference conditions: Possibilities and limitations. Marine Pollution Bulletin 59, 297–310. https://doi.org/10.1016/j.marpolbul.2009.08.011

Alve, E., **1995**. Benthic foraminiferal responses to estuarine pollution; a review. The Journal of Foraminiferal Research 25, 190–203. https://doi.org/10.2113/gsjfr.25.3.190

Alve, E., **1991**. Foraminifera, climatic change and pollution: a study of Late Holocene sediments in Drammensfjord, SE Norway The Holocene. 243-261.

Amaral-Zettler, L.A., McCliment, E.A., Ducklow, H.W., Huse, S.M., **2009**. A method for studying protistan diversity using massively parallel sequencing of V9 hypervariable regions of small-subunit ribosomal RNA Genes. PLoS One 4. https://doi.org/10.1371/journal.pone.0006372

Annali delle Bonificazioni – Anno I – **1858**. Pianta Generale del Bacino Inferiore del Volturno con la indicazione delle opere di strade e di canali eseguite dal Real Governo.

Appleby, P.G., Oldfield, F., **1978**. The calculation of lead-210 dates assuming a constant rate of supply of unsupported 210Pb to the sediment. Catena (Amst) 5, 1–8. https://doi.org/10.1016/S0341-8162(78)80002-2

Arienzo, M., Donadio, C., Mangoni, O., Bolinesi, F., Stanislao, C., Trifuoggi, M., Toscanesi, M., Di Natale, G., Ferrara, L., **2017**. Characterization and source apportionment of polycyclic aromatic hydrocarbons

(pahs) in the sediments of gulf of Pozzuoli (Campania, Italy). Mar. Pollut. Bull 124, 480–487. https://doi.org/10.1016/j.marpolbul.2017.07.006

Armbrecht, L., Weber, M.E., Raymo, M.E., Peck, V.L., Williams, T., Warnock, J., Kato, Y., Hernández-Almeida, I., Hoem, F., Reilly, B., Hemming, S., Bailey, I., Martos, Y.M., Gutjahr, M., Percuoco, V., Allen, C., Brachfeld, S., Cardillo, F.G., Du, Z., Fauth, G., Fogwill, C., Garcia, M., Glüder, A., Guitard, M., Hwang, J.-H., Iizuka, M., Kenlee, B., O'Connell, S., Pérez, L.F., Ronge, T.A., Seki, O., Tauxe, L., Tripathi, S., Zheng, X., **2022**. Ancient marine sediment DNA reveals diatom transition in Antarctica. Nature Communications. 13:1 13, 1–14. https://doi.org/10.1038/s41467-022-33494-4

Armiento, G., Barsanti, M., Caprioli, R., Chiavarini, S., Conte, F., Crovato, C., de Cassan, M., Delbono, I., Montereali, M.R., Nardi, E., Parrella, L., Pezza, M., Proposito, M., Rimauro, J., Schirone, A., Spaziani, F., **2022**. Heavy metal background levels and pollution temporal trend assessment within the marine sediments facing a brownfield area (Gulf of Pozzuoli, Southern Italy). Environmental Monitoring and Assessment. 194:11 194, 1–21. https://doi.org/10.1007/S10661-022-10480-3

Armiento, G., Caprioli, R., Cerbone, A., Chiavarini, S., Crovato, C., de Cassan, M., de Rosa, L., Montereali, M.R., Nardi, E., Nardi, L., Pezza, M., Proposito, M., Rimauro, J., Salerno, A., Salluzzo, A., Spaziani, F., Zaza, F., **2020**. Current status of coastal sediments contamination in the former industrial area of Bagnoli-Coroglio (Naples, Italy). Chemistry and Ecology 36, no. 6, 579-597. https://doi.org/10.1080/02757540.2020.1747448

Armynot du Châtelet, E., Francescangeli, F., Frontalini, F. **2018**. Definition of benthic foraminiferal bioprovinces in transitional environments of the Eastern English Channel and the Southern North Sea." Revue de Micropaléontologie. 61 (3-4), 223-234.

Armynot du Châtelet, E.; Debenay, J.-P., Soulard, R. **2004**. Foraminiferal proxies for pollution monitoring in moderately polluted harbors. Environmental Pollution, 127: 27-40.

Ascione, A., Aucelli, P.P., Cinque, A., di Paola, G., Mattei, G., Ruello, M., Russo Ermolli, E., Santangelo, N., Valente, E., **2021**. Geomorphology of Naples and the Campi Flegrei: human and natural landscapes in a restless land. Journal of Maps 17, 18–28. https://doi.org/10.1080/17445647.2020.1768448

Astraldi, M., Gasparini, G.P., **1994**. The seasonal characteristics of the circulation in the Tyrrhenian Sea. In: La Violette, P. (Ed.), Seasonal and Interannual Variability of the Western Mediterranean SeaCoastal and Estuarine Studies. American Geophysical Union, Washington, D.C. 46, 115–134.

Ausili, A., Bergamin, L., Romano, E., **2020**. Environmental Status of Italian Coastal Marine Areas Affected by Long History of Contamination. Frontiers in Environmental Science 8. https://doi.org/10.3389/fenvs.2020.00034

Aylagas, E., Borja, Á., Tangherlini, M., Dell'Anno, A., Corinaldesi, C., Michell, C.T., Irigoien, X., Danovaro, R., Rodríguez-Ezpeleta, N., **2017**. A bacterial community-based index to assess the ecological status of estuarine and coastal environments. Marine pollution bulletin 114, 679–688. https://doi.org/10.1016/j.marpolbul.2016.10.050

Aylagas, E., Borja, A., Rodriguez-Ezpeleta, N., **2014**. Environmental Status Assessment Using DNA Metabarcoding: Towards a Genetics Based Marine Biotic Index (gAMBI). PLoS ONE. 9. e90529. 10.1371/journal.pone.0090529.

Baran, A., Mierzwa-Hersztek, M., Gondek, K., Tarnawski, M., Szara, M., Gorczyca, O., Koniarz, T., **2019**. The influence of the quantity and quality of sediment organic matter on the potential mobility and toxicity of trace elements in bottom sediment. Environmental Geochemistry and Health 41. https://doi.org/10.1007/s10653-019-00359-7

Barberi, F., Hill, D.P., Innocenti, F., Luongo, G., Treuil, M., **1984**, The 1982-1984 bradyseismic crisis at Phlegrean fields (Italy). Bull Volcanol 47:173–411.

Barnosky, A.D., Matzke, N., Tomiya, S., Wogan, G.O.U., Swartz, B., Quental, T.B., Marshall, C., McGuire, J.L., Lindsey, E.L., Maguire, K.C., Mersey, B., Ferrer, E.A., **2011**. Has the Earth's sixth mass extinction already arrived? Nature 2011 471:7336 471, 51–57. https://doi.org/10.1038/nature09678

Barrenechea Angeles, I., Romero-Martínez, M.L., Cavaliere, M., Varrella, S., Francescangeli, F., Piredda, R., Mazzocchi, M.G., Montresor, M., Schirone, A., Delbono, I., Margiotta, F., Corinaldesi, C., Chiavarini, S., Montereali M.R., Rimauro, J., Parrella, L., Musco, L., Dell'Anno, A., Tangherlini, M., Pawlowski, J., Frontalini, F., **2023**. Encapsulated in sediments: eDNA deciphers the ecosystem history of one of the most polluted European marine sites. 2023. Environment International. In Press. https://doi.org/10.1016/j.envint.2023.107738.

Barras, C., Jorissen, F.J., Labrune, C., Andral, B., Boissery, P., **2014**. Live benthic foraminiferal faunas from the French Mediterranean Coast: Towards a new biotic index of environmental quality. Ecological Indicators 36, 719–743. https://doi.org/10.1016/j.ecolind.2013.09.028

Bergamin, L., Romano, E., Magno, M.C., Ausili, A., Gabellini, M., **2005**. Pollution monitoring of Bagnoli Bay (Tyrrhenian Sea, Naples, Italy), a sedimentological, chemical and ecological approach. Aquatic Ecosystem Health and Management 8, 293–302. https://doi.org/10.1080/14634980500220866

Bergamin, I., Romano, E., Gabellini, M., Ausili, A., Carboni, M.G., **2003**. Chemical-physical and ecological characterisation in the environmental project of a polluted coastal area: the Bagnoli case study. Medit. Mar. Sci. 4, 5. https://doi.org/10.12681/mms.225

Bergamin, L., Di Bella, L., Carboni, M.G.. **1999**. *Valvulineria bradyana* (Fornasini) in organic matter-enriched environment. Il Quaternario. 12. 51-56.

Bertocci, I., Dell'Anno, A., Musco, L., Gambi, C., Saggiomo, V., Cannavacciuolo, M., lo Martire, M., Passarelli, A., Zazo, G., Danovaro, R., **2019**. Multiple human pressures in coastal habitats: variation of meiofaunal assemblages associated with sewage discharge in a post-industrial area. Science of The Total Environment 655, 1218–1231. https://doi.org/10.1016/j.scitotenv.2018.11.121

Birk, S., Bonne, W., Borja, A., Brucet, S., Courrat, A., Poikane, S., Solimini, A., van de Bund, W., Zampoukas, N., Hering, D., **2012**. Three hundred ways to assess Europe's surface waters: An almost complete overview of biological methods to implement the Water Framework Directive. Ecological Indicators 18, 31–41. https://doi.org/10.1016/j.ecolind.2011.10.009

Birks, H. j. b., Braak, C. j. f. T., Line, J.M., Juggins, S., Stevenson, A.C., Battarbee, R.W., Mason, B.J., Renberg, I., Talling, J.F., **1990**. Diatoms and pH reconstruction. Philosophical Transactions of the Royal Society of London. B, Biological Sciences 327, 263–278. https://doi.org/10.1098/rstb.1990.0062

Blanc-Vernet L. **1969**. Contribution à l'étude des Foraminifères de Mèditerranée. Rec. trav. St. Mar. Endoume. 48, 5-281.

Blanchet, H., Lavesque, N., Ruellet, T., Dauvin, J.C., Sauriau, P.G., Desroy, N., Desclaux, C., Leconte, M., Bachelet, G., Janson, A.-L., Bessineton, C., Duhamel, S., Jourde, J., Mayot, S., Simon, S., de Montaudouin, X., **2008**. Use of biotic indices in semi-enclosed coastal ecosystems and transitional waters habitats—Implications for the implementation of the European Water Framework Directive. Ecological

Indicators, Assessing the environmental quality status in estuarine and coastal systems: comparing methodologies and indices 8, 360–372. https://doi.org/10.1016/j.ecolind.2007.04.003

Blott, S., Pye, K. **2012**. Particle size scales and classification of sediment types based on particle size distributions: Review and recommended procedures. Sedimentology. 59. 2071-2096. 10.1111/j.1365-3091.2012.01335.x.

Bolyen, E., Rideout, J.R., Dillon, M.R., Bokulich, N.A., Abnet, C.C., Al-Ghalith, G.A., Alexander, H., Alm, E.J., Arumugam, M., Asnicar, F., Bai, Y., Bisanz, J.E., Bittinger, K., Brejnrod, A., Brislawn, C.J., Brown, C.T., Callahan, B.J., Caraballo-Rodríguez, A.M., Chase, J., Cope, E.K., da Silva, R., Diener, C., Dorrestein, P.C., Douglas, G.M., Durall, D.M., Duvallet, C., Edwardson, C.F., Ernst, M., Estaki, M., Fouquier, J., Gauglitz, J.M., Gibbons, S.M., Gibson, D.L., Gonzalez, A., Gorlick, K., Guo, J., Hillmann, B., Holmes, S., Holste, H., Huttenhower, C., Huttley, G.A., Janssen, S., Jarmusch, A.K., Jiang, L., Kaehler, B.D., Kang, K. bin, Keefe, C.R., Keim, P., Kelley, S.T., Knights, D., Koester, I., Kosciolek, T., Kreps, J., Langille, M.G.I., Lee, J., Ley, R., Liu, Y.X., Loftfield, E., Lozupone, C., Maher, M., Marotz, C., Martin, B.D., McDonald, D., McIver, L.J., Melnik, A. v., Metcalf, J.L., Morgan, S.C., Morton, J.T., Naimey, A.T., Navas-Molina, J.A., Nothias, L.F., Orchanian, S.B., Pearson, T., Peoples, S.L., Petras, D., Preuss, M.L., Pruesse, E., Rasmussen, L.B., Rivers, A., Robeson, M.S., Rosenthal, P., Segata, N., Shaffer, M., Shiffer, A., Sinha, R., Song, S.J., Spear, J.R., Swafford, A.D., Thompson, L.R., Torres, P.J., Trinh, P., Tripathi, A., Turnbaugh, P.J., Ul-Hasan, S., van der Hooft, J.J.J., Vargas, F., Vázquez-Baeza, Y., Vogtmann, E., von Hippel, M., Walters, W., Wan, Y., Wang, M., Warren, J., Weber, K.C., Williamson, C.H.D., Willis, A.D., Xu, Z.Z., Zaneveld, J.R., Zhang, Y., Zhu, Q., Knight, R., Caporaso, J.G., **2019**. Reproducible, interactive, scalable and extensible microbiome data science using QIIME 2. Nature Biotechnology 2019 37:8 37, 852–857. https://doi.org/10.1038/s41587-019-0209-9

Bonomo, S., Cascella, A., Alberico, I., Sorgato S., Pelosi, N., Ferraro, L., Lirer, F., Vallefuoco, M., Agnini, C., Pappone, G., Bellucci, L., **2016**. Reworked Coccoliths as runoff proxy for the last 400 years: the case of Gaeta Gulf (Central Tyrrhenian Sea, Central Italy). Palaeogeography, Palaeoclimatology, Palaeoecology. 459, 15-28.

Bonomo, S., Cascella, A., Alberico, I., Ferraro, L., Giordano, L., Lirer, F., Vallefuoco, M., Marsella, E. **2014**. Coccolithophores from near the Volturno estuary (central Tyrrhenian Sea). Mar. Micropaleontol. 111, 26–37.

Borja, Á., Dauer, D.M., Grémare, A., **2012**. The importance of setting targets and reference conditions in assessing marine ecosystem quality. Ecol Indic 12, 1–7. https://doi.org/10.1016/j.ecolind.2011.06.018

Borja, A., Muxika, I., **2005**. Guidelines for the use of AMBI (AZTI's Marine Biotic Index) in the assessment of the benthic ecological quality. Marine Pollution Bulletin 50, 787–789. https://doi.org/10.1016/j.marpolbul.2005.04.040

Borja, A., Muxika, I., Franco, J., **2003**. The application of a Marine Biotic Index to different impact sources affecting soft-bottom benthic communities along European coasts. Marine Pollution Bulletin 46, 835–845. https://doi.org/10.1016/S0025-326X(03)00090-0

Borja, A., Franco, J., Perez Landa, V., **2000**. A Marine Biotic Index to Establish the Ecological Quality of Soft-Bottom Benthos Within European Estuarine and Coastal Environments. Marine Pollution Bulletin 40, 1100–1114. https://doi.org/10.1016/S0025-326X(00)00061-8

Bouchet, V.M.P., Frontalini, F., Francescangeli, F., Sauriau, P.-G., Geslin, E., Martins, M.V.A., Almogi-Labin, A., Avnaim-Katav, S., Di Bella, L., Cearreta, A., Coccioni, R., Costelloe, A., Dimiza, M.D.,

Ferraro, L., Haynert, K., Martínez-Colón, M., Melis, R., Schweizer, M., Triantaphyllou, M.V., Tsujimoto, A., Wilson, B., Armynot du Châtelet, E., **2021**. Indicative value of benthic foraminifera for biomonitoring: Assignment to ecological groups of sensitivity to total organic carbon of species from European intertidal areas and transitional waters. Marine Pollution Bulletin 164, 112071. https://doi.org/10.1016/j.marpolbul.2021.112071

Bouchet, V.M.P., Goberville, E., Frontalini, F., **2018a**. Benthic foraminifera to assess Ecological Quality Statuses in Italian transitional waters. Ecological Indicators 84, 130–139. https://doi.org/10.1016/j.ecolind.2017.07.055

Bouchet, V.M.P., Telford, R.J., Rygg, B., Oug, E., Alve, E., **2018b**. Can benthic foraminifera serve as proxies for changes in benthic macrofaunal community structure? Implications for the definition of reference conditions. Marine Environmental Research 137, 24–36. https://doi.org/10.1016/j.marenvres.2018.02.023

Bouchet, V.M.P., Alve, E., Rygg, B., Telford, R.J., **2012**. Benthic foraminifera provide a promising tool for ecological quality assessment of marine waters. Ecological Indicators 23, 66–75. https://doi.org/10.1016/j.ecolind.2012.03.011

Bouchet, V.M.P., Sauriau, P.-G., **2008**. Influence of oyster culture practices and environmental conditions on the ecological status of intertidal mudflats in the Pertuis Charentais (SW France): A multi-index approach. Marine Pollution Bulletin 56, 1898–1912. https://doi.org/10.1016/j.marpolbul.2008.07.010

Bouchet, V.M., Debenay, J.P., Sauriau, P.G., Radford-Knoery, J., Soletchnik, P., **2007**. Effects of short-term environmental disturbances on living benthic foraminifera during the Pacific oyster summer mortality in the Marennes-Ol´eron Bay (France). Mar. Environ. Res. 64 (3), 358–383. https://doi.org/10.1016/j.marenvres.2007.02.007.

Brandt, M.I., Trouche, B., Quintric, L., Günther, B., Wincker, P., Poulain, J., Arnaud-Haond, S., **2021**. Bioinformatic pipelines combining denoising and clustering tools allow for more comprehensive prokaryotic and eukaryotic metabarcoding. Molecular Ecology Resources 21, 1904–1921. https://doi.org/10.1111/1755-0998.13398

Brosnahan, M.L., Ralston, D.K., Fischer, A.D., Solow, A.R., Anderson, D.M., **2017**. Bloom termination of the toxic dinoflagellate Alexandrium catenella: Vertical migration behavior, sediment infiltration, and benthic cyst yield. Limnology and oceanography 62, 2829–2849. https://doi.org/10.1002/lno.10664

Brown, S.K., Blois, J.L., **2016**. Ecological Insights from Ancient DNA. eLS 1–7. https://doi.org/10.1002/9780470015902.a0026352

Budillon, F., Esposito, E., Iorio, M., Pelosi, N., Porfido, S., Violante, C., **2005**. The geological record of storm events over the last 1000 years in the Salerno Bay (Southern Tyrrhenian Sea): new proxy evidences. Advances in Geosciences. 2, 123–130.

Burton, G Allen, Burton, G A, **2002**. Sediment quality criteria in use around the world. Limnology 3:2 3, 65–76. https://doi.org/10.1007/S102010200008

Callahan, B.J., McMurdie, P.J., Rosen, M.J., Han, A.W., Johnson, A.J.A., Holmes, S.P., **2016**. DADA2: High-resolution sample inference from Illumina amplicon data. Nature Methods 13, 581–583. https://doi.org/10.1038/nmeth.3869

Camacho, C., Coulouris, G., Avagyan, V., Ma, N., Papadopoulos, J., Bealer, K., Madden, T.L., **2009**. BLAST+: Architecture and applications. BMC Bioinformatics 10, 1–9. https://doi.org/10.1186/1471-2105-10-421

Cao, Y., Lei, Y., Fang, J., Li, T., **2022**. Molecular diversity of foraminiferal eDNA in sediments and their correlations with environmental factors from the Yellow Sea. Ecological Indicators. 142. 109294. https://doi.org/10.1016/j.ecolind.2022.109294.

Capo, E., Giguet-Covex, C., Rouillard, A., Nota, K., Heintzman, P.D., Vuillemin, A., Ariztegui, D., Arnaud, F., Belle, S., Bertilsson, S., Bigler, C., Bindler, R., Brown, A.G., Clarke, C.L., Crump, S.E., Debroas, D., Englund, G., Ficetola, G.F., Garner, R.E., Gauthier, J., Gregory-Eaves, I., Heinecke, L., Herzschuh, U., Ibrahim, A., Kisand, V., Kjær, K.H., Lammers, Y., Littlefair, J., Messager, E., Monchamp, M.E., Olajos, F., Orsi, W., Pedersen, M.W., Rijal, D.P., Rydberg, J., Spanbauer, T., Stoof-Leichsenring, K.R., Taberlet, P., Talas, L., Thomas, C., Walsh, D.A., Wang, Y., Willerslev, E., van Woerkom, A., Zimmermann, H.H., Coolen, M.J.L., Epp, L.S., Domaizon, I., Alsos, I.G., Parducci, L., **2021**. Lake Sedimentary DNA Research on Past Terrestrial and Aquatic Biodiversity: Overview and Recommendations. Quaternary 2021, Vol. 4, Page 6 4, 6. https://doi.org/10.3390/quat4010006

Capotondi, L., Bonomo, S., Graiani, A., Innangi, M., Innangi, S., Giglio, F., Ravaioli, M., Ferraro, L., **2022**. Spatial Distribution of Benthic Foraminifera in the Neretva Channel (Croatia Coast): Faunal Response to Environmental Parameters. Geosciences. 12, 456. https://doi.org/10.3390/geosciences12120456

Carraro, L., Mächler, E., Wüthrich, R., Altermatt, F., **2020**. Environmental DNA allows upscaling spatial patterns of biodiversity in freshwater ecosystems. Nature Communications. 11:1 11, 1–12. https://doi.org/10.1038/s41467-020-17337-8

Cavaliere, M., Barrenechea Angeles, I., Montresor, M., Bucci, C., Brocani, L., Balassi, E., Margiotta, F., Francescangeli, F., Bouchet, V.M.P., Pawlowski, J., Frontalini, F., **2021**. Assessing the ecological quality status of the highly polluted Bagnoli area (Tyrrhenian Sea, Italy) using foraminiferal eDNA metabarcoding. Science of The Total Environment 790, 147871. https://doi.org/10.1016/j.scitotenv.2021.147871

Celico, F., Esposito, L., Mancuso, M., **2000**. Complessità idrodinamica e idrochimica dell'area urbana di Napoli: scenari interpretativi.

Chao, A., Shen. T.-J., **2003.** Nonparametric estimation of Shannon' s index of diversity when there are unseen species in sample. Environmental and Ecological Statistics. 10, 429-443.

Ciacci, C., Betti, M., Abramovich, S., Cavaliere, M., Frontalini, F. **2022**. Mercury-Induced Oxidative Stress Response in Benthic Foraminifera: An In Vivo Experiment on Amphistegina lessonii. Biology,11, 960. https://doi.org/10.3390/biology11070960

Cicchella, D., Vivo, B.D., Lima, A., **2005**. Background and baseline concentration values of elements harmful to human health in the volcanic soils of the metropolitan and provincial areas of Napoli (Italy). Geochemistry: Exploration, Environment, Analysis 5, 29–40. https://doi.org/10.1144/1467-7873/03-042

Cimerman, F., Langer, M., **1991**. Mediterranean foraminifera, Slovenska akademija znanosti in umetnosti. Ljubljana,.

Cirillo, C., Bertoli, B., Acampora, G., Marcolongo, L., 2022. Bagnoli Urban Regeneration through Phytoremediation. Encyclopedia **2022**, Vol. 2, Pages 882-892 2, 882–892. https://doi.org/10.3390/encyclopedia2020058

Cirillo, C., Acampora, G., Bertoli, B., Russo, M., Scarpa, L., **2016**. Napoli e il paesaggio costiero: il recupero ambientale di Bagnoli e la rigenerazione del litorale Flegreo.

Clarke, K.R., Ainsworth, M., **1993**. A method of linking multivariate community structure to environmental variables. Marine Ecology Progress Series 92, 205–219. https://doi.org/10.3354/meps092205

Cobelo-Garcia, A., Prego, R., **2003**. Heavy metal sedimentary record in a Galician Ria (NW Spain): background values and recent contamination. Mar. Pollut. Bull. 46, 1253–1262.

Cordier, T., Alonso-Sáez, L., Apothéloz-Perret-Gentil, L., Aylagas, E., Bohan, D.A., Bouchez, A., Chariton, A., Creer, S., Frühe, L., Keck, F., Keeley, N., Laroche, O., Leese, F., Pochon, X., Stoeck, T., Pawlowski, J., Lanzén, A., **2021**. Ecosystems monitoring powered by environmental genomics: A review of current strategies with an implementation roadmap. Molecular Ecology 30, 2937–2958. https://doi.org/10.1111/MEC.15472

Cordier, T., Frontalini, F., Cermakova, K., Apothéloz-Perret-Gentil, L., Treglia, M., Scantamburlo, E., Bonamin, V., Pawlowski, J., **2019**. Multi-marker eDNA metabarcoding survey to assess the environmental impact of three offshore gas platforms in the North Adriatic Sea (Italy). Marine Environmental Research 146, 24–34. https://doi.org/10.1016/j.marenvres.2018.12.009

Costanza, R., D'Arge, R., de Groot, R., Farber, S., Grasso, M., Hannon, B., Limburg, K., Naeem, S., O'Neill, R. v., Paruelo, J., Raskin, R.G., Sutton, P., van den Belt, M., **1997**. The value of the world's ecosystem services and natural capital. Nature 1997 387:6630 387, 253–260. https://doi.org/10.1038/387253a0

Crutzen, P.J., Stoermer, E.F., **2000**. The "Anthropocene Glob. Chang. News Lett., 41, pp. 17-18

da Silva, L.C., Alves, M.M.V., Figueira, R., Frontalini, F., Pereira, E., Senez-Mello, T.M., Castelo Wellen, F.L., Saibro, M.B., Francescangeli, F., Mello e Sousa, S.H., Bergamaschi, S., Antonioli, L., Bouchet, V.M.P., Terroso, D., Rocha F., **2022**. Unravelling Anthropocene Paleoenvironmental Conditions Combining Sediment and Foraminiferal Data: Proof-of-Concept in the Sepetiba Bay (SE, Brazil). Frontiers in Ecology and Evolution. 10. DOI=10.3389/fevo.2022.852439

Dale, B., **2001**. Marine dinoflagellate cysts as indicators of eutrophication and industrial pollution: a discussion. Science of The Total Environment 264, 235–240. https://doi.org/10.1016/S0048-9697(00)00719-1

Dale, B., Thorsen, T.A., Fjellså, A., **1999**. Dinoflagellate cysts as indicators of cultural eutrophication in the Oslofjord, Norway Estuarine, Coastal and Shelf Science, 48, pp. 371-382.

D'Alisa G., Armiero M., De Rosa S.P., **2015**. Political ecology: Rethink Campania's toxic-waste scandal. Nature. 509-427. http://doi.org/10.1038/509427d

Damiani, V., Baudo, R., Rosa, S., Simone, R., Ferretti, O., Izzo, G., Serena, F., **1987**. A case study: Bay of Pozzuoli (Gulf of Naples, Italy). Hydrobiologia. https://doi.org/10.1007/BF00048661

Danovaro, R., Fanelli, E., Aguzzi, J., Billett, D., Carugati, L., Corinaldesi, C., Dell'Anno, A., Gjerde, K., Jamieson, A.J., Kark, S., McClain, C., Levin, L., Levin, N., Ramirez-Llodra, E., Ruhl, H., Smith, C.R., Snelgrove, P.V.R., Thomsen, L., van Dover, C.L., Yasuhara, M., **2020**. Ecological variables for developing a global deep-ocean monitoring and conservation strategy. Nature Ecology & Evolution. 4:2 4, 181–192. https://doi.org/10.1038/s41559-019-1091-z

de Alteriis, G., Fedi, M., Passaro, P., Siniscalchi, A. **2006.** Magneto-seismic interpretation of subsurface volcanism in the Gaeta Gulf (Italy, Tyrrhenian Sea). Ann. Geophys. 49, 4/5.

De Pippo, T., Donadio, C., Pennetta, M., **2003.** Morphological control on sediment dispersal along the southern Tyrrhenian coastal zones (Italy). Geol. Romana. 37, 113–121.

De Pippo, T., Donadio, C., Pennetta, M., Valente A., Vecchione, C., **1998**. Morphological and sedimentary evolution during the last 5000 years of the Bagnoli volcano-tectonic coastal plain (Naples, Italy). Geologica Romana 34(1):19-30

Di Vito, M.A., Lirer, L., Mastrolorenzo, G., Rolandi, G. **1987**. The Monte Nuovo eruption Campi Flegrei, Italy . Bull. Volcanol. 49, 608–615.

De Vivo, B., Lima, A., **2008**. Characterization and Remediation of a Brownfield Site. The Bagnoli Case in Italy., in: Environmental Geochemistry: Site Characterization, Data Analysis and Case Histories. pp. 355–385. https://doi.org/10.1016/B978-0-444-53159-9.00015-2

Decreto legislativo 3 aprile **2006** n. 152, Norme in materia ambientale. Gazzetta Ufficiale n. 88 del 14 aprile 2006.

Delbono, I., Barsanti, M., Schirone, A., Conte, F., Delfanti, R., **2016**. 210Pb mass accumulation rates in the depositional area of the Magra River (Mediterranean Sea, Italy). Continental Shelf Research 124, 35–48. https://doi.org/10.1016/j.csr.2016.05.010

Del Gaudio, C., Aquino, I., Ricciardi, G.P., Ricco, C., Scandone, R., **2010**. Unrest episodes at Campi Flegrei: a reconstruction of vertical ground movements during 1905-2009. J Volcanol Geotherm Res 195:48–56

Dias, H., Sukumaran, S., **2023**. Are genomic indices effective alternatives to morphology based benthic indices in biomonitoring studies? Perspectives from a major harbour and marine protected area. Marine Pollution Bulletin. 187. 114586. https://doi.org/10.1016/j.marpolbul.2023.114586

Dijkstra, N., Junttila, J., Aagaard-Sørensen, S., **2017**. Environmental baselines and reconstruction of Atlantic Water inflow in BjØrnØyrenna, SW Barents Sea, since 1800 CE. Marine Environmental Research 132, 117–131. https://doi.org/10.1016/j.marenvres.2017.10.012

Dimiza, M.D., Triantaphyllou, M.V., Koukousioura, O., Hallock, P., Simboura, N., Karageorgis, A.P., Papathanasiou, E., **2016**. The Foram Stress Index: A new tool for environmental assessment of soft-bottom environments using benthic foraminifera. A case study from the Saronikos Gulf, Greece, Eastern Mediterranean. Ecological Indicators 60, 611–621. https://doi.org/10.1016/j.ecolind.2015.07.030

Di Rita, F., Lirer, F., Bonomo, S., Cascella, A., Ferraro, L., Florindo, F., Insinga, D.D., Lurcock, P.C., Margaritelli, G., Petrosino, P., Rettori, R., Vallefuoco, M., Magri, D., **2018**. Late Holocene forest dynamics in the Gulf of Gaeta (central Mediterranean) in relation to NAO variability and human impact. Quaternary Science Reviews. 179, 137-152.

Di Rita, F., Lirer, F., Margaritelli, G., Michelangeli, F., Magri, D., **2019**. Climate and human influence on the vegetation of Tyrrhenian Italy during the last 2000 years: new insights from microcharcoal and non-pollen palynomorphs. Geografia Fisica e Dinamica Quaternaria**.,** 42. 203-214. 10.4461/GFDQ.2019.42.10.

Dirzo, R., Young, H.S., Galetti, M., Ceballos, G., Isaac, N.J.B., Collen, B., **2014**. Defaunation in the Anthropocene. Science (1979) 345, 401–406. https://doi.org/10.1126/science.1251817

Djurhuus, A., Closek, C.J., Kelly, R.P., Pitz, K.J., Michisaki, R.P., Starks, H.A., Walz, K.R., Andruszkiewicz, E.A., Olesin, E., Hubbard, K., Montes, E., Otis, D., Muller-Karger, F.E., Chavez, F.P., Boehm, A.B., Breitbart, M., **2020**. Environmental DNA reveals seasonal shifts and potential interactions in a marine community. Nature Communications 2020 11:1 11, 1–9. https://doi.org/10.1038/s41467-019-14105-1

Dolven, J.K., Alve, E., Rygg, B., Magnusson, J., **2013**. Defining past ecological status and in situ reference conditions using benthic foraminifera: a case study from the Oslofjord, Norway. Ecol. Indicat. 29, 219–233. https://doi.org/10.1016/j. ecolind.2012.12.031.

Donadio, C., Vigliotti, M., Valente, R., Stanislao, C., Ivaldi, R., Ruberti, D., **2018**. Anthropic vs. natural shoreline changes along the northern Campania coast, Italy. Journal of Coastal Conservation. 22, 939–955.

Dornelas, M., Gotelli, N.J., McGill, B., Shimadzu, H., Moyes, F., Sievers, C., Magurran, A.E., **2014**. Assemblage time series reveal biodiversity change but not systematic loss. Science (1979) 344, 296–299. https://doi.org/10.1126/SCIENCE.1248484

Dufresne, Y., Lejzerowicz, F., Perret-Gentil, L.A., Pawlowski, J., Cordier, T., **2019**. SLIM: A flexible web application for the reproducible processing of environmental DNA metabarcoding data. BMC Bioinformatics 20. https://doi.org/10.1186/s12859-019-2663-2

Edgar, R.C., Haas, B.J., Clemente, J.C., Quince, C., Knight, R., **2011**. UCHIME improves sensitivity and speed of chimera detection. Bioinformatics 27, 2194–2200. https://doi.org/10.1093/bioinformatics/btr381

El Kateb, A., Stalder, C., Martínez-Colón, M., Mateu-Vicens, G., Francescangeli, F., Coletti, G., Stainbank, S., Spezzaferri, S., **2020**. Foraminiferal-based biotic indices to assess the ecological quality status of the Gulf of Gabes (Tunisia): Present limitations and future perspectives. Ecological Indicators 111. https://doi.org/10.1016/j.ecolind.2019.105962

Esling, P., Lejzerowicz, F., Pawlowski, J., **2015**. Accurate multiplexing and filtering for high-throughput amplicon-sequencing. Nucleic Acids Research 43, 2513–2524. https://doi.org/10.1093/nar/gkv107

Fajemila, O., Martinez-Colon, M., Council, I., Spezzaferri, S., **2022**. Spatial distribution of pollution levels and assessment of benthic foraminifera in Apapa-Badagry Creek, Nigeria. Marine Pollution Bulletin. 185. 114359. https://doi.org/10.1016/j.marpolbul.2022.114359.

Falzoni, F., Petrizzo, M.R., Valagussa, M.. **2018**. A morphometric methodology to assess planktonic foraminiferal response to environmental perturbations: the case study of Oceanic Anoxic Event 2, Late Cretaceous.

Fasciglione, P., Barra, M., Santucci, A., Ciancimino, S., Mazzola, S., Passaro, S., **2016**. Macrobenthic community status in highly polluted area: a case study from Bagnoli, Naples Bay, Italy. Rendiconti Lincei 27, 229–239. https://doi.org/10.1007/S12210-015-0467-5

Ferraro, S., Coccioni, R., Sabatino, N., Del Core, M., Sprovieri, M., **2020**. Morphometric response of late Aptian planktonic foraminiferal communities to environmental changes: A case study of Paraticinella rohri at Poggio le Guaine (central Italy), Palaeogeography, Palaeoclimatology, Palaeoecology. 538, 109384, ISSN 0031-0182, https://doi.org/10.1016/j.palaeo.2019.109384

Fontanier, C., Jorissen, F.J, Licari, L., Alexandre, A., Anschutz, P., Carbonel, P. **2002.** Live benthic foraminiferal faunas from the Bay of Biscay: faunal density, composition, and microhabitats, Deep Sea

Research Part I: Oceanographic Research Papers,, 49, Issue 4, 751-785, ISSN 0967-0637, https://doi.org/10.1016/S0967-0637(01)00078-4.

Fossile, E., Sabbatini, A., Spagnoli, F., Caridi, F., Dell'Anno, A., De Marco, R., Dinelli, E., Droghini, E., Tramontana, M., Negri, A., **2021**. Sensitivity of foraminiferal-based indices to evaluate the ecological quality status of marine coastal benthic systems: A case study of the Gulf of Manfredonia (southern Adriatic Sea). Marine Pollution Bulletin 163, 111933. https://doi.org/10.1016/j.marpolbul.2020.111933

Francescangeli, F., Milker, Y., Bunzel, D., Thomas, H., Norbisrath, M., Schönfeld, J., Schmiedl, G. **2021.** Recent benthic foraminiferal distribution in the Elbe Estuary (North Sea, Germany): A response to environmental stressors. Estuarine, Coastal and Shelf Science. 251, 107198.

Francescangeli, F., Quijada, M., Armynot du Châtelet, E., Frontalini, F., Trentesaux, A., Billon, G., Bouchet, V.M.P., **2020**. Multidisciplinary study to monitor consequences of pollution on intertidal benthic ecosystems (Hauts de France, English Channel, France): Comparison with natural areas. Marine Environmental Research. 160. https://doi.org/10.1016/j.marenvres.2020.105034

Francescangeli, F., Portela, M., Armynot du Chalet, E., Billon, G., Andersen, T.J., Bouchet, V.M.P., Trentesaux, A. **2018.** Infilling of the Canche Estuary (eastern English Channel, France): Insightfrom benthic foraminifera and historical pictures. Marine Micropaleontology.142, 1-12.

Francescangeli, F., Armynot du Chatelet, E., Billon, G., Trentesaux, A., Bouchet, V.M.P., **2016**. Palaeo-ecological quality status based on foraminifera of Boulogne-sur-Mer harbour (Pas-de-Calais, Northeastern France) over the last 200 years. Marine Environmental Research. 117, 32–43. https://doi.org/10.1016/j.marenvres.2016.04.002

Frezza, V., Guillem, M.V., Gaglianone, G., Baldassarre, A., Brandano, M. **2011**. Mixed carbonate-siliclastic sediments and benthic foraminiferal assemblages from Posidonia oceanica seagrass meadows of the central Tyrrhenian continental shelf (Latium, Italy). Italian Journal of Geosciences., 130, 352-369. 10.3301/IJG.2011.07.

Frontalini, F., Cordier, T., Balassi, E., Armynot du Chatelet, E., Cermakova, K., Apothéloz-Perret-Gentil, L., Martins, M.V.A., Bucci, C., Scantamburlo, E., Treglia, M., Bonamin, V., Pawlowski, J., **2020**. Benthic foraminiferal metabarcoding and morphology-based assessment around three offshore gas platforms: Congruence and complementarity. Environment International. 144, 106049. https://doi.org/10.1016/j.envint.2020.106049

Frontalini, F., Greco, M., Di Bella, L., Lejzerowicz, F., Reo, E., Caruso, A., Cosentino, C., Maccotta, A., Scopelliti, G., Nardelli, M.P., Losada, M.T., Armynot du Châtelet, E., Coccioni, R., Pawlowski, J., **2018**. Assessing the effect of mercury pollution on cultured benthic foraminifera community using morphological and eDNA metabarcoding approaches. Marine Pollution Bulletin 129, 512–524. https://doi.org/10.1016/j.marpolbul.2017.10.022

Frontalini, F., Semprucci, F., Armynot du Châtelet, É., Francescangeli, F., Margaritelli, G., Rettori, R., Spagnoli, F., Balsamo, M., Coccioni, R. **2014.** Biodiversity trends of the meiofaunal and foraminiferal assemblages of Lake Varano (southern Italy). Proc. Biol. Soc. Wash. 127, 7–22.

Frontalini, F., Coccioni, R. **2008**. Benthic foraminifera for heavy metal pollution monitoring: A case study from the central Adriatic Sea coast of Italy. Estuarine Coastal and Shelf Science 76(2):404-417. 10.1016/j.ecss.2007.07.024

Frøslev, T.G., Kjøller, R., Bruun, H.H., Ejrnæs, R., Brunbjerg, A.K., Pietroni, C., Hansen, A.J., **2017**. Algorithm for post-clustering curation of DNA amplicon data yields reliable biodiversity estimates. Nature Communications 2017 8:1 8, 1–11. https://doi.org/10.1038/s41467-017-01312-x

Gambi, C., Dell'Anno, A., Corinaldesi, C., lo Martire, M., Musco, L., da Ros, Z., Armiento, G., Danovaro, R., **2020**. Impact of historical contamination on meiofaunal assemblages: The case study of the Bagnoli-Coroglio Bay (southern Tyrrhenian Sea). Marine Environmental Research 156, 104907. https://doi.org/10.1016/J.MARENVRES.2020.104907

Gordon, E., Goni, M., **2003**. Sources and distribution of terrigenous organic matter delivered by the Atchafalaya River to sediments in the northern Gulf of Mexico. Geochimica et Cosmochimica Acta 67, 2359–2375. https://doi.org/10.1016/S0016-7037(02)01412-6

Grimm, E.C., **1987**. CONISS: a FORTRAN 77 program for stratigraphically constrained cluster analysis by the method of incremental sum of squares. Computers & Geosciences 13, 13–35. https://doi.org/10.1016/0098-3004(87)90022-7

Gu, Z., Gu, L., Eils, R., Schlesner, M., Brors, B., **2014**. circlize implements and enhances circular visualization in R. Bioinformatics 30, 2811–2812. https://doi.org/10.1093/bioinformatics/btu393

Guillou, L., Bachar, D., Audic, S., Bass, D., Berney, C., Bittner, L., Boutte, C., Burgaud, G., de Vargas, C., Decelle, J., del Campo, J., Dolan, J.R., Dunthorn, M., Edvardsen, B., Holzmann, M., Kooistra, W.H.C.F., Lara, E., le Bescot, N., Logares, R., Mahé, F., Massana, R., Montresor, M., Morard, R., Not, F., Pawlowski, J., Probert, I., Sauvadet, A.L., Siano, R., Stoeck, T., Vaulot, D., Zimmermann, P., Christen, R., **2013**. The Protist Ribosomal Reference database (PR2): a catalog of unicellular eukaryote Small Sub-Unit rRNA sequences with curated taxonomy. Nucleic acids research 41, D597. https://doi.org/10.1093/nar/gks1160

Hakanson, L., **1980**. An ecological risk index for aquatic pollution control. A sedimentological approach. Water Research 14, 975–1001. https://doi.org/10.1016/0043-1354(80)90143-8

Hammer, Ø., Harper, D.A.T., Ryan, P.D., **2001**. Past: Paleontological Statistics Software Package for Education and Data Analysis. Palaeontologia Electronica 4, 9.

Hausser, J., Strimmer, K. **2014.** Entropy: Estimation of Entropy, Mutual Information and Related Quantities. R package version. Vienna, Austria, R fundation for statistical computing.

Hayward, B.W., Le Coze, F., Vachard, D., Gross, O. World Foraminifera Database. Foraminiferida. **2022**. Accessed through: World Register of Marine Species at: https://www.marinespecies.org/aphia.php?p=taxdetails&id=22528 on 2022-12-22

Hayward, B.W., Wilson, K., Morley, M.S., Cochran, U., Grenfell, H.R., Sabaa, A.T., Daymond- King, R. **2010**. Microfossil record of the Holocene evolution of coastal wetlands in a technologically active region of New Zealand. The Holocene. 20, 405-421.

Hayward, B. W., Sabaa, A. T., Grenfell, H., R., **2004**. Benthic foraminiferal abundance and diversities of ODP Site. Appendix 1, 181-1119. PANGAEA, https://doi.org/10.1594/PANGAEA.464587, In supplement to: Hayward, BW et al. (2004): Benthic foraminifera and the Late Quaternary (last 150 ka) paleoceanographic and sedimentary history of the Bounty Trough, east of New Zealand. Palaeogeography, Palaeoclimatology, Palaeoecology, 211(1-2), 59-93, https://doi.org/10.1016/j.palaeo.2004.04.007

He, X., Sutherland, T.F., Pawlowski, J., Abbott, C.L., **2019**. Responses of foraminifera communities to aquaculture-derived organic enrichment as revealed by environmental DNA metabarcoding. Molecular Ecology 28, 1138–1153. https://doi.org/10.1111/mec.15007

Hess, S., Alve, E., Andersen, T.J., Joranger, T., **2020**. Defining ecological reference conditions in naturally stressed environments–How difficult is it? Mar. Environ. Res. 104885. https://doi.org/10.1016/j.marenvres.2020.104885.

Hill, M.O., **1973**. Diversity and Evenness: A Unifying Notation and Its Consequences. Ecology 54, 427–432. https://doi.org/10.2307/1934352

Holt, E. A., Miller, S. W., **2010**. Bioindicators: Using Organisms to Measure Environmental Impacts. Nature Education Knowledge 3(10):8

Horner-Devine, A.R., Hetland, R.D., MacDonald, D.G. **2015**. Mixing and transport in coastal river plumes. Annu. Rev. Fluid Mech., 47, 569–594. doi: 10.1146/annurev-fluid-01031141408

Horner, R.A., Greengrove, C.L., Davies-Vollum, K.S., Gawel, J.E., Postel, J.R., Cox, A.M., **2011**. Spatial distribution of benthic cysts of Alexandrium catenella in surface sediments of Puget Sound, Washington, USA. Harmful Algae 11, 96–105. https://doi.org/10.1016/j.hal.2011.08.004

Horrocks, M., Nichol, S.L., D'Costa, D.M., Augustinus, P., Jacobi, T., Shane, P.A., Middleton, A. **2007**. A late quaternary record of natural change and human impact from Rangihoua Bay, bay of islands, northern New Zealand. J. Coast. Res. 592–604.

Iermano, I., Liguori, G., Iudicone, D., Nardelli, B., Colella, S., Zingone, A., Saggiomo, V., Ribera d'Alcalà, M., **2012**. Filament formation and evolution in buoyant coastal waters: observation and modelling. Prog. Oceanogr.106, 118–137.

Incarbona, A., Ziveri, P., Di Stefano, E., Lirer, F., Mortyn, G., Patti, B., Pelosi, N., Sprovieri, M., Tranchida, G., Vallefuoco, M., Albertazzi, S., Bellucci, L.G., Bonanno, A., Bonomo, S., Censi, P., Ferraro, L., Giuliani, S., Mazzola, S., Sprovieri, R. **2010**. Calcareous nannofossil assemblages from the Central Mediterranean Sea over the last four centuries: the impact of the Little Ice Age. Climate of the Past. 6, 817–866.

Istituto Centrale per la Ricerca Scientifica e Tecnologica Applicata al Mare (ICRAM) & Agenzia per la Protezione dell'Ambiente e per i Servizi Tecnici (APAT), **2007**. Manuale per la movimentazione di sedimenti marini. Ministero dell'Ambiente e della Tutela del Territorio e del Mare.

Istituto Geografico Militare, **1914**, Cartografia 1:25000

Jahan, S., Strezov, V., **2019**. Assessment of trace elements pollution in the sea ports of New South Wales (NSW), Australia using oysters as bioindicators. Sci Rep 9, 1416. https://doi.org/10.1038/s41598-018-38196-w

Jorissen, F., Nardelli, M.P., Almogi-Labin, A., Barras, C., Bergamin, L., Bicchi, E., El Kateb, A., Ferraro, L., McGann, M., Morigi, C., Romano, E., Sabbatini, A., Schweizer, M., Spezzaferri, S., **2018**. Developing Foram-AMBI for biomonitoring in the Mediterranean: Species assignments to ecological categories. Marine Micropaleontology 140, 33–45. https://doi.org/10.1016/j.marmicro.2017.12.006

Jorissen, F.J., Barmawidjaja, D.M. , Puskaric, S., van der Zwaan, G.J., **1992.** Vertical distribution of benthic foraminifera in the northern Adriatic Sea: The relation with the organic flux. Marine Micropaleontology. 19, Issues 1–2,131-146, ISSN 0377-8398.

Juggins S. *rioja: Analysis of Quaternary Science Data*. **2022.** R package version 1.0-5, https://cran.r-project.org/package=rioja.

Kaiho, K., **1994.** Benthic foraminiferal dissolved-oxygen index and dissolved-oxygen levels in the modern ocean. Geology. 22. 719-722. 10.1130/0091-7613(1994)022<0719:BFDOIA>2.3.CO,2.

Keck, F., Millet, L., Debroas, D., Etienne, D., Galop, D., Rius, D., Domaizon, I. **2020**. Assessing the response of micro-eukaryotic diversity to the Great Acceleration using lake sedimentary DNA. Nat Commun 11, 3831. https://doi.org/10.1038/s41467-020-17682-8

Keeley, N., Wood, S. A., Pochon, X. **2018**. Development and preliminary validation of a multi-trophic metabarcoding biotic index for monitoring benthic organic enrichment, Ecological Indicators, Volume 85, 1044-1057, https://doi.org/10.1016/j.ecolind.2017.11.014.

Kelly, R.P., Port, J.A., Yamahara, K.M., Martone, R.G., Lowell, N., Thomsen, P.F., Mach, M.E., Bennett, M., Prahler, E., Caldwell, M.R., Crowder, L.B., **2014**. Harnessing DNA to improve environmental management. Science (1979) 344, 1455–1456. https://doi.org/10.1126/science.1251156

Keyes, A.A., McLaughlin, J.P., Barner, A.K., Dee, L.E., **2021**. An ecological network approach to predict ecosystem service vulnerability to species losses. Nature Communications 2021 12:1 12, 1–11. https://doi.org/10.1038/s41467-021-21824-x

Klootwijk, A., Alve, E., Hess, S., Renaud, P., Sørlie, C., Dolven, J., **2020**. Monitoring environmental impacts of fish farms: Comparing reference conditions of sediment geochemistry and benthic foraminifera with the present. Ecological Indicators. 120. 10.1016/j.ecolind.2020.106818.

Kowalska, J.B., Mazurek, R., Gąsiorek, M., Zaleski, T., **2018**. Pollution indices as useful tools for the comprehensive evaluation of the degree of soil contamination–A review. Environmental geochemistry and health 40, 2395–2420. https://doi.org/10.1007/S10653-018-0106-Z

Kranner, M., Harzhauser, M. Beer, C., Auer, G., Piller, W. E. **2022.** Calculating dissolved marine oxygen values based on an enhanced Benthic Foraminifera Oxygen Index. Scientific Reports. 12(1), 1376.

Lanzén, A., Dahlgren, T.G., Bagi, A., Hestetun, J.T., **2021**. Benthic eDNA metabarcoding provides accurate assessments of impact from oil extraction, and ecological insights. Ecological Indicators 130, 108064. https://doi.org/10.1016/j.ecolind.2021.108064

Laroche, O., Wood, S.A., Tremblay, L.A., Ellis, J.I., Lear, G., Pochon, X., **2018**. A cross-taxa study using environmental DNA/RNA metabarcoding to measure biological impacts of offshore oil and gas drilling and production operations. Marine Pollution Bulletin 127, 97–107. https://doi.org/10.1016/j.marpolbul.2017.11.042

Laroche, O., Wood, S.A., Tremblay, L.A., Ellis, J.I., Lejzerowicz, F., Pawlowski, J., Lear, G., Atalah, J., Pochon, X., **2016**. First evaluation of foraminiferal metabarcoding for monitoring environmental impact from an offshore oil drilling site. Marine Environmental Research 120, 225–235. https://doi.org/10.1016/j.marenvres.2016.08.009

Legambiente. Rapporto Ecoma I numeri e le storie della criminalità ambientale Legambiente: Roma, Italy. **2014**. http://www.amblav.it/download/0417_ecomafia_introduzione.pdf

Leray, M., Yang, J.Y., Meyer, C.P., Mills, S.C., Agudelo, N., Ranwez, V., Boehm, J.T., Machida, R.J., **2013**. A new versatile primer set targeting a short fragment of the mitochondrial COI region for metabarcoding metazoan diversity: Application for characterizing coral reef fish gut contents. Frontiers in Zoology 10, 1–14. https://doi.org/10.1186/1742-9994-10-34

Lewis, S.L., Maslin, M.A., **2015**. Defining the Anthropocene. Nature 2015, 519:7542 519, 171–180. https://doi.org/10.1038/nature14258

Li, X., Wai, O.W.H., Li, Y.S., Coles, B.J., Ramsey, M.H., Thrnton, I., **2000**. Heavy metal distribution in sediment profiles of the pearl river estuary, south China. Appl. Geochem. 15, 567–581.

Lirer, F., Sprovieri, M., Vallefuoco, M., Ferraro, L., Pelosi, N., Giordano, L., Capotondi, L., **2014.** Planktonic foraminifera as bio-indicators for monitoring the climatic changes that have occurred over the past 2000 years in the southeastern Tyrrhenian Sea. Integrative Zoology. 9, 542–554.

Lirer, F., Sprovieri, M., Ferraro, L., Vallefuoco, M., Capotondi, L., Cascella, A., Petrosino, P., Insinga, D.D., Pelosi, N., Tamburrino, S., Lubritto, C., **2013**. Integrated stratigraphy for the late Quaternary in the eastern Tyrrhenian Sea. Quaternary International. 292, 71–85.

Liu, C., Cui, Y., Li, X., Yao, M., **2021**. microeco: an R package for data mining in microbial community ecology. FEMS Microbiology Ecology 97, 255. https://doi.org/10.1093/femsec/fiaa255

Logemann, A. Reininghaus, M. Schmidt, M. Ebeling, A. Zimmermann, T. Wolschke, H. Friedrich, J., Brockmeyer, B. Pröfrock, D. Witt, G., **2022**. Assessing the chemical anthropocene – Development of the legacy pollution fingerprint in the North Sea during the last century, Environmental Pollution, Volume 302, 2022, 119040, ISSN 0269-7491, https://doi.org/10.1016/j.envpol.2022.119040

Long, E.R., MacDonald, D.D., Severn, C.G., Hong, C.B., **2000**. Classifying probabilities of acute toxicity in marine sediments with empirically derived sediment quality guidelines. Environmental Toxicology and Chemistry: an International Journal 19, 2598–2601. https://doi.org/10.1002/etc.5620191028

Long, E. R., Macdonald, D.D., Smith, S. L., Calder, F. D., **1995**. Incidence of Adverse Biological Effects Within Ranges of Chemical Concentration in Marine and Estuarine Sediments. Environmental Management. 19. 81-97. 10.1007/BF02472006.

Long, E. R., Morgan, L.G. **1990.** The potential for biological effects of the national status and trends program. OAA Tech. Memo NOS OMA 52. NOAA, Seattle, WA. 175.

Lu, G.Y., Wong, D.W., **2008**. An adaptive inverse-distance weighting spatial interpolation technique. Computers & Geosciences 34, 1044–1055. https://doi.org/10.1016/j.cageo.2007.07.010

Lu, Y., Yuan, J., Lu, X., Su, C., Zhang, Y., Wang, C., Cao, X., Li, Q., Su, J., Ittekkot, V., Garbutt, R.A., Bush, S., Fletcher, S., Wagey, T., Kachur, A., Sweijd, N., **2018**. Major threats of pollution and climate change to global coastal ecosystems and enhanced management for sustainability. Environmental Pollution 239, 670–680. https://doi.org/10.1016/j.envpol.2018.04.016

MacDonald, D.G., Carlson, J., Goodman, L., **2013.** On the heterogeneity of stratified-shear turbulence: Observations from a near-field river plume. J. Geophys. Res. Oceans. 118, 6223–6237. doi: 10.1002/2013JC008891

Mancini, L., Cero, C. D., Gucci, P., Venturi, L., Carlo, M. D., Volterra, L., **1994.** Il fiume Volturno-la definizione dello stato di salute del corpo idrico. Inquinamento. 10, 70–83.

Marbà, N., Díaz-Almela, E., Duarte, C.M., **2014**. Mediterranean seagrass (Posidonia oceanica) loss between 1842 and 2009. Biological Conservation 176, 183–190. https://doi.org/10.1016/j.biocon.2014.05.024

Margaritelli, G., Vallefuoco, M., Di Rita, F., Capotondi, L., Bellucci, L.G., Insinga, D.D., Petrosino, P., Bonomo, S., Cacho, I., Cascella, A., Ferraro, L., Florindo, F., Lubritto, C., Lurcock, P.C., Magri, D., Pelosi, N., Rettori, R., Lirer, F., **2016.** Marine response to climate changes during the last five millennia in the central Mediterranean Sea. Glob. Planet. Change. 142, 53e72. https://doi.org/10.1016/j.gloplacha.2016.04.007.

Martins, M.V., Alves, M., Yamashita, C., Sousa, S., Apostolos, E., Koutsoukos, M., Disaró, S., Debenay, J.P., Duleba, W., **2019**. Response of Benthic Foraminifera to Environmental Variability: Importance of Benthic Foraminifera in Monitoring Studies. 10.5772/intechopen.81658.

Martin, M., **2011**. Cutadapt removes adapter sequences from high-throughput sequencing reads. EMBnet Journal 17, 10–12. https://doi.org/10.14806/ej.17.1.200

McGrath, J., A., Joshua, N., Bess, A. S., Parkerton, T. F., **2019**. Review of Polycyclic Aromatic Hydrocarbons (PAHs) Sediment Quality Guidelines for the Protection of Benthic Life. Integrated Environmental Assessment and Management, (), ieam.4142–. doi:10.1002/ieam.4142

McKinney, M.L., **1990**. Trends in body-size evolution. In: McNamara, K.J. (Ed.), Evolutionary Trends, pp. 75–118.

McMichael, A.J. **1993**., Planetary Overload. Global Environ- mental Change and the Health of the Human Species. Cam- bridge University Press, Cambridge.

McMurdie, P.J., Holmes, S., **2013**. phyloseq: An R Package for Reproducible Interactive Analysis and Graphics of Microbiome Census Data. PLoS One 8, e61217. https://doi.org/10.1371/journal.pone.0061217

Meyers, P.A., **1994**. Preservation of elemental and isotopic source identification of sedimentary organic matter. Chemical Geology 114, 289–302. https://doi.org/10.1016/0009-2541(94)90059-0

Milker, Y., Schmiedl, G., **2012**. A taxonomic guide to modern benthic shelf foraminifera of the western Mediterranean Sea. Palaeontologia Electronica. https://doi.org/10.26879/271

Misuraca, M., Budillon, F., Tonielli, R., Di Martino, G., Innangi, S., Ferraro, L., **2018.** Coastal Evolution, Hydrothermal Migration Pathways and Soft Deformation along the Campania Continental Shelf (Southern Tyrrhenian Sea): Insights from High-Resolution Seismic Profiles. *Geosciences. 8,* 121. https://doi.org/10.3390/geosciences804012

Molisso, F., Caccavale, M., Capodanno, M., Di Gregorio, C., Gilardi, M., Guarino, A., Oliveri, E., Tamburrino, S., Sacchi, M., **2020**. Sedimentological analysis of marine deposits off the Bagnoli-Coroglio Site of National Interest (SNI), Pozzuoli (Napoli) Bay. Chemistry and Ecology, 36(6), 565–578. doi:10.1080/02757540.2020.1747447

Monchamp, M.E., Spaak, P., Domaizon, I., Dubois, N., Bouffard, D., Pomati, F., **2017**. Homogenization of lake cyanobacterial communities over a century of climate change and eutrophication. Nature Ecology & Evolution 2017 2:2 2, 317–324. https://doi.org/10.1038/s41559-017-0407-0

Montuori, P., De Rosa, E., Di Duca, F., Provvisiero, D.P., Sarnacchiaro, P., Nardone, A., Triassi, M., **2021**. Estimation of Polycyclic Aromatic Hydrocarbons Pollution in Mediterranean Sea from Volturno River,

Southern Italy: Distribution, Risk Assessment and Loads. Int. J. Environ. Res. Public Health. 18(4):1383. doi: 10.3390/ijerph18041383

Montuori, P, De Rosa, E., Sarnacchiaro, P., Di Duca, F., Provvisiero, D.P., Nardone, A., Triassi, M., **2020**. Polychlorinated biphenyls and organochlorine pesticides in water and sediment from Volturno River, Southern Italy: occurrence, distribution and risk assessment. Environmental Sciences Europe. 32, 123. 10.1186/s12302-020-00408-4.

Moretti, M., Sansone, E., Spezie, G., Vultaggio, M., De Maio, A., **1977**. Alcuni aspetti del movimento delle acque del Golfo di Napoli. Annali IUN. 45–46:207–217.

Morroni, L., d'Errico, G., Sacchi, M., Molisso, F., Armiento, G., Chiavarini, S., Rimauro, J., Guida, M., Siciliano, A., Ceparano, M., Aliberti, F., Tosti, E., Gallo, A., Libralato, G., Patti, F.P., Gorbi, S., Fattorini, D., Nardi, A., di Carlo, M., Mezzelani, M., Benedetti, M., Pellegrini, D., Musco, L., Danovaro, R., Dell'Anno, A., Regoli, F., **2020**. Integrated characterization and risk management of marine sediments: The case study of the industrialized Bagnoli area (Naples, Italy). Marine Environmental Research 160, 104984. https://doi.org/10.1016/j.marenvres.2020.104984

Müller, G., **1979**. Schwermetallen in den Redimen des rheins. Umschau 79, 778–783.

Murray, J. **2006**. Ecology and Applications of Benthic Foraminifera. Cambridge: Cambridge University Press. doi:10.1017/CBO9780511535529

Nava, M.L., Giampaola, D., Laforgia, E., Boenzi, G. **2007**. Tra il Clanis e il Sebeto: nuovi dati sull'occupazione della piana campana tra il Neolitico e l'eta del Bronzo. Atti della XL Riunione Scientifica Istituto Italiano di Preistoria e Protostoria., 1 101-126.

O'Connor T.P. **2004**. The sediment quality guideline, ERL, is not a chemical concentration at the threshold of sediment toxicity. Mar Pollut Bull. Sep;49(5-6):383-5. doi:10.1016/j.marpolbul.2004.06.024

Obura, D., Gudka, M., Samoilys, M., Osuka, K., Mbugua, J., Keith, D.A., Porter, S., Roche, R., van Hooidonk, R., Ahamada, S., Araman, A., Karisa, J., Komakoma, J., Madi, M., Ravinia, I., Razafindrainibe, H., Yahya, S., Zivane, F., **2021**. Vulnerability to collapse of coral reef ecosystems in the Western Indian Ocean. Nature Sustainability 2021 5:2 5, 104–113. https://doi.org/10.1038/s41893-021-00817-0

Oksanen, J., Guillaume Blanchet, F., Friendly, M., Kindt, R., Legendre, P., McGlinn, D., Minchin, P.R., O'Hara, R.B., Simpson, G.L., Solymos, P., Henry, M., Stevens, H., Szoecs, E., Wagner, H., **2019**. vegan: Community Ecology Package. R package version 2.5-5. [WWW Document]. https://CRAN.R-project.org/package=vegan.

Oksanen, O., Blanchet, F.G., Kindt, R., Legendre, P., Minchin, P.R., O'Hara, B., Simpson, G.L., Solymos, P., Stevens, H., Wagner, H.H., **2016.** Vegan: Community Ecology Package. R.

Oksanen, J., Kindt, R., Legendre, P., O'Hara, B., Stevens, M.H.H., Oksanen, M.J., Suggests, M., **2007**. The vegan package. Community ecology package 10, 631–637.

Parada, A.E., Needham, D.M., Fuhrman, J.A., **2016**. Every base matters: assessing small subunit rRNA primers for marine microbiomes with mock communities, time series and global field samples. Environmental Microbiology 18, 1403–1414. https://doi.org/10.1111/1462-2920.13023

Parent, B., Hyams-Kaphzan, O., Barras, C., Lubinevsky, H., Jorissen, F., **2021**. Testing foraminiferal environmental quality indices along a well-defined organic matter gradient in the Eastern Mediterranean. Ecological Indicators 125, 107498. https://doi.org/10.1016/j.ecolind.2021.107498

Parent, B., **2019**. Développement d'un indice biotique basé sur les foraminifères benthiques ; application sur la façade méditerranéenne française (Thèse de doctorat). Angers University.

Parrella, A., Isidori, M., Lavorgna, M., **2003**. Dell'Aquila, A. Stato di qualità del fiume Volturno integrato da indagini di tossicità e genotossicità. Ann. Ig. 15, 147–157.

Passaro, S., Gherardi, S., Romano, E., Ausili, A., Sesta, G., Pierfranceschi, G., Tamburrino, S., Sprovieri, M., **2020**. Coupled geophysics and geochemistry to record recent coastal changes of contaminated sites of the Bagnoli industrial area, Southern Italy. Estuarine, Coastal and Shelf Science 246, 107036. https://doi.org/10.1016/j.ecss.2020.107036

Pawlowski, J., Bruce, K., Panksep, K., Aguirre, F.I., Amalfitano, S., Apothéloz-Perret-Gentil, L., Baussant, T., Bouchez, A., Carugati, L., Cermakova, K., Cordier, T., Corinaldesi, C., Costa, F.O., Danovaro, R., Dell'Anno, A., Duarte, S., Eisendle, U., Ferrari, B.J.D., Frontalini, F., Frühe, L., Haegerbaeumer, A., Kisand, V., Krolicka, A., Lanzén, A., Leese, F., Lejzerowicz, F., Lyautey, E., Maček, I., Sagova-Marečková, M., Pearman, J.K., Pochon, X., Stoeck, T., Vivien, R., Weigand, A., Fazi, S., **2021**. Environmental DNA metabarcoding for benthic monitoring: A review of sediment sampling and DNA extraction methods. Science of The Total Environment 151783. https://doi.org/10.1016/j.scitotenv.2021.151783

Pawlowski, Jan, Esling, P., Lejzerowicz, F., Cedhagen, T., Wilding, T.A., **2014a**. Environmental monitoring through protist next-generation sequencing metabarcoding: assessing the impact of fish farming on benthic foraminifera communities. Mol Ecol Resour 14, 1129–1140. https://doi.org/10.1111/1755-0998.12261

Pawlowski, J., Lejzerowicz, F., Esling, P., **2014b**. Next-generation environmental diversity surveys of foraminifera: Preparing the future. Biological Bulletin 227, 93–106. https://doi.org/10.1086/BBLv227n2p93

Pawlowski, J., Lecroq, B., **2010**. Short rDNA barcodes for species identification in foraminifera. Journal of Eukaryotic Microbiology 57, 197–205. https://doi.org/10.1111/j.1550-7408.2009.00468.x

Pedersen, M.W., Overballe-Petersen, S., Ermini, L., der Sarkissian, C., Haile, J., Hellstrom, M., Spens, J., Thomsen, P.F., Bohmann, K., Cappellini, E., Schnell, I.B., Wales, N.A., Carøe, C., Campos, P.F., Schmidt, A.M.Z., Gilbert, M.T.P., Hansen, A.J., Orlando, L., Willerslev, E., **2015**. Ancient and modern environmental DNA. Philosophical Transactions of the Royal Society B: Biological Sciences 370, 20130383. https://doi.org/10.1098/rstb.2013.0383

Peréz-Cruz, L.L., Machain-Castilho, M.L. **1990**. Benthic foraminifera of the oxygen minimum zone, continental shelf of the Gulf of Tehuantepec, Mexico. Journal of Foraminiferal Research, 20: 312-325.

Pergent-Martini, C., Leoni, V., Pasqualini, V., Ardizzone, G., Balestri, E., Bedini, R., Belluscio, A., Belsher T., Borg, J., A Boudouresque, C., Boumaza, S., Bouquegneau, M., Buia, M., Calvo, S., Cebrian, J., Charbonnel, E., Cinelli, F., Cossu, A., Di Maida, G., Velimirov, B. **2005**. Descriptors of Posidonia oceanica meadows: Use and application. Ecological Indicators. 5. 213-230. 10.1016/j.ecolind.2005.02.004.

Pergent-Martini, C., **1998**. Posidonia oceanica: a biological indicator of past and present mercury contamination. Mar. Environ. Res. 45 (2), 101–111

Pergent, G., Pergent-Martini, C., Lepidochronological analysis in the mediterranean seagrass posidonia-oceanica state-of-the-art and future-developments. **1995**. Oceanologica Acta (0399-1784) (Gauthier-Villars), 1994 , Vol. 17 , N. 6 , P. 673-681

Peterson, B.G., Carl, P., Boudt, K., Bennett, R., Ulrich, J., Zivot, E., Cornilly, D., Hung, E., Lestel, M., Balkissoon, K., Wuertz, D., Christidis, A.A., Martin, R.D., Zhou, Z. "Zenith", Shea, J.M., **2020**. PerformanceAnalytics: Econometric Tools for Performance and Risk Analysis.

Peterson, B., Carl, P., Boudt, K., Bennett Ross, Ulrich, J., Zivot, E., Cornilly, D., **2014**. Econometric Tools for Performance and Risk Analysis.

Plant, J., Smith, D., Smith, B., Williams, L., **2000**. Environmental Geochemistry at the Global Scale. Journal of the Geological Society. 157. 837-849. 10.1144/jgs.157.4.837.

Pochon, X., Wood, S.A., Keeley, N.B., Lejzerowicz, F., Esling, P., Drew, J., Pawlowski, J., **2015**. Accurate assessment of the impact of salmon farming on benthic sediment enrichment using foraminiferal metabarcoding. Marine Pollution Bulletin 100, 370–382. https://doi.org/10.1016/j.marpolbul.2015.08.022

Porzio, L., Grech, D., Buia, M.C., **2020**. Long-term changes (1800–2019) in marine vegetational habitats: Insights from a historic industrialised coastal area. Marine Environmental Research 161, 105003. https://doi.org/10.1016/j.marenvres.2020.105003

Radicati di Brozolo, F., Di Girolamo, P., Turi, B., Oddone, M., **1988.** 40Ar/39Ar and K-Ar dating of K-rich rocks from the Roccamonfina volcano, roman comagmatic region, Italy. Geochimica Cosmochimica Acta. 52, 1435-1441.

Rezza, C., Albanese, S., Lima, A., De Vivo, B., **2015.** Geochemical characterization, isotopic approach and environmental risk assessment in the Domizio Flegreo and Agro Aversano area (Campania region). European Congress on Regional Geoscientific Cartography and Information System.

Rognes, T., Flouri, T., Nichols, B., Quince, C., Mahé, F., **2016**. VSEARCH: a versatile open source tool for metagenomics. PeerJ 4. https://doi.org/10.7717/peerj.2584

Romano, E., Bergamin, L., Celia Magno, M., Pierfranceschi, G., Ausili, A., **2018**. Temporal changes of metal and trace element contamination in marine sediments due to a steel plant: The case study of Bagnoli (Naples, Italy). Applied Geochemistry 88, 85–94. https://doi.org/10.1016/j.apgeochem.2017.05.012

Romano, E., Bergamin, L., Ausili, A., Pierfranceschi, G., Maggi, C., Sesta, G., Gabellini, M., **2009**. The impact of the Bagnoli industrial site (Naples, Italy) on sea-bottom environment. Chemical and textural features of sediments and the related response of benthic foraminifera. Marine Pollution Bulletin 59, 245–256. https://doi.org/10.1016/j.marpolbul.2009.09.017

Romano, E., Bergamin, L., Finoia, M.G., Carboni, M.G., Ausili, A., Gabellini, M., **2008**. Industrial pollution at Bagnoli (Naples, Italy): Benthic foraminifera as a tool in integrated programs of environmental characterisation. Marine Pollution Bulletin 56, 439–457. https://doi.org/10.1016/j.marpolbul.2007.11.003

Romano, E., Ausili, A., Zharova, N., Celia Magno, M., Pavoni, B., Gabellini, M., **2004**. Marine sediment contamination of an industrial site at Port of Bagnoli, Gulf of Naples, Southern Italy. Marine pollution bulletin 49, 487–95. https://doi.org/10.1016/j.marpolbul.2004.03.014

Ruberti, D., Buffardi, C., Sacchi, M., Vigliotti, M., **2022**. The late Pleistocene-Holocene changing morphology of the Volturno delta and coast (northern Campania, Italy): Geological architecture and human influence. Quaternary International. 625, 14-28, ISSN 1040-6182, https://doi.org/10.1016/j.quaint.2022.03.023.

Ruberti, D., Sacchi, M., Pepe, F., Vigliotti, M., **2018.** LGM incised valley in a volcanic setting. The northern campania plain (Southern Italy). In Alpine and Mediterranean Quaternary. In Proceedings of the Quaternary: Past, Present, Future—AIQUA Conference, Florence, Italy. 13–14, 35–38.

Rumolo, P., Barra, M., Gherardi, S., Marsella, E., Sprovieri, M., **2011**. Stable isotopes and C/N ratios in marine sediments as a tool for discriminating anthropogenic impact. Journal of Environmental Monitoring 13, 3399–3408. https://doi.ORG/10.1039/C1EM10568J

S. dos S. de Jesus, M., Frontalini, F., Bouchet, V.M.P., Yamashita, C., Sartoretto, J.R., Figueira, R.C.L., de Mello e Sousa, S.H., **2020**. Reconstruction of the palaeo-ecological quality status in an impacted estuary using benthic foraminifera: The Santos Estuary (São Paulo state, SE Brazil). Marine Environmental Research 162, 105121. https://doi.org/10.1016/j.marenvres.2020.105121

Sacchi, E., Conti, M.A., D'Orazi Porchetti, S., Logoluso, A., Nicosia, U., Perugini, G., Petti, F.M., **2009.** Aptian dinosaur footprints from the Apulia platform (Bisceglie, southern Italy) in the framework of the periadriatic ichnosites. Palaeogeogr. Palaeoclimatol. Palaeoecol. 271, 104- 116.

Salomons, W., de Rooij, N.M., Kerdijk, H., Bril, J., **1987**. Sediments as a source for contaminants? Hydrobiologia 149, 13–30. https://doi.org/10.1007/BF00048643

Samir, A.M., El-Din, A.B. **2001**. Benthic foraminiferal assemblages and morphological abnormalities as pollution proxies in two Egyptian bays. Marine Micropaleontology, 41: 193-227.

Sarkar, D., **2008**. Lattice. https://doi.org/10.1007/978-0-387-75969-2

Satellite Imagery, Google Earth, **1990**

Savvides, C., Papadopoulos, A., Haralambous, K.J., Loizidou, M., **1995**. Sea sediments contaminated with heavy metals: Metal speciation and removal. Water Science and Technology, Pollution of the Mediterranean Sea 32, 65–73. https://doi.org/10.1016/0273-1223(96)00077-7

Scandone, R., Giacomelli, L., Speranza, F.F., **2008**. Persistent activity and violent strombolian eruptions at Vesuvius between 1631 and 1944. Journal of Volcanology and Geothermal Research 170, 167–180. https://doi.org/10.1016/j.jvolgeores.2007.09.014

Schönfeld, J., Alve, E., Geslin, E., Jorissen, F., Korsun, S., Spezzaferri, S., Abramovich, S., Almogi-Labin, A., Châtelet, E., Barras, C., Bergamin, L., Bicchi, E., Bouchet, V., Cearreta, A., Bella, L.,Dijkstra, N., Disaró, S., Ferraro, L., Frontalini, F., Tsujimoto, A. **2012**. The FOBIMO (FOraminiferal BIo-MOnitoring) initiative. Towards a standardised protocol for soft-bottom benthic foraminiferal monitoring studi. Marine Micropaleontology. 94-95. 1-13. 10.1016/j.marmicro.2012.06.001.

Scott, D. B., Poag, C. W., Watts, A. B., **2005**. Quaternary benthic foraminifera abundance of Hole 95-612. PANGAEA, https://doi.org/10.1594/PANGAEA.251267

Sen Gupta, B.K., **1999**. Foraminifera in marginal marine environments. In: Sen Gupta, B.K. (Ed.), Modern Foraminifera. KluwerAcademic Publishing, London, pp. 217–23.

Segata, N., Izard, J., Waldron, L., Gevers, D., Miropolsky, L., Garrett, W.S., Huttenhower, C., **2011**. Metagenomic biomarker discovery and explanation. Genome Biology 12, 1–18. https://doi.org/10.1186/gb-2011-12-6-r60

Selvaggio, M.A., **2015**. A case study, Bagnoli: a difficult transition. Academicus International Scientific Journal MMXV, 40–50. https://doi.org/10.7336/academicus.2015.11.03

Sgarella, F., Moncharmont Zei, M., **1993**. Benthic foraminifera of the Gulf of Naples (Italy): systematics and autoecology. Boll. soc. paleontol. ital 32, 145–264

Siano, R., Lassudrie, M., Cuzin, P., Briant, N., Loizeau, V., Schmidt, S., Ehrhold, A., Mertens, K.N., Lambert, C., Quintric, L., Noël, C., Latimier, M., Quéré, J., Durand, P., Penaud, A., **2021**. Sediment archives reveal irreversible shifts in plankton communities after World War II and agricultural pollution. Current Biology 31, 2682-2689.e7. https://doi.org/10.1016/j.cub.2021.03.079

Simpson, G.L., Oksanen, J., **2020**. Analogue and Weighted Averaging Methods for Palaeoecology, R.

Sorgente, R., Di Maio, A., Pessini, F., Ribotti, A., Bonomo, S., Perilli, A., Alberico, I., Lirer, F., Cascella, A., Ferraro, L., **2020.** Impact of Freshwater Inflow From the Volturno River on Coastal Circulation. Frontiers in Marine Science. 7. doi.org/10.3389/fmars.2020.00293

Sprovieri, M., Passaro, S., Ausili, A., Bergamin, L., Finoia, M., Gherardi, S., Molisso, F., Quinci, E., Sacchi, M., Sesta, G., Trincardi, F., Romano, E., **2020**. Integrated approach of multiple environmental datasets for the assessment of sediment contamination in marine areas affected by long-lasting industrial activity: the case study of Bagnoli (southern Italy). Journal of Soils and Sediments 20, 1692–1705. https://doi.org/10.1007/s11368-019-02530-0

Tangherlini, M., Corinaldesi, C., Rastelli, E., Musco, L., Armiento, G., Danovaro, R., Dell'Anno, A., **2020**. Chemical contamination can promote turnover diversity of benthic prokaryotic assemblages: The case study of the Bagnoli-Coroglio bay (southern Tyrrhenian Sea). Marine Environmental Research 160, 105040. https://doi.org/10.1016/J.marenvres.2020.105040

Tomlinson, D.L., Wilson, J.G., Harris, C.R., Jeffrey, D.W., **1980**. Problems in the assessment of heavy-metal levels in estuaries and the formation of a pollution index. Helgolander Meeresunters 33, 566–575. https://doi.org/10.1007/BF02414780

Triassi, M., Montuori, P., Provvisiero D.P., De Rosa E., Di Duca, F., Sarnacchiaro, P., Díez, S. **2022.** Occurrence and spatial-temporal distribution of atrazine and its metabolites in the aquatic environment of the Volturno River estuary, southern Italy, Science of The Total Environment. 803, 149972, ISSN 0048-9697, https://doi.org/10.1016/j.scitotenv.2021.149972.

Trifuoggi, M., Donadio, C., Mangoni, O., Ferrara, L., Bolinesi, F., Nastro, R.A., Stanislao, C., Toscanesi, M., Di Natale, G., Arienzo, M., **2017**. Distribution and enrichment of trace metals in surface marine sediments in the Gulf of Pozzuoli and off the coast of the brownfield metallurgical site of Ilva of Bagnoli (Campania, Italy). Mar Pollut Bull 124, 502–511. https://doi.org/10.1016/j.marpolbul.2017.07.033

Triki, H.Z., Laabir, M., Lafabrie, C., Malouche, D., Bancon-Montigny, C., Gonzalez, C., Deidun, A., Pringault, O., Daly-Yahia, O.K., **2017**. Do the levels of industrial pollutants influence the distribution and abundance of dinoflagellate cysts in the recently-deposited sediment of a Mediterranean coastal ecosystem? Science of The Total Environment 595, 380–392. https://doi.org/10.1016/J.SCITOTENV.2017.03.183

Troise, C., De Natale, G., Pingue, F., Obrizzo, F., De Martino, P., Tammaro. U., Boschi, E., **2007**, Renewed ground uplift at Campi Flegrei caldera (Italy): new insight on magmatic processes and forecast. Geophys Res Lett 34:L03301.

Tsujimoto, A., Yasuhara, M., Nomura, R., Yamazaki H., Sampei, Y., Hirose, K., Yoshikawa, S., 2008. Development of modern benthic ecosystems in eutrophic coastal oceans: The foraminiferal record over the last 200 years, Osaka Bay, Japan Marine Micropaleontology, 69, pp. 225-239.

United Nations, **2015**. Transforming our World. The 2030 Agenda for Sustainable Development. Resolution Adopted by the General Assembly on 25 September 2015, 42809, 1-13. https://doi.org/10.1007/s13398-014-0173-7.2

Urbanek, A., **1993**. Biotic crises in the history of Upper Silurian graptoloids: a palaeobiological model. Hist. Biol. 7 (1), 29–50.

Vallefuoco, M., Lirer, F., Ferraro, L., Pelosi, N., Capotondi, L., Sprovieri, M., Incarbona, A., **2012.** Climatic variability and anthropogenic signatures in the Gulf of Salerno (southern-eastern Tyrrhenian Sea) during the last half millennium. Rendiconti Accademia Lincei. 23, 13-23.

van de Bund, W., Solimini, A.G., **2007**. Ecological Quality Ratios for Ecological Quality Assessment in Inland and Marine Waters. REBECCA Deliverable 10.

Vilela, C.G.; Batista, D.S.; Baptista Neto, J.A., Ghiselli Jr., R.O. **2011**. Benthic foraminifera distribution in a tourist lagoon in Rio de Janeiro, Brazil: A response to anthropogenic impacts. Marine Pollution Bulletin, 62: 2055-2074.

Voltaggio, M., Branca, M., Tedesco, D., Tuccimei, P., di Pietro, L., Voltaggio, M., Branca, M., Tedesco, D., Tuccimei, P., di Pietro, L., **2004**. 226Ra-excess during the 1631-1944 activity period of Vesuvius (Italy) . A model of alpha-recoil enrichment in a metasomatized mantle and implications on the current state of the magmatic system. Geochimica et Cosmochimica Acta 68, 167–181. https://doi.org/10.1016/S0016-7037(03)00236-9

Ward, T.J., **1989**. The Accumulation and Effects of Metals in Seagrasses Habitats. In: Larkum, A.W.D., McComb, A.J. and Shepherd, S.A., Eds., Biology of Seagrasses, Elsevier, Amsterdam, 797-820

Worm, B., Barbier, E.B., Beaumont, N., Duffy, J.E., Folke, C., Halpern, B.S., Jackson, J.B.C., Lotze, H.K., Micheli, F., Palumbi, S.R., Sala, E., Selkoe, K.A., Stachowicz, J.J., Watson, R., **2006**. Impacts of biodiversity loss on ocean ecosystem services. Science (1979) 314, 787–790. https://doi.org/10.1126/science.1132294

Wright, L. D., **1977**. Sediment transport and deposition at river mouths: a synthesis. GSA Bull. 88, 857–868. https://doi.org/10.1130/0016-7606(1977)88<857:STADAR>2.0.CO,2

Zhang, C., Qiao, Q., Piper, J.D.A., Huang, B., **2011**. Assessment of heavy metal pollution from a Fe-smelting plant in urban river sediments using environmental magnetic and geochemical methods. Environmental Pollution 159, 3057–3070. https://doi.org/10.1016/j.envpol.2011.04.006

Acknowledgments

I would like to thank all the people who supported me during this path lasted more than three years.

A special and huge thank to Fabrizio Frontalini. For his passion, patience, encouragements and kindness. It's not easy to describe the sense of joyfulness that he shared with me at each step of my PhD. This is something not common, it doesn't happen only when a scientist loves his research. You should also love people for being a great researcher and a great person, and I am just so glad to have met you, Fabrizio, and have learnt from you.

Many thanks to Carla Bucci for her support in the laboratory. A solid help for preparing mesocosms, measuring pH and for samples preparation.

A lot of thanks to all the people I worked with: in particular, Michele Betti, Caterina Ciacci, Inés Barrenechea, Luciana Ferraro, Fabio Francescangeli, Marina Montresor and Jan Pawlowski and I apologize if I am forgetting somebody. Hopefully we will collaborate to more investigations in the future.

Many thanks to Lorenzo Brocani, Andrea Buresta, Giulia Persichini, and Vittoria Scipioni who worked with me for their bachelor thesis. Their help has been very important, and you all become great geologists.

Special thanks to my PhD cycle colleagues: Benedetta Amicizia, Gioele Bigini, Matteo Corrieri, Arianna Malaguti, Luca Mancini and Nicole Marittimo. Although coming from different backgrounds, we shared a "normal" start of our PhD, it was great knowing to have their support during our common steps.

Lot of thanks to my colleagues: Michele Curuzzi, Agnese Mannucci, Federica Rebecchi and Davide Torre for the friendship and the coffees. You made me feel the campus like home, like a place where to find laughs and support, where to share ideas and thoughts. Good luck with the rest of your PhD!

In my family we all studied sciences, but among us the real scientist is just my sister. She has always been my pole star, especially during this journey, when I always looked for her last suggestions on many aspects of my life and career. It makes me smile we are going to discuss our PhD thesis in the same weeks, but when they ask me about my work, I always underline yours. Because you have always shined brighter.

My last and biggest thank is for my parents. After following my father's footsteps for a lifelong, studying geology, going to explore ores in arid lands, apparently, as noticeable from this thesis, I have started to move toward marine-biological topics, more like what my mother used to do. Honestly, I still don't know where waters are carrying me, but the times I have been afraid to drown, your sights on the banks, always ready to encourage me and proud for how I was rafting, have been enough to give a sense to every direction the flow was following.

Supplementary materials

Station ID	B4/40	B4/20	B4/10	B3/40	B3/20	B3/10	B2/40	B2/20	B2/10	B1/40	B1/20	B1/10
As	39	67	75	42	59	84	34	45	20	26	31	23
Cd	0.59	0.42	0.37	0.7	0.27	0.31	0.06	0.03	0.14	0.14	0.03	0.13
Co	6.8	8.9	6.8	6	5.5	7	6.2	4.8	3.8	7.2	6.7	13.2
Cr	41	24	15	38	21	21	18	9	7	19	14	26
Cu	45	33	42	47	24	21	17	8	20	20	9	26
Hg	0.73	0.34	0.36	0.65	0.43	0.25	0.36	0.11	0.04	0.28	0.11	0.12
Ni	11	9.9	8.3	9.7	8.2	10.6	6.7	4.9	3.7	8.6	5.6	11.8
Pb	277	229	262	279	230	322	122	61	31	81	64	50
V	71	85	74	64	66	87	61	56	57	76	95	272
Zn	603	777	795	669	667	674	249	116	102	164	127	165
PLI	1.22	1.14	1.12	1.21	1.05	1.09	0.83	0.64	0.61	0.84	0.66	0.84
mCd	4.14	1.29	0.82	3.98	0.25	0.49	0.00	0.00	0.00	0.00	0.00	0.00
EF (As)	1.13	2.01	2.03	1.28	1.96	3.17	0.85	1.38	0.58	0.75	0.95	0.76
EF (Hg)	3.07	1.47	1.40	2.82	2.03	1.34	1.28	0.51	0.18	1.15	0.49	0.57
EF (Pb)	4.87	4.12	4.26	5.06	4.57	7.27	1.81	1.13	0.55	1.39	1.19	0.99
EF (Zn)	4.03	5.31	4.91	4.61	5.04	5.79	1.41	0.82	0.69	1.06	0.89	1.24

from	Background	ERM	ERL
De Vivo & Lima 2008	36	85	33
Cicchella et al. 2005	0.25	9	5
De Vivo & Lima 2008	35	n/a	n/a
Damiani et al. 1987	30	145	80
Damiani et al. 1987	20	390	70
Damiani et al. 1987	0.25	1.3	0.15
Damiani et al. 1987	20	50	30
Damiani et al. 1987	60	110	35
De Vivo & Lima 2008	100	n/a	n/a
De Vivo & Lima 2008	158	270	120

Table S2.1 PTEs concentrations (ppm), references values: effect range median (ERM); effect range low (ERL), background (ppm), pollution load index (PLI).

EF	Classification	mCd	Classification	PLI	Classification
≤ 2	Low enrichment	1.5-2	Low	0-1	Unpolluted
2–5	Moderate enrichment	2-4	Moderate	>1	Polluted
5–20	High enrichment	4-8	High		
20–40	Very high enrichment	8-16	Very high		
> 40	Extreme enrichment	16-32	Extremely high		
		>32	Ultra high		

Table S2.2 Categories of different geochemical indices: Enrichment factor (EF) after Müller (1979), contamination index (mCd) after mCd Hakanson (1980) and pollution load index (PLI).

		B1_10	B1_20	B1_40	B2_10	B2_20	B2_40	B3_10	B3_20	B3_40	B4_10	B4_20	B4_40
C/N		14.14	10.22	14.25	9.79	4.95	16.73	14.88	52.53	34.85	41.27	15.83	31.08
TN	%	0.02273	0.02754	0.03356	0.01191	0.02709	0.04372	0.06581	0.39298	0.44627	0.13753	0.12368	0.20716
TOC	%	0.31914	0.28167	0.47591	0.11623	0.13003	0.73308	0.97673	20.26586	14.31825	5.6986	1.96812	6.41898
Mud	%	1.421801	1.146789	5.908419	0.346741	0.105597	9.751773	12.24087	8.082409	27.16346	4.786681	9.243697	21.38965

Table S2.3 Raw data of C/N, TN (%), TOC (%), and mud (%).

	Mean	Min	Perc 10	Perc 25	Perc 50	Perc 75	Perc 98	Max	Std dev
C/N	21.7	5.0	9.8	13.2	15.4	32.0	50.1	52.5	14.7
TN (%)	0.1	0.0	0.0	0.0	0.1	0.2	0.4	0.4	0.1
TOC (%)	4.3	0.1	0.1	0.3	0.9	5.9	19.0	20.3	6.6
Mud (%)	8.5	0.1	0.4	1.4	7.0	10.4	25.9	27.2	8.5
Sand	88.3	71.7	73.5	87.3	91.6	92.8	95.4	95.5	8.1
As (ppm)	40.0	16.0	19.0	21.0	34.0	52.0	82.0	84.0	22.0
Cd (ppm)	0.0	0.0	0.0	0.0	0.0	0.0	1.0	1.0	0.0
Co (ppm)	7.0	4.0	5.0	6.0	7.0	8.0	12.0	13.0	2.0
Cr (ppm)	23.0	7.0	11.0	17.0	21.0	28.0	43.0	44.0	11.0
Cu (ppm)	27.0	8.0	12.0	20.0	26.0	35.0	46.0	47.0	12.0
Hg (ppm)	0.0	0.0	0.0	0.0	0.0	0.0	1.0	1.0	0.0
Ni (ppm)	9.0	4.0	5.0	7.0	9.0	10.0	12.0	12.0	3.0
Pb (ppm)	151.0	31.0	54.0	66.0	99.0	246.0	310.0	322.0	102.0
V (ppm)	85.0	56.0	59.0	65.0	70.0	81.0	222.0	272.0	53.0
Zn (ppm)	372.0	102.0	121.0	149.0	172.0	668.0	790.0	795.0	281.0

Table S2.4 Basic statistics of grain size (%), organic matter content (%), and PTE concentrations (ppm).

https://docs.google.com/spreadsheets/d/1_Z2RZTKyW5O6wbluw-AODk1eLzYFaR_o/edit?usp=sharing&ouid=116551334897653390439&rtpof=true&sd=true

Table S2.5 Benthic foraminiferal morphological data

https://docs.google.com/spreadsheets/d/1yD0Q9u2YjN-z34Pwuc8bezFpgxYmngO8/edit?usp=sharing&ouid=116551334897653390439&rtpof=true&sd=true

Table S2.6 Benthic foraminiferal molecular data.

https://docs.google.com/spreadsheets/d/1T-geH160RFeFGDitwTD3k_99ZKzS2ESH/edit?usp=sharing&ouid=116551334897653390439&rtpof=true&sd=true

Table S2.7 Assigned MOTUs and ecological group

https://docs.google.com/spreadsheets/d/1LLTtqwFkfTZ0otHfofhVu2h4V7RJx35t/edit?usp=sharing&ouid=116551334897653390439&rtpof=true&sd=true

Table S2.8 Unassigned MOTUs and ecological group

https://docs.google.com/spreadsheets/d/1QNIIoFynQM7g81qOcZbTDsp8BbV2-bK4/edit?usp=sharing&ouid=116551334897653390439&rtpof=true&sd=true

Table S2.9 Abbreviation of morphospecies and MOTUs as reported in Figure 2.4.

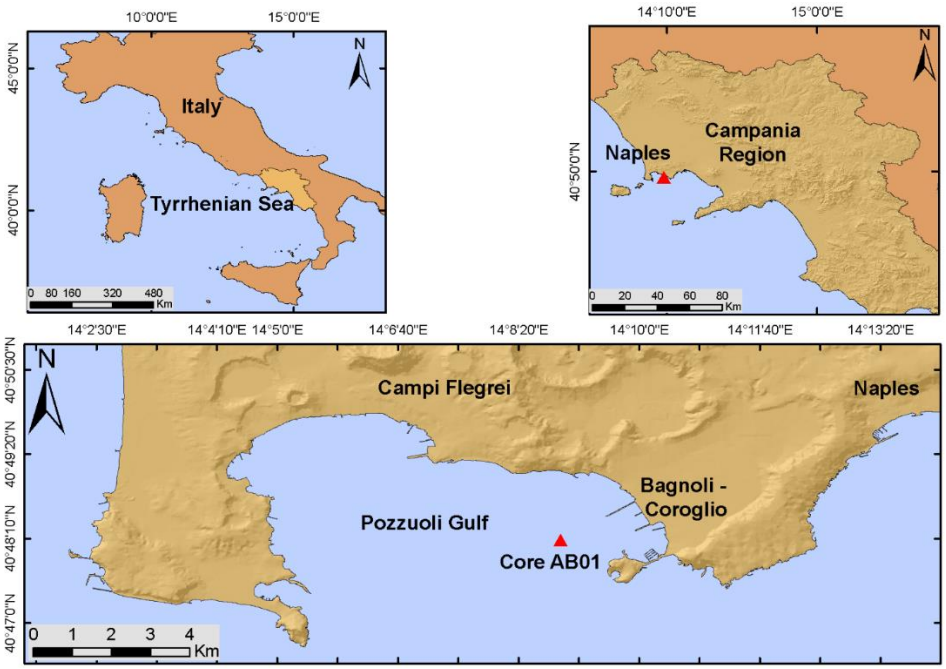

Figure S3.1. Location of the Bagnoli-Coroglio SIN in the Pozzuoli Gulf (Tyrrhenian Sea) and position of the AB01 sediment core (55m water depth).

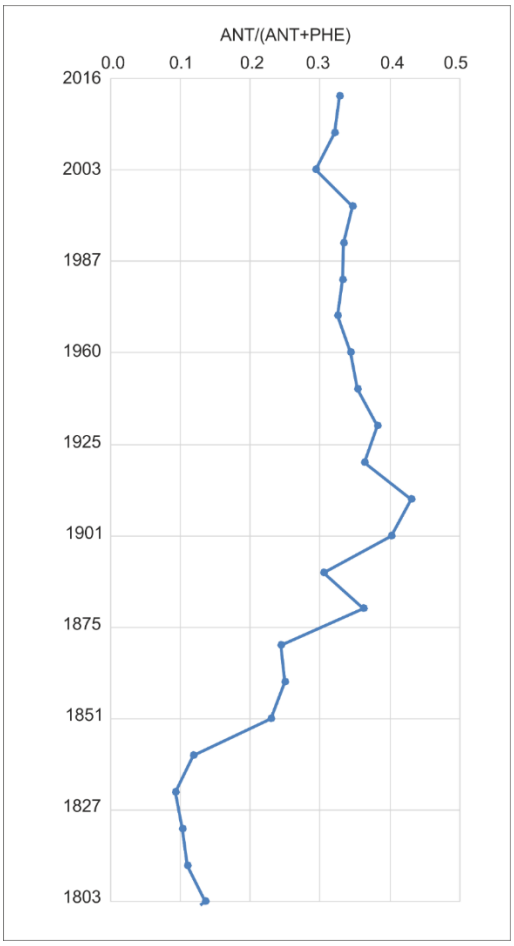

Figure S3.2. Plot of Anthracene/(Anthracene + Phenanthrene) along the AB01 sediment core.

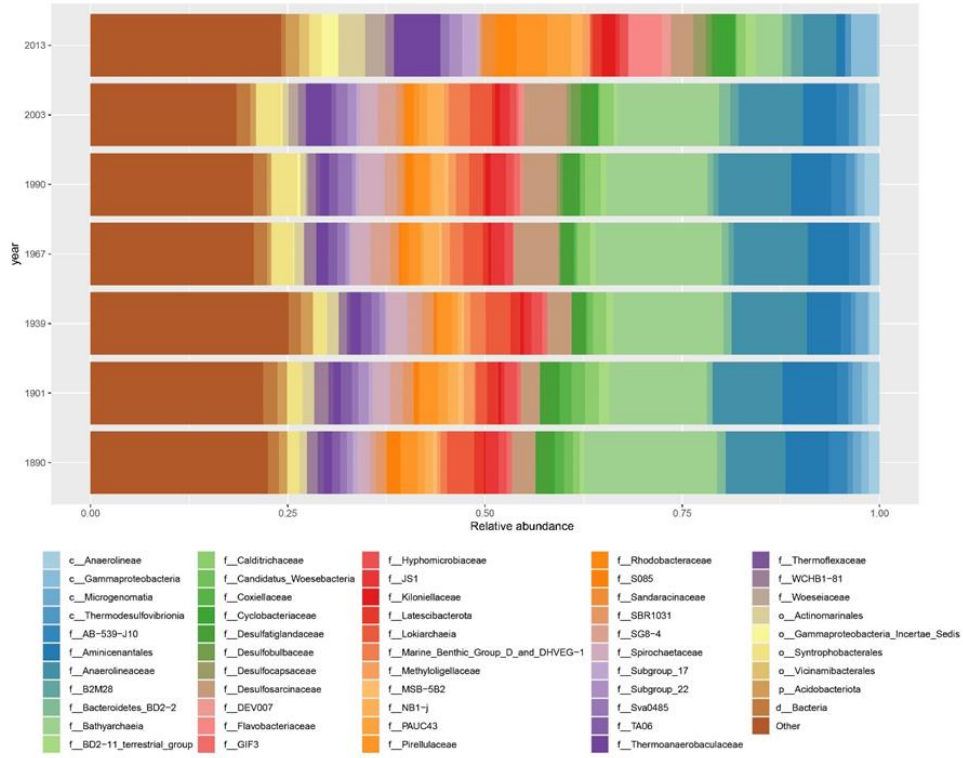

Figure S3.3. Bar-plot showing the taxonomic composition of the bacterial assemblages along the AB01 sediment core at the lowest taxonomic level in terms of sequence contribution to each bacterial taxa. Taxa contributing less than 1% were summed and indicated as "Other". Taxa names are preceded by a letter according to the maximum depth of taxonomic assignment: "d" for domain, "c" for class, "o" for order and "f" for family.

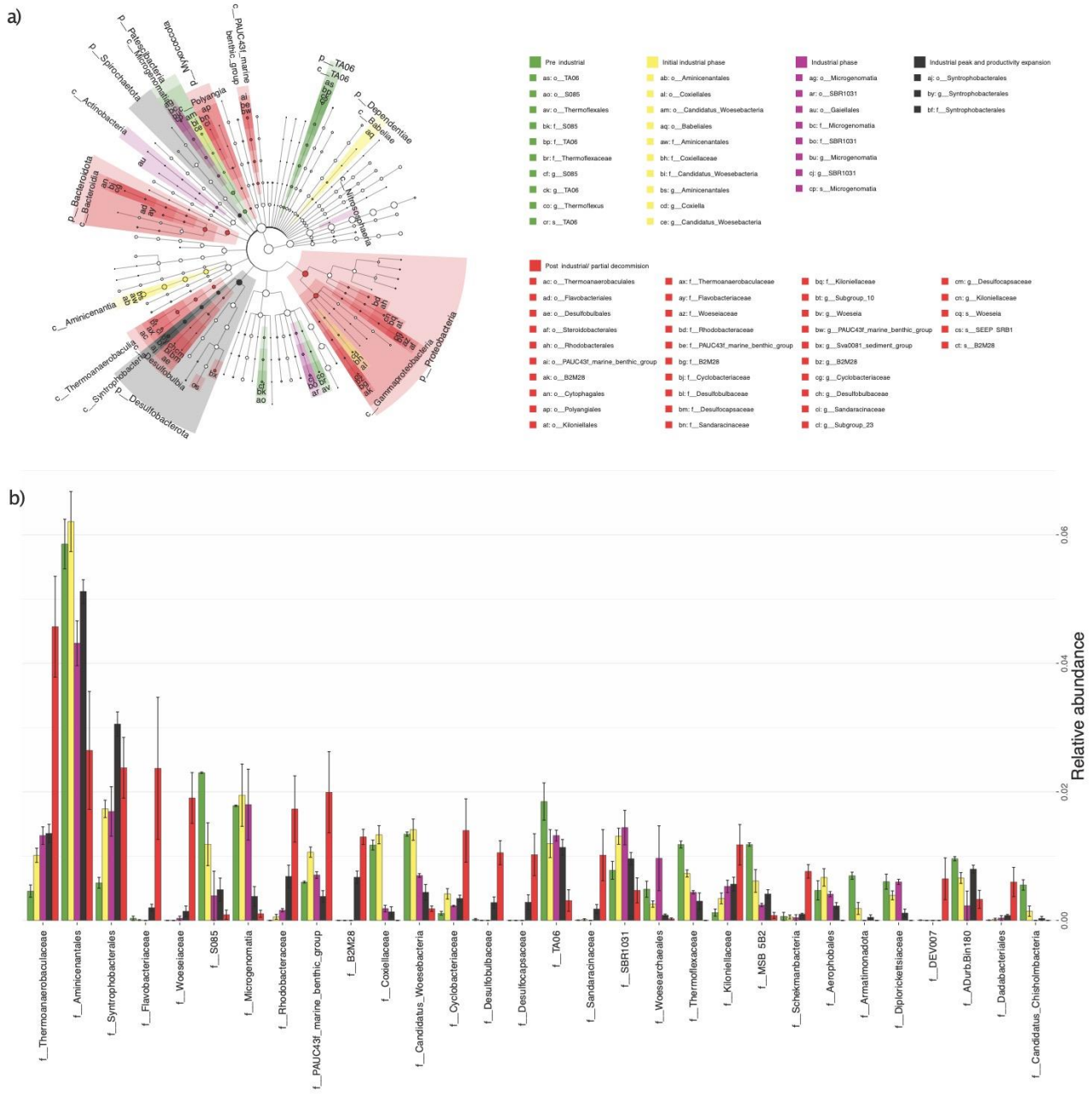

Figure S3.4. Results of LEfSe analysis carried out on the prokaryotic assemblage composition. A) Cladogram reporting the main prokaryotic taxa associated with the different historical periods; B) Barplot reporting the relative abundances (from 0 to 1) of the differentially abundant taxa at family level; error bars represent the standard error, and all bars are colored according to the related temporal phase.

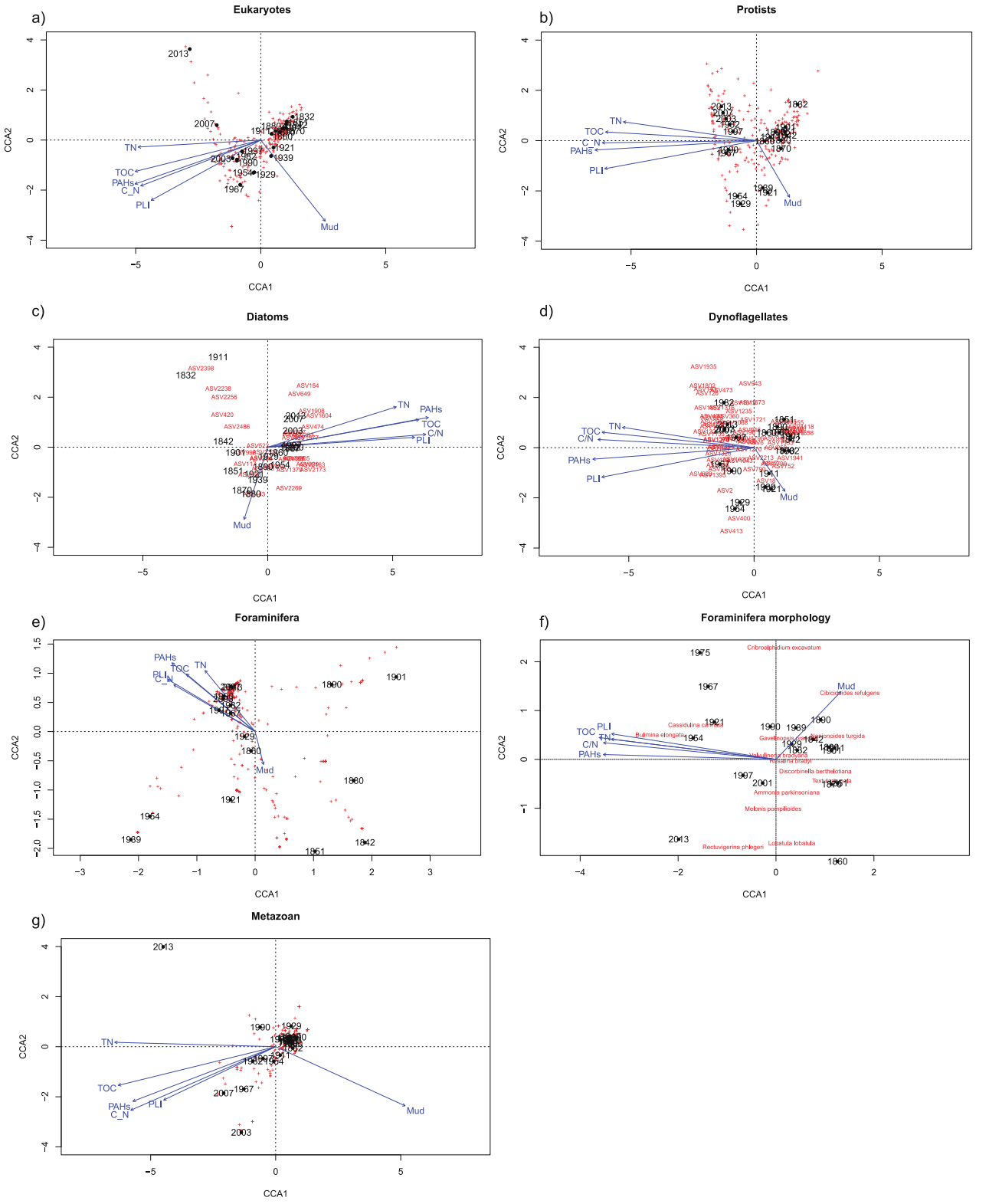

Figure S3.5. Correspondence canonical analysis (CCA) plots show the ASVs or taxa in red, the sediment layers (dates) and environmental parameters (arrows) for each of taxonomical group's a) eukaryotes, b) protists, c) diatoms d) dinoflagellates, e) foraminifera and f) foraminifera morphology and g) metazoan.

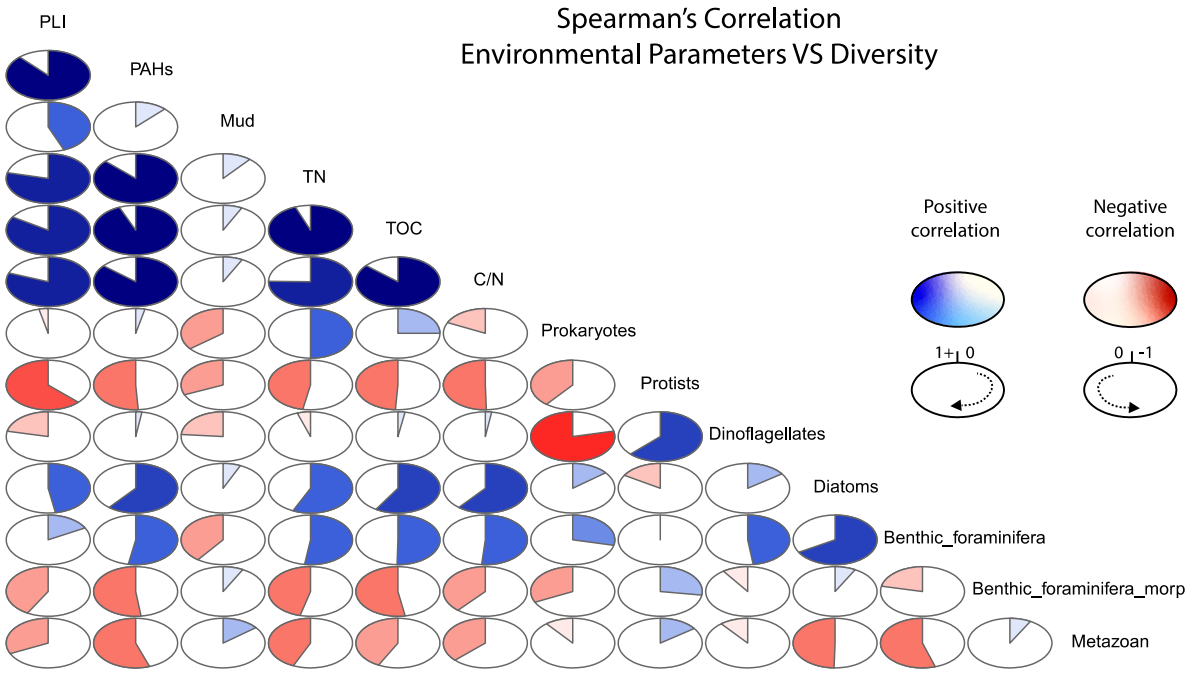

Figure S3.6. Spearman's correlation between environmental parameters and diversity: blue circles (positive correlation) and rad circles (negatives correlation).

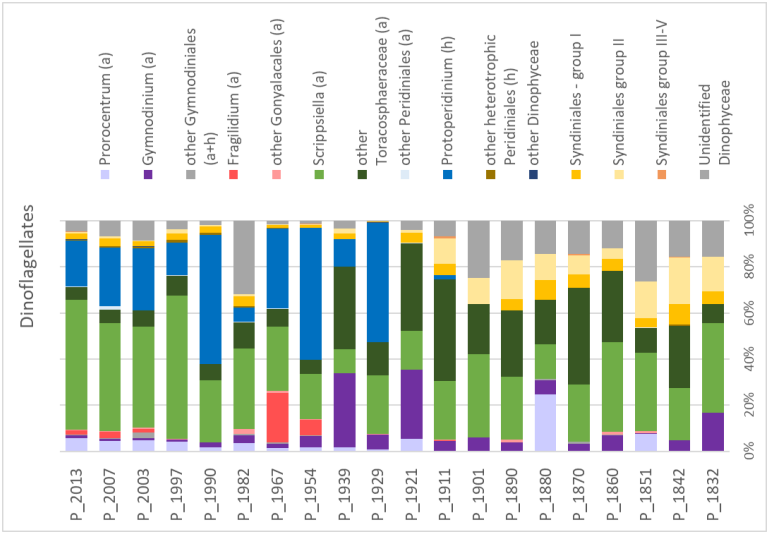

Figure S3.7. Dinoflagellates in the sediment layers of the AB01 core inferred by metabarcoding of V9 18S rDNA from sedimentary DNA. Taxa are expressed as relative abundance of reads from the normalized dataset. (a) = taxa with chloroplasts; (h) = heterotrophic taxa.

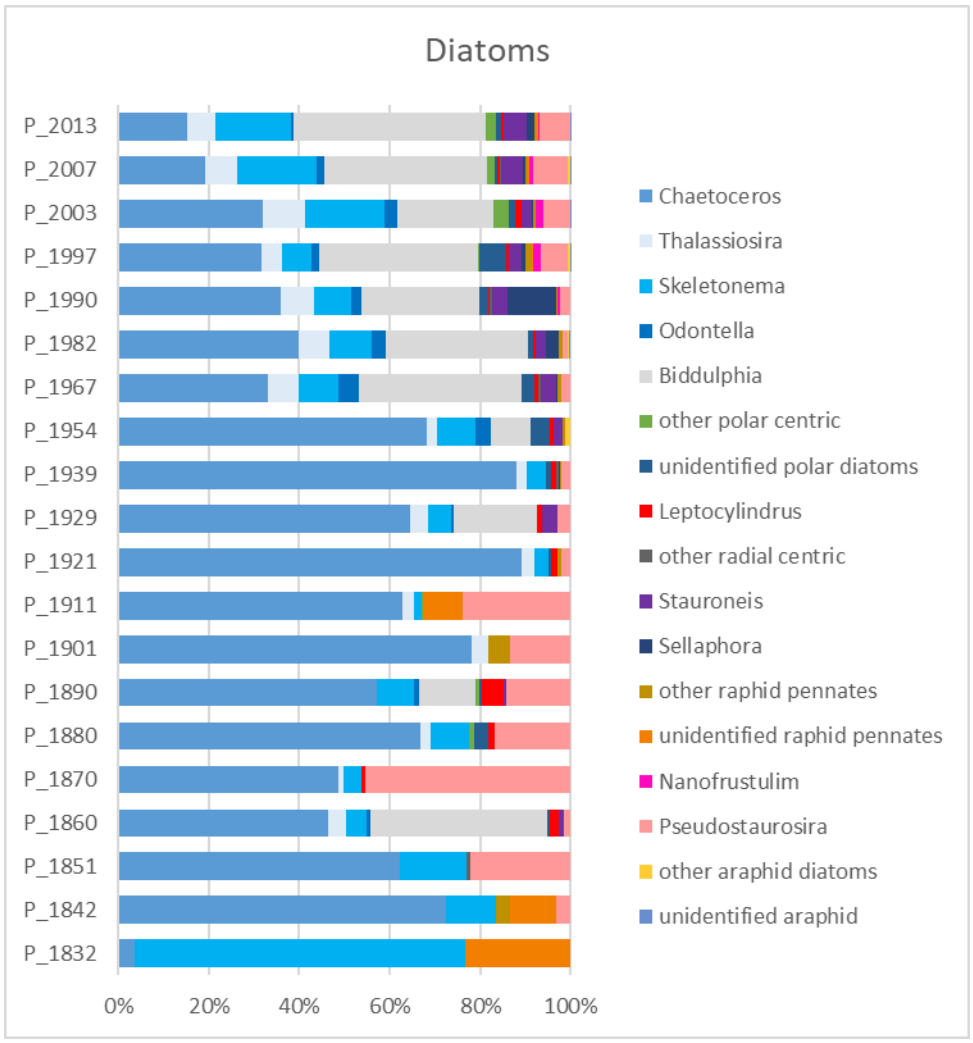

Figure S3.8. Diatoms in the sediment layers of the AB01 core inferred by metabarcoding of V9 18S rDNA from sedimentary DNA. Taxa are expressed as relative abundance of reads from the normalized dataset.

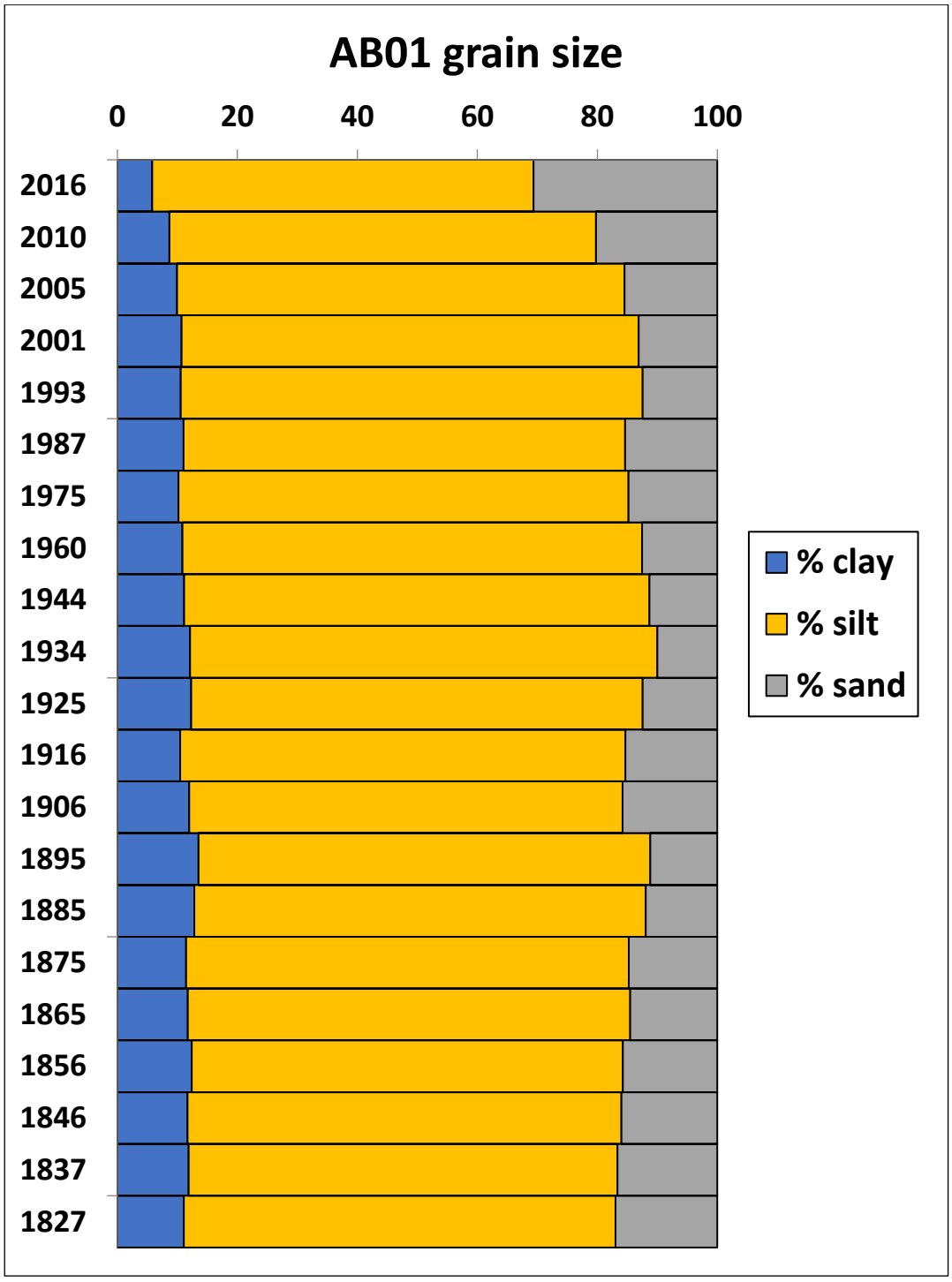

Figure S3.9. AB01 sediment core grain-size plot: volume percentage of sand, silt and clay (on x axe) vs ages (on y axe) of each odd sediment layer (1 cm resolution) as derived from the geochronology (see Supplementary Table 3.1).

Layer	Year	u(Year)	Environmental variables				sedaDNA				Morphology
cm	a	a	Grain-size	PLI	PAHs	Organic matter	Eukaryotes	Foraminifera	Metazoan	Prokaryotic	Foraminifera
0-1	2016	1	X	X	X						
1-2	2013	1				X	X	X	X	X	X
2-3	2010	1	X	X	X						
3-4	2007	1				X	X	X	X		X
4-5	2005	1	X	X	X						
5-6	2003	1				X	X	X	X	X	X
6-7	2001	1	X	X	X						
7-8	1997	2				X	X	X	X		X
8-9	1993	2	X	X	X						
9-10	1990	2				X	X	X	X	X	X
10-11	1987	2	X	X	X						
11-12	1982	2				X	X	X	X		X
12-23	1975	3	X	X	X						
13-14	1967	4				X	X	X	X	X	X
14-15	1960	4	X	X	X						
15-16	1954	5				X	X	X	X		X
16-17	1944	3	X	X	X						
17-18	1939	3				X	X	X	X	X	X
18-19	1934	3	X	X	X						
19-20	1929	3				X	X	X	X		X
20-21	1925	3	X	X	X						
21-22	1921	3				X	X	X	X		X
22-23	1916	3	X	X	X						
23-24	1911	3				X	X	X	X		X
24-25	1906	3	X	X	X						
25-26	1901	3				X	X	X	X	X	X
26-27	1895	3	X	X	X						
27-28	1890	3				X	X	X	X	X	X
28-29	1885	3	X	X	X						
29-30	1880	4				X	X	X	X		X
30-31	1875	4	X	X	X						
31-32	1870	4				X	X	X	X		X
32-33	1865	4	X	X	X						
33-34	1860	4				X	X	X	X		X
34-35	1856	4	X	X	X						
35-36	1851	4				X	X	X	X		X
36-37	1846	4	X	X	X						
37-38	1842	3				X	X	X	X		X
38-39	1837	3	X	X	X						
39-40	1832	3				X	X		X		X
40-41	1827	3	X	X	X						
Number of analyzed samples		**41**	**21**	**21**	**21**	**20**	**20**	**19**	**20**	**7**	**20**

Table S3.1. AB01 sediment core chronology. For every layer, ages and age uncertainties arepresented.

Genetic markers used for this study					
Organism	**region**	**primers name**	**forward sequence (5'-3')**	**reverse sequence (5'-3')**	**ref**
Prokaryotes	V4-V5	515F-Y 926R	GTGYCAGCMGCCGCGGTAA	CCGYCAATTYMTTTRAGTTT	Parada et al., 2016
Eukaryotes	nc 18S V9	1389F - 1510R	TTGTACACACCGCCC	CCTTCYGCAGGTTCACCTAC	Amaral-Zettler, et al., 2009
metazoan	mt COI	mlCOIintF - dgHCO2198	AAGGGCACCACAAGAACGC	CCACCTATCACAYAATCATG	Leray et al 2013
foraminifera	nc 18S 37F	s14F1 - s15R	GGWACWGGWTGAACWGTWTAYCCYCC	TAAACTTCAGGGTGACCAAARAAYCA	Pawlowski and Lecroq, 2010
PCR programs for V9, COI and foraminifera					
V9					
94°C	3'				
94°	30"	30X			
57°	60"				
72°	90"				
72°C	10"				
COI					
95°C	5'				
94°C	10"				
62-47°C	30"	16 cycles	(1°C decrease every cycle)		
72°C	1'				
95°C	10"				
46°C	30"	35 cycles			
72°C	1'				
72°C	2'				
Foraminifera					
94°C	5'				
94°	30''				
52°	30''	50 cycles			
72°	30''				
72°	2'				

Table S3.2. Genetic markers and PCR programs used for eukaryotes, metazoa and foraminifera.

PLI values

Age	PLI
2016	3.47
2010	3.27
2005	4.76
2001	3.83
1993	5.32
1987	4.18
1975	6.35
1960	5.61
1944	4.74
1934	4.17
1925	4.44
1916	2.38
1906	1.73
1895	1.57
1885	1.22
1875	1.21
1865	1.27
1856	1.03
1846	0.79
1837	0.91
1827	0.79

PLI class

0-1	unppolluted
1-2	moderately to unpolluted
2-3	moderately polluted
3-4	moderately to highly polluted
4-5	highly polluted
5-6	very highly polluted
6-7	extremely polluted

Table S3.3. AB01 sediment core a) Pollution Load Index (PLI) values and classes; b) Polycyclic Aromatic Hydrocarbons (PAHs) and thresholds; c) site specific background concentration of trace elements

Age	TN	TOC	C/N
	%	%	
2013	0.12	4.41	37.2
2007	0.07	2.09	30.9
2003	0.08	3.61	43.4
1997	0.08	2.97	37.4
1990	0.09	3.02	33.7
1982	0.11	4.95	46.5
1967	0.09	3.89	43.6
1954	0.07	2.35	34.4
1939	0.06	1.92	30.4
1929	0.07	1.91	25.9
1921	0.07	1.96	27.6
1911	0.06	1.27	21.2
1901	0.06	1.30	20.1
1890	0.06	1.25	20.5
1880	0.05	1.16	21.3
1870	0.05	1.12	22.2

TOC
%

>4.1
3.4-4.1
2.5-3.4
2.0-2.5
<2.0

1860	0.05	1.19	22.5
1851	0.05	1.21	22.7
1842	0.06	1.24	21.3
1832	0.06	1.16	19.0

Table S3.4. AB01 sediment core Total Nitrogen (TN), Total Organic Carbon (TOC) and C/N values.

Group	Best correlation variables	Correlation
Terrestial plants and posidonia	PLI, Mud	0.69
Diatoms	PLI, PAHs, Mud	0.32
Dynoflagellates	PLI, PAHs	0.6
Eukaryotes	PLI, PAHs, Mud	0.79
Metazoan	PAHs, Mud, TOC	0.57
Protists	PLI, PAHs	0.82
Foraminifera_genetic	PLI	0.12
Foraminifera_morph	TOC	0.54

Table S3.5. Results of biological environmental (BIOENV) analysis applied to different taxa groups. The BIOENV exhibited the environmental variables with the highest correlation with biological data.

https://docs.google.com/spreadsheets/d/1bIUmhtEMGLgFwzC4moxJekKAF9hKMKUp/edit?usp=sharing&ouid=116551334897653390439&rtpof=true&sd=true

Table S3.6. Diversity (H') and ecological indices (Foram-AMBI, g-AMBI, microgAMBI).

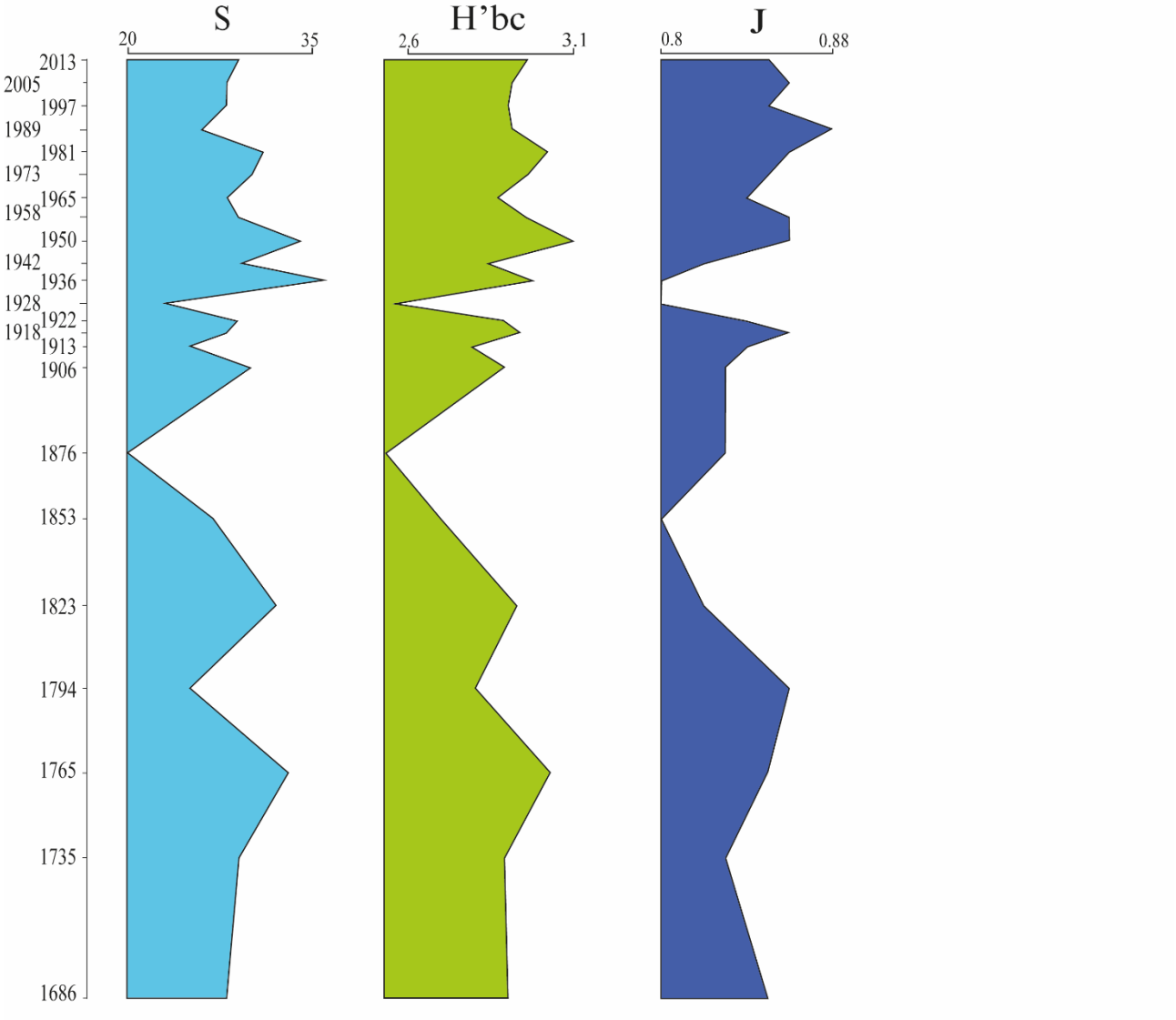

Figure S5.1. Plot of diversity indices (S), H'bc and equitability (J).

https://docs.google.com/spreadsheets/d/19BA8FMMI7fUKcn84k8S-_1inXsQVJTL9/edit?usp=sharing&ouid=116551334897653390439&rtpof=true&sd=true

Table S5.1. Abundance and relative abundance of benthic foraminifera species.